AN ABSTRACT OF THE DISSERTATION OF

Elizabeth R. Jachens for the degree of Doctor of Philosophy in Water Resources Engineering presented on March 9, 2020.

Title: Using Recession Analysis to Characterize Watershed Responses to Drought.

Abstract approved:

John S. Selker

In the face of climate change droughts are predicted to become more persistent, further intensifying the need for accurately predicting the timing and magnitude of summer streamflow in rivers. In order to determine the sensitivity of a watershed to drought, there is a need to describe what these drought conditions will look like and to quantify how severe the effects on the rivers and aquifers will be. Discrepancies between model predictions and observed streamflow motivate us to improve our current understanding of watershed responses to drought in order to better characterize it. This dissertation attempts to identify issues surrounding the current understanding of watershed responses to drought. First, we introduce a methodology that can greatly expand the number of watersheds analyzed using recession analysis with water height instead of discharge. Using water height for recession analysis instead of discharge reduces the fieldwork associated with data collection and thus with the same resources more watersheds can be characterized using water height alone. Second, we focused on quantifying the impacts of different recession analysis methods on the parameter estimations and consequences for drought sensitivity interpretation. We conclude that analyzing the recessions collectively is flawed and that analysis should consider individual recessions in order to quantify watershed responses to different hydrological scenarios. Third, we examined how hillslope drainage pathways and residence time varies during a drought event and the associated effects of modeling the process in 2D

vs 3D. In 3D, the hillslope drainage path rotates from stream perpendicular to stream parallel as the contributing driving gradient changes with the lowering water table. This results in an increased path length and residence time that is not captured in a 2D model, ultimately changing the timing and magnitude of aquifer contributions to streamflow during drought. While this dissertation has developed a framework for better understanding and predicting streamflow during drought, there are still opportunities to improve the characterization by monitoring more small watersheds, describing the variability in individual recession at low flows, and gaining a deeper understanding of drainage timescale. Knowing how streams and aquifers will respond to drought in future climate scenarios has great implications for water management as it may enable us to identify watersheds that are sensitive or resilient to future drought.

Using Recession Analysis to Characterize Watershed Responses to Drought

by
Elizabeth R. Jachens

A DISSERTATION

submitted to

Oregon State University

in partial fulfillment of
the requirements for the
degree of

Doctor of Philosophy

Presented March 9, 2020
Commencement June 2020

Doctor of Philosophy dissertation of Elizabeth R. Jachens presented on March 9, 2020.

APPROVED:

Major Professor, representing Water Resources Engineering

Director of the Water Resources Graduate Program

Dean of the Graduate School

I understand that my dissertation will become part of the permanent collection of Oregon State University libraries. My signature below authorizes release of my dissertation to any reader upon request.

Elizabeth R. Jachens, Author

ACKNOWLEDGMENTS

I would like to extend my sincerest appreciation to my advisor, John Selker, who has provided support throughout my path in pursuit of my Ph.D. John has always encouraged me to pursue projects that I find interesting, many of which seemed divergent from my main goals at the time. It has been truly remarkable to problem-solve together, and I couldn't imagine any advisor more supportive than John.

A huge thanks to my committee for supporting me from the beginning, on numerous other projects as well as on this one. Together, they have helped me understand my own capabilities necessary to get where I am today.

Thank you to everyone who has read version of my papers, proving valuable perspective and undoubtedly improving my manuscripts. I am thankful for my co-authors for reading and re-reading drafts. The author contribution section doesn't do you justice, I couldn't have done this without you. Thank you Gordon Godshalk for being an amazing "naïve but intelligent reader" for your honest reviews.

I am grateful for the Water Resources Graduate Program and BEE staff for going out of your way to answer all of my questions and helping me navigate my time at OSU. I know you ladies are always on my side and I loved seeing your kind smiles in the office.

Thank you to my officemates and peers for providing distractions, comic relief, help with code, and sympathy. I loved the daily lunch gatherings, snack breaks, birthday celebrations, and pretty much every other social event that inevitably involved good food and great company. And to my Gilmore Girls, I couldn't imagine my time at OSU without you.

Finally, I would not have done this without the love and support of my family. My family has always believed in my abilities and taught me how to believe in myself. They have raised me with the understanding that with hard work I can reach every goal I set, an invaluable skill that I will take with me as I continue in life. This is just the beginning, and I'm excited to tackle what comes next.

CONTRIBUTION OF AUTHORS

Clément Roques, David. E. Rupp, and John S. Selker were involved in each of the three following manuscripts. They each provided valuable contributions throughout the process. All authors provided substantial contributions to intellectual content development and revising the manuscript.

Clément Roques was a primary contributor in setting up and performing analysis. He provided the initial code for analysis and related support that benefited all chapters of this work. Clément also provided expert knowledge on model setup and interpretation.

David. E. Rupp was involved in the conceptualization of ideas and the development of methodology. He provided technical support and expert advice on mathematics. David significantly contributed to addressing reviewer concerns during the peer-review process.

John S. Selker was the principal investigator for all research. He provided much of the theoretical framework and supervised the projects.

TABLE OF CONTENTS

Page

TABLE OF CONTENTS (Continued)

Page

LIST OF FIGURES

Figure Page

LIST OF FIGURES (Continued)

Figure Page

LIST OF TABLES

Chapter 1. General Introduction

In the face of climate change droughts are predicted to become more persistent, further intensifying the need for accurately predicting the timing and magnitude of summer streamflow. In the absence of recharge, as is the case in prolonged droughts where overland flow is negligible, streamflow originates from aquifer drainage (Troch et. al 2013). The rate a draining aquifer can sustain streamflow during drought, described by baseflow recession analysis, provides insight into aquifer parameters and hydrologic properties (Brutsaert & Nieber 1977). Recession analysis is a well-accepted technique to describe how water moves in a landscape and is contributed over time. Recession analysis is a means of using characteristics of this receding limb to quantify hydraulic properties of the connected aquifer system. Recession analysis is visualized in log-log space as the time rate of change in discharge as a function of discharge expressed by $-dQ/dt$ vs Q. The derivative of flow with respects to time is expressed as a power function $-dQ/dt=aQ^b$ such that the recession plot parameter a is graphically represented by the y-intercept and b is the slope.

Since recession analysis was established in 1977, there have been methodological improvements but not all of the scientific community has accepted and incorporated the improvements. The original methodology for baseflow recession analysis consists of taking the derivative of flow using a constant time step (Brutsaert and Nieber, 1977). Using the constant time step has since been shown to be confounded with artifacts, particularly at low flows when the change in discharge is large relative to instrument precision (Kirchner, 2009; Roques *et al.*, 2017; Rupp and Selker, 2006a). The artifacts contribute to point clouds for low flow values that make the interpretation of parameters at low values difficult (Rupp and Selker, 2006a). However, a recent paper on new computational methodology and procedures for taking the derivatives for the recession analysis has shed light on low flow behaviors by removing artifacts and errors associated with taking the derivative at low flows (Figure 1) (Roques *et al.*, 2017). Comparing the exponential time step (ETS) to the constant time step (CTS) method, recession analysis using the ETS method reduces the scatter and spread of the data points within the point cloud allowing for an improved understanding of the underlying

watershed response processes. The improvements in recession analysis allow for this work to focus on low flow ranges, where previous works wouldn't have been possible because of computational artifacts obscuring interpretation of results. Each advancement in recession analysis has increased the amount of usable information and opened the door to advance our thinking about advancing our thinking about how we can use recession analysis, conceptually and methodologically.

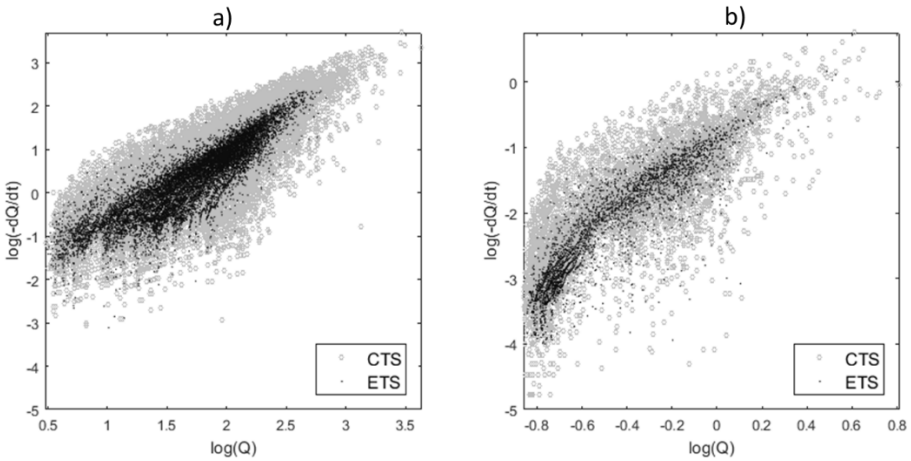

Figure 1. Recession analysis comparing the constant time step (CTS) method with the exponential time step (ETS) method for a) McKenzie River at Clear Lake, OR (USGS no. 14158500) and b) Lookout Creek near Blue Lake, OR (USGS no. 14161500)

An application for recession analysis using improved low flow characterization could be insights of droughts on summer streamflow. In the Oregon Cascades, the winter snow conditions in 2015 were equivalent to a 4ºC climate warming scenario, presenting a unique opportunity to test fundamental hypotheses of headwater stream response to changes in the amount and timing of recharge during low snowpack conditions. With the Oregon Cascade Mountain range receiving less than 20% of the average snowfall in the winter of 2015, we seek to describe the hydrological responses of such anomalous - but near future normal – recharge and runoff conditions.

Previous regional studies focused on the regional characterization in the Cascades have characterized low flow sensitivity with snowmelt runoff based on air temperature (Kormos *et al.*, 2016), whether a stream is spring fed vs surface fed (Manga, 1997, 1996; Safeeq *et al.*, 2013), on the underlying geology and aquifer

(Godsey *et al.*, 2014; Jefferson *et al.*, 2008; Tague *et al.*, 2008; Tague and Grant, 2004, 2009), or as a direct response to snowpack (Manga, 1997; Tague and Grant, 2009). These studies aim to analyze streamflow responses of timing and magnitude to climate change scenarios, with implicating predictions about large regional responses to future climate scenarios as sensitivities of low streamflow affect terrestrial and aquatic ecosystems, and water management practices.

The winter of 2015 provided such an opportunity when the winter snowpack was less than 20% of the average annual snowpack but precipitation totals were near historical averages. This snow and rain combination, with precipitation regimes changing from snow dominated to rain dominated, is similar to that of a 4°C warming scenario, presenting a unique opportunity to test the fundamental hypotheses about the hydrogeological impact on expected stream flow under climate change. Despite being the lowest snowpack on record (Mote *et al.*, 2018), the 2015 summer streamflow did not reach the record lows that the climate models predicted or breaking historical records (Figure 2) (Tague and Grant, 2004, 2009). The near-normal precipitation but low-snowpack was consistent with climate models, but the response was different than streamflow predictions from those climatic conditions (Tague and Grant, 2004, 2009). The hydrographs in Figure 2 show the 2015 water year (highlighted in blue) follows the lower envelope of historic streamflow, instead of reaching record flows predicted based on the low recharge winter, indicating a streamflow that unexpectedly stabilized, instead of continuing to decline, more than current theory can describe. The presence of a stabilized streamflow response to drought is absent in the predictive models. This indicates that the models are not capturing the hydrology and can be improved by a deeper understanding of the temporal pattern of streamflow during drought. This motivated us to explain the observations of sustained summer baseflow for the watersheds in the Oregon Cascades and why the current models weren't capturing the low flows.

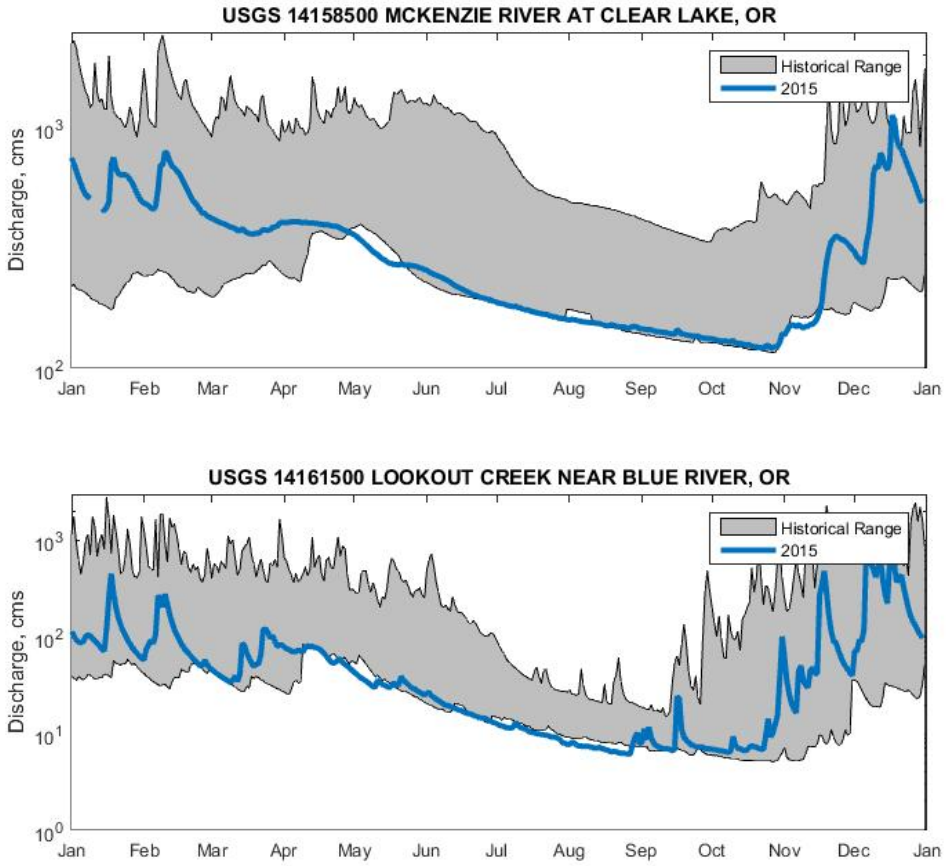

Figure 2. Clear Lake USGS no. 14158500 (top) and Lookout Creek USGS no. 14161500 (bottom) comparison between historical streamflow and 2015 streamflow

While understanding the summer streamflow after the 2015 snow drought in the Oregon Cascades is outside the scope of this dissertation, we do seek to develop a better conceptual and mythological understanding of recession analysis that ultimately could be applied to larger regional questions. This work will seek to provide to answers such as characterizing what drought looks like, how watersheds and stream systems respond to drought, and how severely climate change will affect the hydrology of the watershed streamflow. Reliable predictions for streamflow response to future warming scenarios are important for water managers to identify vulnerable drinking water sources and ecological services, validating the need for studies and models to determine the relationships between watershed characteristics and their streamflow response. While models have usefulness for representing future scenarios, they will continue to

fail to capture the true complexity of the system and therefore there is no substitute for field data for validation.

For the purposes of this dissertation, we were motivated by describing streamflow response to drought and the predictive models to address where and how models might be improved. This work aims to characterize watersheds' sensitivity to drought conditions based on the capacity to develop a sustained summer baseflow, developing a conceptual framework for understanding and improving predictions for drought flow. The rationale underlying the proposed research is that, once representative hydrologic responses to drought can be modeled, streamflow sensitivity to drought can be predicted and water resources can be managed efficiently. The objective of this work is to increase accessibility of recession analysis by using water height measurements, create a standard procedure for interpretation of recession analysis parameters, and to develop a 3D model shallow groundwater drainage to better model path lengths and residence times.

Chapter 2 provides a methodology for recession analysis using water height instead of discharge. By using water height directly, there is not a need for in-stream discharge measurements to create a rating curve. And because rating curves are field intensive and expensive to obtain, using water height greatly reduces the time and money required to perform recession analysis and thus expands the number of watersheds that can be monitored. While values of b are not conserved when using water height for recession analysis compared to discharge, we find that the variability in values of b within and between events is captured in recession analysis using both water height and discharge. This methodology is validated using two USGS watersheds and a batch analysis of 37 Swiss watersheds. With the advent of low-cost reliable pressure loggers, as well as satellites that provide global reporting of river stage, recession analysis using water height expands the number of river systems where recession analysis can be conducted and provides the potential for insights into the variability of watershed drainage characteristics without the need for a discharge record. This chapter introduced a new methodology to increase the number of small

watersheds that can be characterized, matching the scale of many questions about the critical zone and small scale watershed processes.

Chapter 3 evaluates the interpretation methods of recession analysis parameters through the lens of climate variables controlling the hydrograph. Recent studies have highlighted major differences in the estimation of the recession parameters depending on the method, casting doubt on our ability to properly evaluate and compare hydrological properties across watersheds based on $-dQ/dt$ vs. Q recession analysis. This chapter shows that estimation based on collective recessions as an average watershed response is strongly affected by the distributions of event inter-arrival time, magnitudes, and antecedent conditions, implying that the resulting recession parameters do not represent watershed properties as much as they represent the climate. The chapter emphasizes that proper evaluation of watershed properties is only ensured by considering independently individual recession events. While average properties can be assessed by considering the average (or median) values of a and b, their variabilities provide critical insight into the sensitivity of a watershed to the initial conditions involved prior to each recharge event. This chapter deconstructs how individual recessions are organized into the point cloud, concluding that using individual recessions is an methodological approach to increase the amount of information about watershed responses.

Chapter 4 looks at how water flows within a shallow hillslope aquifer. Traditionally, hillslopes are modeled in 2D where water drains perpendicularly to the stream, where the aquifer width is constant in space which assumes the stream slope is negligible. However, for many watersheds the stream does have a measurable slope making the effective aquifer 3D. For these 3D watersheds, the stream angle will contribute to the angle and path of water draining from the aquifer. This chapter presents preliminary analysis exploring the theoretical framework of hillslope drainage resulting in the fundamental changes the driving gradient for flow. The driving gradient is determined by the ratio of the stream angle to the hillslope angle, thus the driving gradient controlled by the downslope direction for very large hillslope angles compared to the driving gradient of downstream for comparatively large stream angles. While the

geometry of the watershed does not change, the effective hillslope angle decreases as the aquifer drains, thus transitioning from a driving gradient primarily down hillslope to down streamslope that corresponds to streamlines rotating from stream perpendicular to stream parallel. This results in the path of steepest descent that the water will drain, shifting the actual flow lines from being primarily perpendicular to the stream rotating until they are stream parallel, resulting in a longer the path length and residence time of hillslope drainage. Water managers need accurate streamflow predictions to effectively manage water resources within a basin, but this can't be met if models are not capturing the temporal evolution of hillslope drainage and streamflow during drought. This chapter looks at aquifer geometry and drainage patterns as a reason for an incomplete conceptual model and explores the conceivable impact of topographic expression on recession analysis.

Chapter 5 synthesizes the findings from Chapters 2-4 and provides suggestions on paths forward to strengthen characterization watershed responses to drought.

Chapter 2. Streamflow Recession Analysis using Water Height

Elizabeth R. Jachens[1], Clément Roques[2], David E. Rupp[3], John S. Selker[1]

[1]Department of Biological and Ecological Engineering, Oregon State University, USA.

[2]Department of Earth Sciences, ETH Zürich, Switzerland.

[3]Oregon Climate Change Research Institute, College of Earth, Oceanic and Atmospheric Sciences, Oregon State University, USA.

For Submission to:

Water Resources Research

Status: In review

2.1 Abstract

Recession analysis is a well-accepted technique for characterizing aquifer and basin properties based on the falling limb of the hydrograph. However, recession analysis using streamflow discharge requires a relationship (the rating curve) between simultaneous measurements of water height, h, and discharge, Q, across a wide range of flows which is expensive to obtain. We leverage the relationship between h and Q (typical power law) to perform recession analysis using h directly, thus permitting identification of transient flow regimes where only h is available. Recession analysis evaluates the rate of change in discharge, $-dQ/dt$, as a function of discharge, Q, in a bi-logarithmic plot where the slope, b, contains information about aquifer characteristics. While values of b are not conserved when replacing Q with h, we find that the variability in values of b within and between events is captured in recession analysis for both Q and h. For example, when considering individual recessions, a change from a larger b at high discharge to a smaller b at lower discharge may indicate the transition from early to late-time behaviors as predicted by theory for idealized aquifers and would be present using both Q and h. With the advent of low-cost reliable pressure loggers, as well as satellites that provide global reporting of river stage, recession analysis using water height expands the number of river systems where recession analysis can be conducted and provides the potential for insights into the variability of watershed drainage characteristics without the need for a discharge record.

2.2 Introduction

The understanding of streamflow dynamics is fundamental for water resources management, flood prediction, sediment transport, and drought assessment. The establishment of accurate hydrographs is critical but is expensive to obtain. Though measuring continuous water height has become easy using automatic pressure transducers, estimating discharge requires a local rating curve constructed from field-collected discharges measurements paired with concurrent water height measurements over the range of flows of interest, typically covering peak to baseflow discharges. These extreme discharges are cause for uncertainties in a rating curve due to their low frequency of occurrence, safety concerns at high discharges, and instrument precision

impeding the collection of reliable estimates at low discharges (Kiang *et al.*, 2018). Extrapolation of a rating curve to include extreme events compromises the validity of the hydrograph (Lang *et al.*, 2010). Additionally, a rating curve is no longer valid if the stream undergoes any major channel changes at the monitoring location, a common consequence of exceptionally high flows.

After streamflow is no longer dominated by overland flow, the falling limb of a hydrograph is an expression of the processes controlling groundwater discharge to a stream. Recession analysis (RA) is a means of using characteristics of this receding limb to quantify hydraulic properties of the connected aquifer system. Traditional recession analysis frequently uses the Boussinesq equation to describe drainage from a 1-dimensional aquifer (Brutsaert and Nieber, 1977; Troch *et al.*, 2013). In the absence of recharge or evapotranspiration, the falling limb of the hydrograph can be described by an analytical solution that takes the form of a power law in Equation (1).

$$-\frac{dQ}{dt} = a \cdot Q^b \tag{1}$$

where Q is a stream discharge [m^3/s] and a is a constant that contain information about watershed characteristics including geometry, storativity, and hydraulic conductivity and b is another constant for which theories predict values ranging from 1-3. Parameters a and b are estimated by carefully fitting Equation (1) on single or a collection/cloud of recessions on bi-logarithmic space, where $\log(a)$ is the intercept and b is the slope (Brutsaert and Nieber, 1977; Roques *et al.*, 2017; Rupp and Selker, 2006a)

Analytical solutions to the Boussinesq equation of an idealized, initially fully saturated, and unconfined draining horizontal aquifer predict values of $b=3$ for early-time and $b=1.5$ for late-time recession (Brutsaert and Nieber, 1977). Early-time recession occurs immediately after a recharge event when the drainage rate is mostly controlled by the near-stream boundary condition. Late-time recession is characterized by a slower drainage rate that is principally controlled by the boundary provided by the aquifer's groundwater divide or other remote no-flow boundary condition. Theory suggests that a transition from early to late-time can be identified in an RA plot by a break in slope from 3 to 1.5. In order to account for the uncertainty in the transition

from early to late-time aquifer draining behavior, this analysis will consider transient flow regimes from high-flow to low-flow instead of early to late-time behavior.

Traditionally, recession analysis has been performed on data from many recession events together and undifferentiated on a single plot (the "point cloud") with the assumption that the ensemble of recessions stacked on the $-dQ/dt$ vs Q plot reflects an underlying average/bulk behavior of a watershed. More recently, studies have considered individual recession events and the variability in watershed response as an alternative to the point cloud to estimate recession parameters, a and b (Biswal and Marani, 2010; Dralle *et al.*, 2015; Jachens *et al.*, 2019; Shaw and Riha, 2012; Tashie *et al.*, 2019; Thomas *et al.*, 2015). Individual recessions have been found to have larger b values than those obtained by the point cloud with some research relating the variability of individual recessions to season of year (Bart and Hope, 2014; McMillan *et al.*, 2011; Tashie *et al.*, 2019). Additionally, *Jachens et al.* [2019] suggest that the point cloud results from the convolution of successive recessions with different inter-arrival time which has led to misinterpretation in the estimation of average watershed behavior and properties. As a result, this paper will only consider individual recessions for determining recession analysis parameters, a and b.

We define the ratio of b (the "slope ratio") measured at high and low flows, $R_b = b_h/b_l$, to describe the magnitude of change in flow regime occurring during a recession. According to the Boussinesq theory reviewed above, b transitions from 3 and 1.5 such that R_b takes on a value of 2. In a more general case, $R_b > 1$ (i.e., b is greater at high flows than at low flows) indicates that streamflow is more stable, or sustaining, at high flows. In contrast, $R_b < 1$ (i.e., b is smaller at high flows than at low flows) indicates a more stable streamflow decline rate a low flows than at high flows. Cases where the high flows exhibit a smaller slope than low flows (resulting in a slope ratio less than 1) have been observed (Clark *et al.*, 2009; Mutzner *et al.*, 2013; Rupp and Selker, 2006a).

A change in the upslope boundary condition is not the only hypothesis to explain observed variability in R_b. Various hypotheses have been proposed including stream network morphological effects, drainage density, and aquifer

compartmentalization (Biswal and Marani, 2010; Sánchez-Murillo *et al.*, 2015; Shaw and Riha, 2012; Stoelzle *et al.*, 2013). The slope ratio is a useful proxy to easily identify if a transition in streamflow regimes controlled by hydraulic or geometrical factors exists.

Classical characterization of streamflow recession can be described as a linear relationship between $-dQ/dt$ vs. Q in log-log space plot with the intercept defined as $\log(a)$ and the slope defined by b. However, because of the complexity of natural watersheds, RA performed on streamflow data reveals strong variability in a and b values beyond the simple linear representation for high and low flows [*e.g.*, *Biswal & Marani*, 2014; *D. Dralle et al.*, 2015; *McMillan et al.*, 2011; *Mutzner et al.*, 2013; *Ploum et al.*, 2019; *Shaw & Riha*, 2012; *Tashie et al.*, 2019; *Wang*, 2011]. The variability in recession parameters can reveal information about the complexities in watershed response, often evident from visual examination of the general organization of the individual $-dQ/dt$ vs Q data points representing the range of behaviors. The general organization of the RA plot includes any breaks in slope as well as other trends that can be identified in individual or collective/cloud of recession events is a graphical manifestation of what we refer to hereafter as the "structural decay of flow." The structural decay of flow captures the physical organization of the rate of change of discharge as a function of discharge represented in the RA plot, including a and b of the collective/cloud and individual recessions.

This paper aims at demonstrating the reliability of performing RA on measured water height directly (hereafter referred to as WHRA) in order to estimate R_b and describe the structural decay of streamflow recession without introducing bias through the definition and uncertainty of a rating curve. Although this methodology does not allow quantification of the hydrodynamic properties of the aquifer, which frankly is in question in the case of RA itself, it is shown to shed light on the main transient streamflow characteristics and the over-arching trends of drought flow. We first present the mathematical framework to compare RA and WHRA. We then test the methodology on two real-data watersheds, one with $R_b > 1$ and one with $R_b < 1$. Finally, we test the universality of this methodology on a batch of 54 Swiss watersheds.

2.3 Methods

Here we describe a method for analyzing recession hydrographs using water height instead of discharge rate, leveraging the power law rating curve equation. Rating curves employ a variety of mathematical forms including power law, linear, parabolic, exponential, or a compound segment fit (Kennedy, 1984; Lovellford, 2013).

The power law equation for rating curves Equation (2) is standard (Clarke, 1999; Degagnea *et al.*, 1996; Reitan and Petersen-Øverleir, 2004) and is consistent with the form of discharge resistance equations such as Manning's and Chezy's (Herschy, 1993; Kennedy, 1984):

$$Q = c \cdot h^m \tag{2}$$

where h is water height [m], and c and m are constants. The transformation of Equation (1) for WHRA plots substitutes the right-hand side of Equation (2) for discharge, resulting in an expression that is a function of water height in Equation (3).

$$\frac{-dQ}{dt} = \frac{-d}{dt}(c \cdot h^m) \tag{3}$$

$$\frac{-dQ}{dt} = c \cdot m \cdot h^{m-1} \cdot \frac{-dh}{dt} \tag{4}$$

Thus $-dQ/dt$ vs. Q can be expressed in terms of h for the WHRA axes using Equation (2) and Equation (4) using Equation (5):

$$\left[c \cdot m \cdot h^{m-1} \cdot \frac{-dh}{dt}\right] vs. [\, c \cdot h^m] \tag{5}$$

The fitting coefficient c appears on both axes in Equation (5) and thus the mathematical simplification holds true for bi-logarithmic space, shown in Equation (6).

$$\left[m \cdot h^{m-1} \cdot \frac{-dh}{dt}\right] vs. [h^m] \tag{6}$$

Without a rating curve providing the parameter m, Equation (6) can be simplified to Equation (7) by letting $m = 1$.

$$\ln\left[\frac{-dh}{dt}\right] vs. \ln[h] \tag{7}$$

The simplification from Equation (6) to Equation (7) is not mathematically equivalent and thus the scale is not preserved. However, the assumption of m=1 is necessary because otherwise m is an unknown from the rating curve. Values of m in the literature for power-law rating curves tend to be close to 2, which is consistent with our findings and allows for our assumption of m=1 (Fenton and Keller, 2001; Reitan and Petersen-Øverleir, 2004, 2008). The slope of the WHRA plot can be related to the slope of the RA plot by substituting Equation (2) and (4) into the slope calculation as shown in Equation (8) and simplified in Equation (9).

$$\begin{aligned} b_{RA} &= \frac{\ln\left(\frac{-dQ_2}{dt}\right) - \ln\left(\frac{-dQ_1}{dt}\right)}{\ln(Q_2) - \ln(Q_1)} \\ &= \frac{\ln\left(c \cdot m \cdot {h_2}^{m-1} \cdot \frac{-dh_2}{dt}\right) - \ln\left(c \cdot m \cdot {h_1}^{m-1} \cdot \frac{-dh_1}{dt}\right)}{\ln(c \cdot {h_2}^{m}) - \ln(c \cdot {h_1}^{m})} \end{aligned} \tag{8}$$

$$b_{RA} = \frac{m - 1 + b_{WHRA}}{m} \tag{9}$$

where b_{RA} is b estimated with RA plot $\ln\left[\frac{-dQ}{dt}\right] vs. \ln[Q]$ and b_{WHRA} is b estimated from WHRA plot $\ln\left[\frac{-dh}{dt}\right] vs \ln[h]$ from Equation (7). For a rating curve taking the form of a power law (Equation (2)), the ratio of b values during high and low flows, R_b, is expressed in Equation (10).

$$R_b = \frac{b_{(RA,h)}}{b_{(RA,l)}} = \frac{m - 1 + b_{WHRA,h}}{m - 1 + b_{WHRA,l}} \tag{10}$$

where the subscripts h and l indicate the slope during the high-flow and low-flow recession, respectively. As proof of concept, we tested the methodology by analyzing in detail data from two watersheds from the USGS database for which both water height and discharge measurements were available for at least 10 years: West Conewago

Creek near Manchester, PA (USGS Station# 01574000) and the South Fork of the McKenzie River, OR (USGS Station# 14159200). We then performed similar analysis on a batch of streamflow time series in order to evaluate the validity of WHRA across different watershed characteristics. For this purpose, we selected 37 watersheds across Switzerland where 40 years of both water height and stream discharge data were available. For the dataset, discharge data is given in m^3/s and water height is given in meters above mean sea level as daily averages. Without additional information about a published datum or rating curve equations for each watershed, we set to optimize a datum and rating curve for each watershed. We assumed a power law rating curve equation for each watershed and optimized the datum so that the resulting rating curve minimized the root mean square error for water height vs. discharge in log-log space. The optimized datum was subtracted from that watershed's water height data to represent the effective water depth that was used for the final rating curve for the watershed. The watersheds all have rating curve root mean square logarithmic error (RMSLE) above 0.25 [-] which indicates a rating curve without multiple segments that hasn't changed significantly over time making them suitable to compare WHRA with RA. WHRA performed given only water height was compared with the RA using discharge data from the same time period.

When performing recession analysis, it is essential to take a special care in the computation of the time derivative at low flow. Here the exponential time step method was used (Roques *et al.*, 2017). Additionally, mean daily data (discharge or water height) was calculated from 15-minute data to further reduce noise. The beginning of the recession was defined as 1 day after the peak in discharge to exclude the potential influence of overland flows. Only recession events were included that had a minimum duration of 5 days and whose discharge monotonically decreased throughout the event. The end of the recession was defined to be the minimum discharge or height prior to an increase. The sensitivity of recession parameters to the precise hydrograph recession definition was found to be low, consistent with previous studies. For the slope of the individual recessions, individual estimates of a and b are based on direct linear fitting using least squares regression in bi-logarithms space and the median of all values are

used to describe the variation in watershed behavior. The individual recession slope is classified as either high or low-flow based on whether the peak flow is greater than or less than the median streamflow.

2.4 Results

2.4.1 Case Study: West Conewago Creek, PA

West Conewago Creek has published data for discharge and water height starting in October of 2007 at 15-minute increments. The USGS provisional rating curve for West Conewago Creek is best fit by a power law rating curve with c = 16.4 and m = 3.4 (R^2=0.96) using Equation (2) (USGS, 2018). A total of 244 recession events were identified.

The similarity of the pattern of points in RA and WHRA plots are evident in Figure 3. While the instantaneous slope of a recession event in the WHRA plot (Figure 3b) cannot be directly interpreted physically, the structural decay of flow is consistently represented in the WHRA and RA methods. For West Conewago Creek, the ratio of slopes calculated from the median of the individual recession slopes for traditional RA of 0.66 is comparable to the power law WRHA value of 0.60. Notably, this method produces a slope ratio, R_b, less than 1 indicating that the individual recessions at low flow show larger slopes that at high flows (Figure 3), contradictory to the observations from taking the slope ratio of the point cloud, consistent with previous studies (Roques *et al.*, 2017; Tashie *et al.*, 2019).

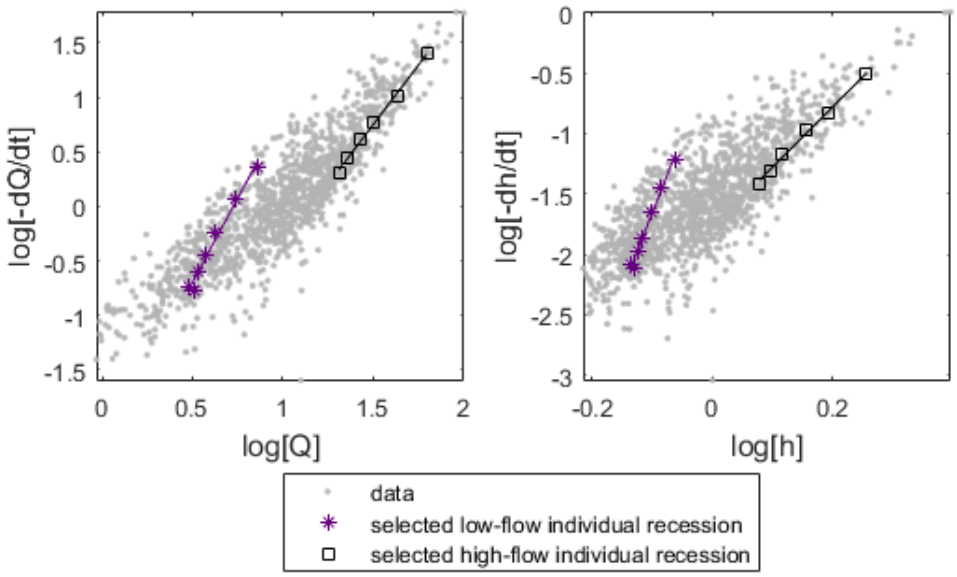

Figure 3**.** Example individual recessions for high-flow and low-flow for discharge recession analysis (a), and water height recession analysis (b), for West Conewago Creek at USGS station 01574000. Individual recessions at higher ranges of *Q* or *h* tend to have smaller slopes that those at lower ranges, resulting in a slope ratio < 1.

In addition to the structural decay of flow, the trends in WHRA are also preserved compared to RA. For each individual event, the values of *b* for WHRA and RA are positively correlated (Figure 4). Using the water height and discharge data directly, the rating curve with an m=3.4 is compared to the best fit line with a slope of 3.9 between *b* values for all 244 individual events for WHRA and RA. Some of the discrepancies between these two values are based on the use of a single rating curve *m* for the entire period of record when the data suggests some variation in the rating curve though time or a rating curve with a low R^2 for the power law fit. When *m* is assumed to be 1, RA is equal to WHRA *b* values (Figure 4- red asterisk). For other values of *m*, the scale of *b* is not preserved but the relationship between the individual recessions (Figure 4- green open triangles). Trends in *b* such as seasonality or initial discharge can be analyzed with WHRA as the relationship between values is preserved from RA. Regardless of the value of *m* assumed, WHRA maintains the relationship between individual recession *b* values and is a valid substitute for the slope ratio of RA because the fundamental structural decay of flow is preserved.

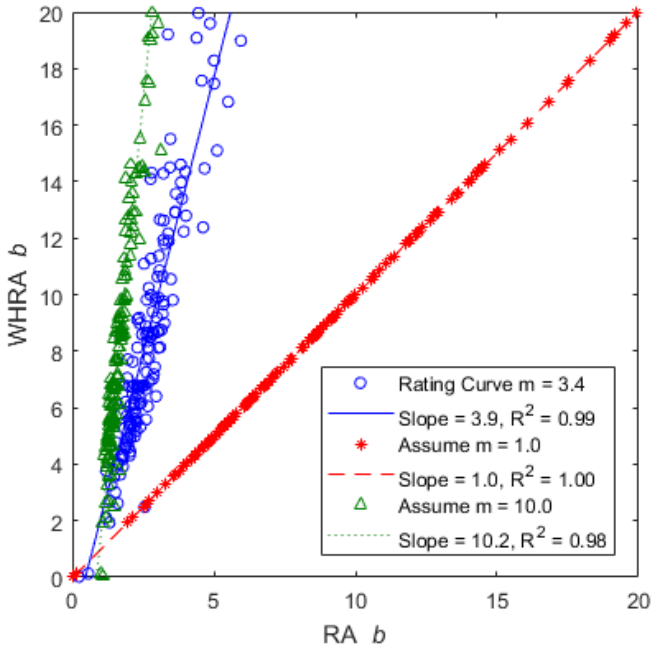

Figure 4. Comparison of individual event *b* values for RA and WHRA for all events identified for West Conewago Creek at USGS station 01574000. The blue open circles show the data using a rating curve *m=3.4* from the rating curve and the best fit line between the RA and WHRA *b* with a slope of 4.5. For m=1 (red asterisk) and m=10 (green open triangles), the range of RA *b* values is different as the scale is not preserved but the relationship between individual recessions is preserved with an R^2 of 1 and 0.98 respectively.

2.4.2 Case Study: South Fork of McKenzie River, OR

The South Fork of the McKenzie River (USGS station 14159200) has 15-minute published discharge data beginning in October 2000, however, gage height records start in October 2007. The USGS provisional rating curve for the South Fork of the McKenzie River is best fit by a power law rating curve with c = 6.2 and m = 2.6 (R^2=0.99). Traditional RA was performed using the mean daily discharges while WHRA was performed using mean daily stage records. We analyzed 345 recession events from 1 October 2007 to 8 May 2018. Power-law (Figure 5b) water height recession plots show structural decay consistent with the RA plot (Figure 5a), evident by the distinct organization of data points in the lower envelope. Using the slope ratio of the median individual slopes, RA has a slope ratio of 0.21 compared to 0.19 for WHRA. The slope ratio less than 1 indicates a smaller slope for high flows and a greater

slope for low flows that can be identified in both traditional RA and WHRA using individual recessions (Figure 5). A larger slope at the low flow ranges indicates a more stable flow rate than compared to higher flow ranges. Regardless of the *m* value assumed, the trends for WHRA and RA are preserved (Figure 6).

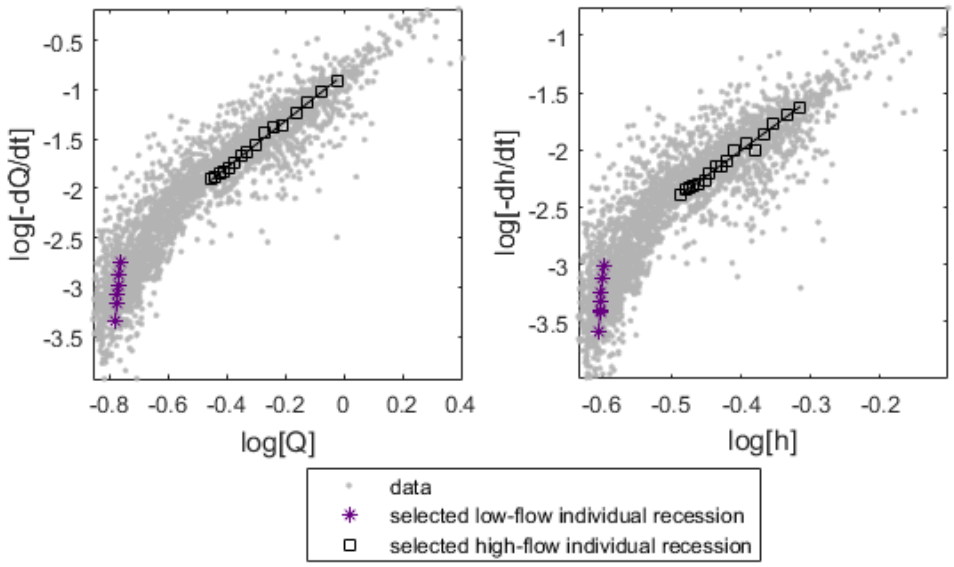

Figure 5. Same as Figure 3 but for the South Fork of the McKenzie River at USGS station 14159200.

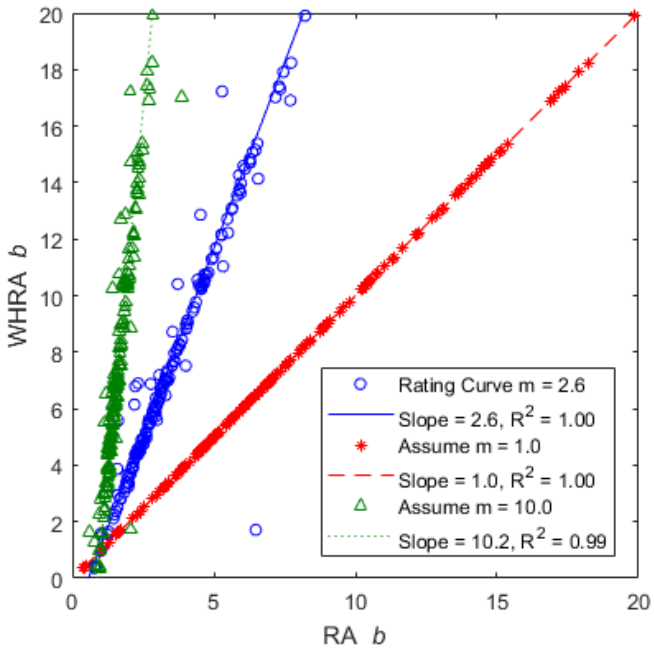

Figure 6. Comparison of individual event *b* values for RA and WHRA for all events identified for the South Fork of the McKenzie River at USGS station 14159200. The blue open circles show the data using a rating curve *m=2.6* from the rating curve and the best fit line between the RA and WHRA *b* with the same slope. For m=1 (red asterisk) and m=10 (green open triangles), the range of RA *b* values is different as the scale is not preserved but the relationship between individual recessions is preserved with an R^2 of 1 and 0.99 respectively.

2.4.3 Batch Analysis of Swiss Watersheds

The wide applicability of WHRA was tested on 37 relatively undisturbed watersheds across Switzerland that have river discharge and water level record ("FOEN," 2019). For the 37 watersheds, rating curve exponents ranged from *m*=1.54 - 6.11 with a median of 3.13 with and a median RMSLE of 0.09 [-]. Recession analysis is performed independently using the corrected water height data and the discharge. Overland flow and the minimum event duration are consistent from the previous examples at 1 and 5 days respectively. The results from WHRA and RA are compared using the ratio of high to low median individual slopes of WHRA to RA shown in Figure 7. WHRA does preserve the slope ratio when compared to RA, and thus correctly identifies the change in hydraulic regime without knowing the value of *m*. Only 2 watersheds are incorrectly characterized using WHRA compared to RA, both with a slope ratio for WHRA less than 1 and greater than 1 for RA. Of the 37 watersheds, 33 watersheds have a slope RA slope ratio less than 1 indicating that the change in hydraulic regime is contrary to the early to late-time transition to smaller slopes at low flows predicted by Boussinesq theory for an idealized aquifer and suggested by many point cloud analyses.

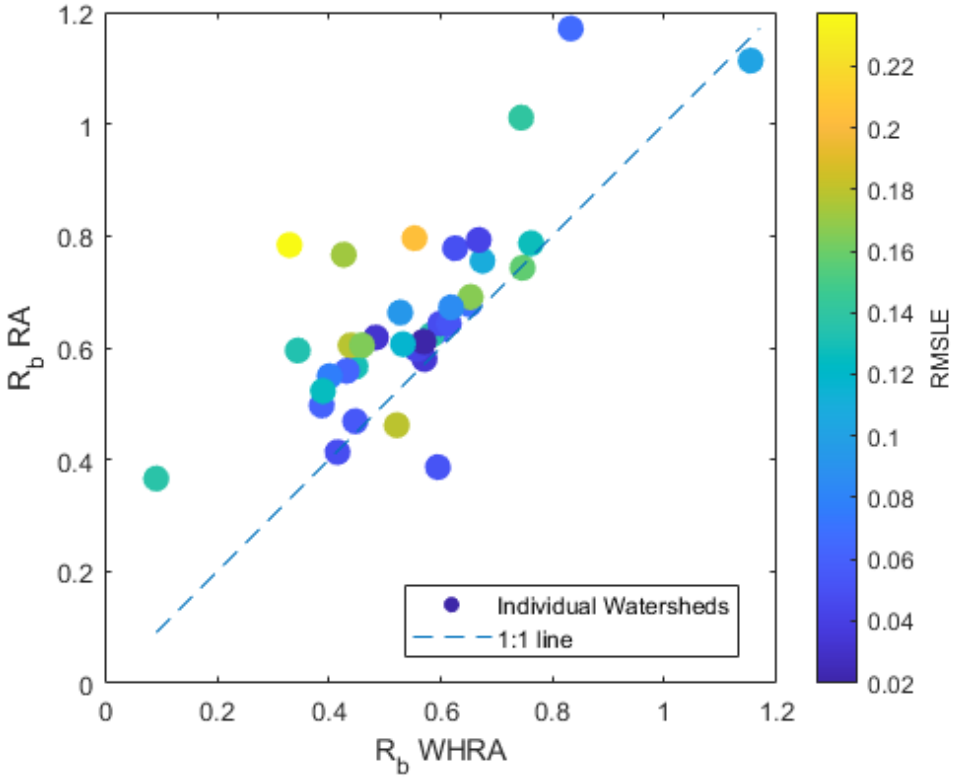

Figure 7**.** Ratio of high to low median individual slopes for WHRA and RA compared to the 1:1 line. The color of the symbol is based on the RMSLE of the power-law rating curve as fit in log-log space.

From Figure 7, *m* is unknown and assumed to be 1 when calculating the slope ratio using Equation (10). However, the slope ratio using *m=1* is consistent with the slope ratio from Equation (10) with the m value from the rating curve (Figure 8). The slope ratio is relatively insensitive to values of *m*, leading to the correct interpretation of WHRA even when *m* is unknown.

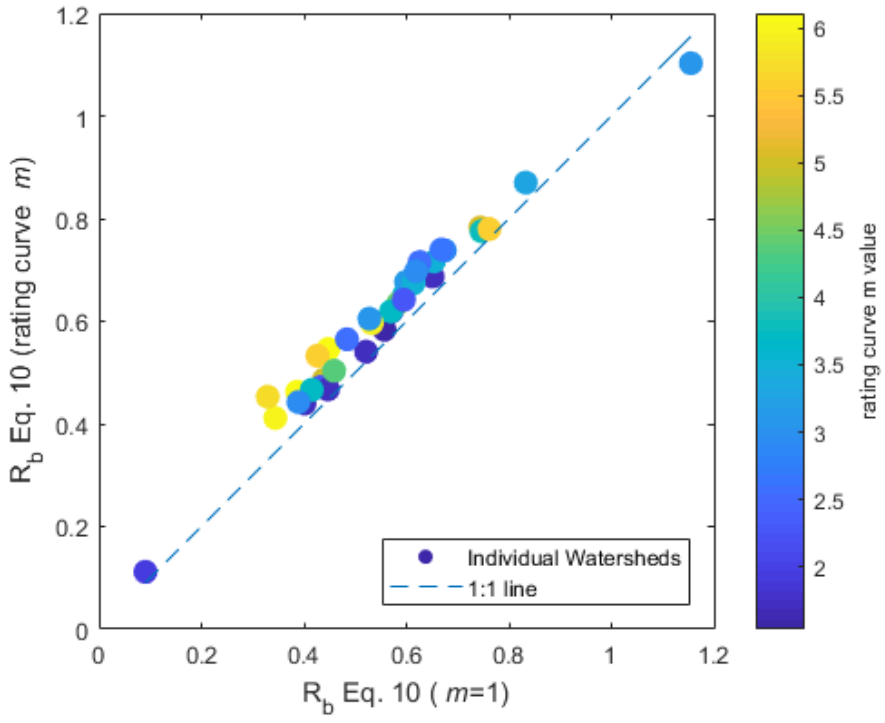

Figure 8**.** Comparison of the slope ratio for the assumed m=1 vs the m from the rating curve show that the slope ratio is relatively insensitive to the value of m chosen.

2.5 Conclusions

We demonstrate that water height recession analysis (WHRA) can provide insight into transient stream discharge regimes in basins where fieldwork required to create rating curves is difficult. While the magnitude of the actual values of the recession constant b obtained by WHRA is not preserved compared to RA, relative comparisons between individual recessions can indicate a change in the hydrologic regime between high and low flow. Based on the form of the rating curve, a transformed rating curve axes can be plotted on a bi-logarithmic scale using water height as $\ln\left[\frac{-dh}{dt}\right] vs. \ln[h]$ which preserves the structural decay of flow

For the power law rating curve, we have shown how the RA slope (b_{RA}) is a function of the m rating curve exponent. Values of m based on Manning's equation plus the assumption that the cross-sectional area is proportional to the water height suggests a value of 1.7 but could be 2.0 or larger for coarse-grained rivers [e.g., *Rupp & Smart*,

2007]. When doing WHRA, the value *m* is unknown and thus the exact value of b_{RA} is unknown (except when b_{WHRA} =1, in which case b_{RA} must also be 1 according to Equation (10). The ratio of slopes between the high-flow and low-flow segments of the recession curve can help to identify changes in stream hydraulic regimes during a recession which can be related between RA and WHRA using Equation 10. For the power law case, the slope ratio relationship is shown in Equation (11).

$$\frac{b_{WHRA,h}}{b_{WHRA,l}} = \frac{m(b_{RA,h} - 1) + 1}{m(b_{RAl} - 1) + 1} \tag{11}$$

where the subscripts *h* and *l* indicate the slope during the high to low flows, respectively. From Equation (11), if the RA slope ratio is 1 then the WHRA slope ratio is also 1. The slope ratio is valid when comparing WHRA for an unknown value of *m* to the slope ratio for RA. However, as the RA slope ratio or value of *m* diverge from a value of one, the WHRA ratio of slopes ($b_{WHRA,h}/b_{WHRA,l}$) diverges from the RA slope ratio. For example, if high-flow to low-flow corresponds with early ($b_{RA,h}$ = 3) to late ($b_{RA,l}$ = 1.5) -time behavior the ratio of slopes for is 2 for RA, the WHRA slope ratio is 2.3 or 2.5 for *m* = 1.7 or 2.0 respectively. For the two watersheds examined in this analysis, *m* = 2.4 and 2.6, which is above the range given by Rupp & Smart (2007) of 1.7 to 2.0 for *m*. However, a larger *m* has been correlated to a decrease in hydraulic depth (Smart *et al.*, 2002). Interestingly if *m* tends toward infinity, $b_{WHRA,h}/b_{WHRA,l}$ has an upper limit of 4 when $b_{RA,h}$ = 3 and $b_{RA,2}$ = 1.5. For the same RA slope ratio, greater differences between $b_{RA,h}$ and $b_{RA,l}$ will result in WHRA slope ratios approaching the RA slope ratio as *m* becomes large. For the small range of slopes from 1 to 3 and values of *m* based on Manning's equation, the ratio of slopes from WHRA suggests similar trends to the ratio of slope from RA plots.

Regardless of the rating curve equation, WHRA generally reproduces the structural decay of flow and the slope ratio present in RA. The structural decay of flow and the ratio of slopes present in WHRA can indicate a transition from high to low-flows where the slope of the WHRA plot decreases at lower discharges just as in the RA plot, but the methodology can also identify a break in slope that increases for low discharge. A change in slope is important because it reveals the fundamental flow

behavior, signifying a possible boundary-condition driven transition from high to low-flows if the slope ratio is greater than 1, or describing a decreased rate of discharge decline for lower flows expressed with a slope ratio less than 1. With a slope ratio less than 1, the sudden increase in slope at low discharge is not consistent with the traditional theory of a constant slope for late-time and has been identified but not adequately addressed in the literature (Clark *et al.*, 2009; Mutzner *et al.*, 2013). Understanding how aquifers drive streamflow during low discharge events is important for streamflow estimation and water management during a hydrologic drought. Preliminary analysis using WHRA can be interpreted based on the ratio of the slopes where a break occurs between late-time behaviors or at low discharges. Water height recession analysis (WHRA) can provide insight into relative watershed characteristics at different flow regimes in basins where dedicated fieldwork for discharge measurements to create rating curves is not feasible.

Acknowledgments, Samples, and Data

The datasets used in this paper are freely available from the USGS website for the watersheds in the US and at http://www.hydroshare.org/resource/58801283d02c4dbcac876bfa86749082 for the watersheds from the Federal Office for the Environment (FOEN), Bern, Switzerland. Respective codes can be obtained from the corresponding author. The authors declare that they have no conflict of interest.

References

Bart, R., & Hope, A. (2014). Inter-seasonal variability in baseflow recession rates: The role of aquifer antecedent storage in central California watersheds. Journal of Hydrology, 519(PA), 205–213. https://doi.org/10.1016/j.jhydrol.2014.07.020

Biswal, B., & Marani, M. (2010). Geomorphological origin of recession curves. Geophysical Research Letters, 37(24), 1–5. https://doi.org/10.1029/2010GL045415

Biswal, B., & Marani, M. (2014). "Universal" recession curves and their geomorphological interpretation. Advances in Water Resources, 65, 34–42. https://doi.org/10.1016/j.advwatres.2014.01.004

Brutsaert, W., & Nieber, J. L. (1977). Regionalized drought flow hydrographs from a mature glaciated plateau. Water Resources Research, 13(3), 637–643. https://doi.org/10.1029/WR013i003p00637

Clark, M. P., Rupp, D. E., Woods, R. A., Tromp-van Meerveld, H. J., Peters, N. E., & Freer, J. E. (2009). Consistency between hydrological models and field observations: Linking processes at the hillslope scale to hydrological responses at the watershed scale. Hydrological Processes. https://doi.org/10.1002/hyp.7154

Clarke, R. T. (1999). Technical Note: Uncertainty in the estimation of mean annual flood due to rating-curve indefinition, 222, 185–190.

Degagnea, M. P. J., Douglas, G. G., Hudson, H. R., & Simonovic, S. P. (1996). A decision support system for the analysis and use of stage-discharge rating curves. Journal of Hydrology, 184, 225–241.

Dralle, D., Karst, N., & Thompson, S. E. (2015). A, b careful: The challenge of scale invariance for comparative analyses in power law models of the streamflow recession. Geophysical Research Letters, 42(21). https://doi.org/10.1002/2015GL066007

Fenton, J. D., & Keller, R. J. (2001). The Calculation of Streamflow from Measurements of Stage. Cooperative research centre for catchment hydrology, (Report 01/6), 84. Retrieved from http://www.catchment.crc.org.au/pdfs/technical200106.pdf

Federal Office for the Environment (FOEN) (2019). Retrieved from https://www.hydrodaten.admin.ch/en/current-situation-table-discharge-and-water-levels.html

Herschy, R. (1993). The stage-discharge relation. Flow Measurement and Instrumentation, 4(1), 10–15. Retrieved from https://doi.org/10.1016/0955-5986(93)90005-4

Jachens, E. R., Rupp, D. E., Roques, C., & Selker, J. S. (2019). Recession analysis 42 years later - work yet to be done (in review). Hydrology and Earth System Sciences Discussions, 1–16. https://doi.org/10.5194/hess-2019-205

Kennedy, E. J. (1984). Discharge Ratings at Gaging Stations: Techniques of water-resource investigations of the United States Geological Survey. https://doi.org/10.1016/0022-1694(70)90079-X

Kiang, J. E., Gazoorian, C., McMillan, H., Coxon, G., Le Coz, J., Westerberg, I. K., et al. (2018). A Comparison of Methods for Streamflow Uncertainty Estimation. Water Resources Research, 54(10), 7149–7176. https://doi.org/10.1029/2018WR022708

Lang, M., Pobanz, K., Renard, B., Renouf, E., & Sauquet, E. (2010). Hydrological Sciences Journal Extrapolation of rating curves by hydraulic modelling, with application to flood frequency analysis Extrapolation of rating curves by hydraulic modelling, with application to flood frequency analysis. https://doi.org/10.1080/02626667.2010.504186

Lovellford, R. (2013). Variation in the Timing of Coho Salmon (Oncorhynchus kisutch) Migration and Spawning Relative to River Discharge and Temperature. Master of Science Thesis in Water Resources Science at Oregon State University.

McMillan, H. K., Clark, M. P., Bowden, W. B., Duncan, M., & Woods, R. A. (2011). Hydrological field data from a modeller's perspective: Part 1. Diagnostic tests for model structure. Hydrological Processes, 25(4), 511–522. https://doi.org/10.1002/hyp.7841

Mutzner, R., Bertuzzo, E., Tarolli, P., Weijs, S. V., Nicotina, L., Ceola, S., et al. (2013). Geomorphic signatures on Brutsaert base flow recession analysis. Water Resources Research, 49(9), 5462–5472. https://doi.org/10.1002/wrcr.20417

Ploum, S. W., Lyon, S. W., Teuling, A. J., Laudon, H., & van der Velde, Y. (2019). Soil frost effects on streamflow recessions in a sub-arctic catchment. Hydrological Processes. https://doi.org/10.1002/hyp.13401

Reitan, T., & Petersen-Øverleir, A. (2004). Estimating the discharge rating curve by nonlinear regression - The frequentist approach, (2). Retrieved from http://www.nve.no/Global/Publikasjoner/Publikasjoner%5Cn2004/Report%5Cn2004/Trykkefil%5Cnreport%5Cn6-04.pdf

Reitan, T., & Petersen-Øverleir, A. (2008). Bayesian power-law regression with a location parameter, with applications for construction of discharge rating curves. Stochastic Environmental Research and Risk Assessment, 22(3), 351–365. https://doi.org/10.1007/s00477-007-0119-0

Roques, C., Rupp, D. E., & Selker, J. S. (2017). Improved streamflow recession parameter estimation with attention to calculation of − dQ/dt. Advances in Water Resources, 108, 29–43. https://doi.org/10.1016/j.advwatres.2017.07.013

Rupp, D. E., & Selker, J. S. (2006). Information, artifacts, and noise in dQ/dt - Q recession analysis. Advances in Water Resources, 29(2), 154–160. https://doi.org/10.1016/j.advwatres.2005.03.019

Rupp, D. E., & Smart, G. M. (2007). Comment on "Flow resistance equations without explicit estimation of the resistance coefficient for coarse-grained rivers" by Raul Lopez, Javier Barragan, and M. Angels Colomer. Journal of Hydrology, 346(3–4), 174–178. https://doi.org/10.1016/j.jhydrol.2007.08.024

Sánchez-Murillo, R., Brooks, E. S., Elliot, W. J., Gazel, E., & Boll, J. (2015). Baseflow recession analysis in the inland Pacific Northwest of the United States. Hydrogeology Journal, 23(2), 287–303. https://doi.org/10.1007/s10040-014-1191-4

Shaw, S. B., & Riha, S. J. (2012). Examining individual recession events instead of a data cloud: Using a modified interpretation of dQ/dt-Q streamflow recession in glaciated watersheds to better inform models of low flow. Journal of Hydrology, 434–435, 46–54. https://doi.org/10.1016/j.jhydrol.2012.02.034

Smart, G. M., Duncan, M. J., & Walsh, J. M. (2002). Relatively Rough Flow Resistance Equations. Journal of Hydraulic Engineering, 128(6), 568–578. https://doi.org/10.1061/(asce)0733-9429(2002)128:6(568)

Stoelzle, M., Stahl, K., & Weiler, M. (2013). Are streamflow recession characteristics really characteristic? Hydrology and Earth System Sciences, 17(2). https://doi.org/10.5194/hess-17-817-2013

Tashie, A., Scaife, C. I., & Band, L. E. (2019). Transpiration and Subsurface Controls of Streamflow Recession Characteristics. Hydrological Processes, 0–2. https://doi.org/10.1002/hyp.13530

Thomas, B. F., Vogel, R. M., & Famiglietti, J. S. (2015). Objective hydrograph baseflow recession analysis. Journal of Hydrology, 525. https://doi.org/10.1016/j.jhydrol.2015.03.028

Troch, P. A., Berne, A., Bogaart, P., Harman, C., Hilberts, A. G. J., Lyon, S. W., et al.

(2013). The importance of hydraulic groundwater theory in catchment hydrology: The legacy of Wilfried Brutsaert and Jean-Yves Parlange. Water Resources Research, 49(9), 5099–5116. https://doi.org/10.1002/wrcr.20407

USGS. (2018). WaterWatch: Customized Rating Curve Builder. Retrieved September 10, 2018, from https://waterwatch.usgs.gov/?id=mkrc

Wang, D. (2011). On the base flow recession at the Panola Mountain Research Watershed, Georgia, United States. Water Resources Research, 47(3), 1–10. https://doi.org/10.1029/2010WR009910

Chapter 3. Recession Analysis Revisited: Impacts of Climate on Parameter Estimation

Elizabeth R. Jachens[1], David E. Rupp[2], Clément Roques[3], John S. Selker[1]

[1]Department of Biological and Ecological Engineering, Oregon State University, USA.

[2]Oregon Climate Change Research Institute, College of Earth, Oceanic and Atmospheric Sciences, Oregon State University, USA.

[3]Department of Earth Sciences, ETH Zürich, Switzerland.

For Submission to:

Hydrology and Earth System Science (HESS)

Status: Accepted

3.1 Abstract

Recession analysis is a classical method in hydrology to assess watersheds' hydrological properties by means of the receding limb of a hydrograph, frequently expressed as the rate of change in discharge (-*dQ/dt*) against discharge (*Q*). This relationship is often assumed to take the form of a power law $-dQ/dt=aQ^b$, where *a* and *b* are recession parameters. Recent studies have highlighted major differences in the estimation of the recession parameters depending on the method, casting doubt on our ability to properly evaluate and compare hydrological properties across watersheds based on recession analysis of -*dQ/dt* vs. *Q*. This study shows that estimation based on collective recessions as an average watershed response is strongly affected by the distributions of event inter-arrival time, magnitudes, and antecedent conditions, implying that the resulting recession parameters do not represent watershed properties as much as they represent the climate. The main outcome from this work highlights that proper evaluation of watershed properties is only ensured by considering independent individual recession events. While average properties can be assessed by considering the average (or median) values of *a* and *b*, their variabilities provide critical insight into the sensitivity of a watershed to the initial conditions involved prior to each recharge event.

3.2 Introduction

Accurate representations of watershed-scale hydrological processes are urgent in a global- and anthropogenic-change perspective. Streamflow recession analysis has been routinely used for about half a century to assess watershed properties (Brutsaert and Nieber, 1977; Kirchner, 2009; McMillan et al., 2014) and more recently their vulnerability to climatic and anthropogenic factors (Berghuijs et al., 2016; Brooks et al., 2015; Buttle, 2018; Fan et al., 2019). Recession analysis is commonly done by plotting the time rate of change in discharge -*dQ/dt* vs. discharge *Q* with bi-logarithmic axes. Theory for an idealized single aquifer predicts a power law relationship with parameters *a* and *b* (Brutsaert and Nieber, 1977; Rupp and Selker, 2005) is shown in Equation (12).

$$-dQ/dt = aQ^b \quad (12)$$

However, it has long been recognized that the accuracy in the estimation of those parameters is highly sensitive to the methods used (Chen et al., 2018; Dralle et al., 2017; Roques et al., 2017; Rupp and Selker, 2006a; Santos et al., 2019; Stoelzle et al., 2013).

Two categories of parameter estimation methods are based on: 1) the aggregation of all observations in the space of *-dQ/dt* vs. *Q*, hereafter referred to as the "point cloud", to describe the average watershed behavior and 2) the identification of individual recession events in the space of *-dQ/dt* vs. *Q* to look at the variability of a watershed's response. There is a long history of recession analysis parameter estimation using the point cloud beginning with Brutsaert and Nieber (1977), and it remains common (Buttle, 2018; Liu et al., 2016; Meriö et al., 2019; Ploum et al., 2019; Sánchez-Murillo et al., 2015; Stewart, 2015; Vannier et al., 2014; Yeh and Huang, 2019). In recent literature there has been a shift toward using individual recessions to estimate recession parameters (Basso et al., 2015; Karlsen et al., 2019; Roques et al., 2017), and Santos et al. (2019) go as far as to question the validity of point cloud estimation methods.

When Brutseart and Nieber (1977) first proposed their recession analysis method, aquifer recession behavior was identified by fitting a lower envelope to the point cloud, thus assuming small values of *-dQ/dt* for a given *Q* represent aquifer discharge flow, and anything larger has contributions from faster pathways such as overland flow. This lower-envelope (LE) method of estimating recession analysis parameters was shown to be highly subject to artifacts arising from measurement noise and recording precision (Rupp and Selker, 2006a; Troch et al., 1993), and improvements to fitting a lower envelope have been proposed (Stoelzle et al., 2013; Thomas et al., 2015). An alternative fitting method wherein *b* was estimated as the best linear fit to the point cloud was introduced by Vogel and Kroll (1992) as the central tendency (CT). The central tendency method was adapted by Kirchner (2009) to address the undue weight of highly uncertain extreme points. Kirchner (2009) also suggested fitting a polynomial function to averages within bins of the cloud data. All

of these point cloud fitting approaches fundamentally treat each computation of $-dQ/dt$ and Q as reflecting a single average underlying curve, with deviations from a single curve effectively treated as noise. In other studies, data have been subset by season or month (e.g., Szilagyi et al., 2007; Thomas et al., 2015) to examine seasonal variations in the recession characteristics with the subsets still treated to point cloud analyses.

In contrast, the variability in watershed response to individual recharge events can be depicted by fitting recession parameters to individual recession events. Several authors have observed that individual recessions had greater b values than the point cloud did (Biswal and Marani, 2010; Mcmillan et al., 2011; 2014; Mutzner et al., 2013; Shaw and Riha, 2012); a larger value of b indicates a time rate of decline that decreases more quickly with decreasing streamflow. Consistent with these studies, we have also observed individual recessions that have a larger b values than the point cloud fit across watersheds in the Oregon Cascades. As an example, we present in Fig. 1 recessions for Lookout Creek, Oregon, USA, using daily discharge data (m^3/s) from 1949 to 2016 (USGS station no. 14161500; United States Geological Survey) (Johnson and Rothacher, 2019; USGS, 2019). In the 66 years of data presented, a total of 1309 recession events are identified with an average of 19 events per year. It is clear that values of b for individual recession events tend to be larger than b for the point cloud, particularly at lower discharges. In this example, individual event selection criteria include recessions lasting longer than 5 days, starting 1 day after the peak to exclude the influence of overland flow, and ending at the next precipitation event, following other studies (Biswal and Marani, 2010; Shaw and Riha, 2012). The b parameter estimated using point cloud analysis (binning average method; BA) is smaller ($b = 1.5$) compared to the median of b values from the individual recessions ($b = 2.8$ with 50% of individual recessions taking values from 2.0 to 4.7; see the color bar of Figure 9). The frequency distribution of the b parameter from the individual recessions is skewed right and roughly log-normal which suggests that b from the point cloud does not represent an average or 'master' recession behavior.

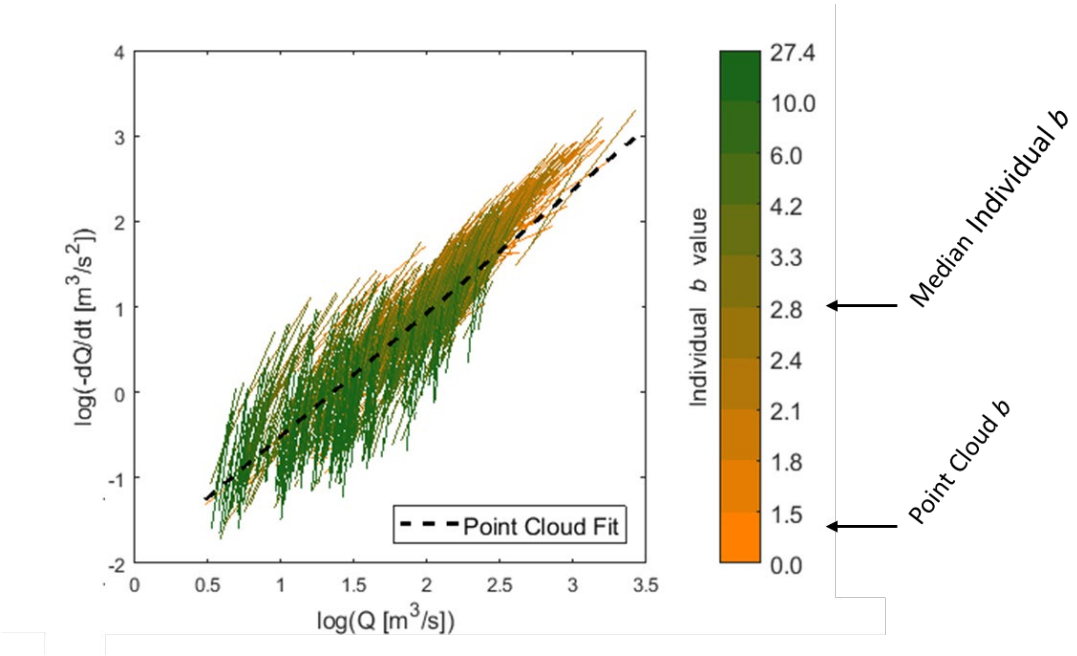

Figure 9. Recession analysis plot in log-log space for Lookout Creek (USGS no. 14161500). Individual recession fits are displayed with color scale differencing by values following a discretization according to decile groups. This discretization allows for the description of the organization of individual recessions where recessions with similar b values that appear to be horizontally offset. The point cloud has a value of $b = 1.4$ (binning average shown as a black dotted line) compared to $b = 2.8$ for the median individual recession.

For a given discharge range in Figure 9, there appears to be multiple individual recessions with similar values of b that are horizontally offset, implying a common b but a variable a value. The offset of individual recession events suggests that antecedent conditions may be influencing the location of the recession curves (e.g., Rupp et al., 2009), consistent with various theoretical definitions of a that include the aquifer saturated thickness at the onset of the recession as a parameter (Rupp and Selker, 2006b). Many authors have associated the pattern of shifted individual recessions with seasonality (Bart and Hope, 2014; Dralle et al., 2015; Karlsen et al., 2019; McMillan et al., 2011; Shaw and Riha, 2012; Tashie et al., 2019). Authors describe a generally sinusoidal relationship with larger a values associated with summer months (Dralle et al., 2015; Shaw and Riha, 2012) and a weaker seasonal relationship for values of b (Karlsen et al., 2019; Tashie et al., 2019). Seasonality associated with meteorological conditions may well be used as a predictor of a or b, but seasonality alone fails to

address the underlying climatic conditions that control streamflow recession. Instead of describing the variability between events based on seasonality as a proxy, parameter estimation should focus on antecedent and meteorological conditions that control streamflow recession in order to form a more comprehensive physically based understanding of recession parameters (e.g., Bart and Hope, 2014; Karlsen et al., 2018).

This paper explores the source of the offset ($\ln(a)$) and slope (b) on individual recessions. Using a time series of synthetic hydrographs with known parameters, we compare different methods for estimating the recession analysis parameters and the sensitivity to the method on the frequency and magnitude of events that make up the hydrograph. We are particularly concerned with how individual recessions collectively create the emergent point cloud and seek to describe how recession parameter estimation of the point cloud is affected by the distribution of individual recessions.

3.3 Methods

This section presents methods for (3.3.1) the definition of three synthetic hydrographs, (3.3.2) the description of recession extraction from the hydrograph, and (3.3.3) the comparisons between four fitting methods for parameter estimation applied to a discharge time series for Lookout Creek.

3.3.1 Synthetic Hydrograph Methods

This chapter makes use of synthetic hydrographs to explore factors that change b for individual recession events as well as the inter-arrival times of individual events that create the point cloud. Our synthetic hydrographs are created by defining individual recession events and stitching them together to create a long time series. Synthetic hydrographs were chosen for this study because each individual recession can be definitively identified, as the characteristics are known which is unrealistic when considering real watersheds. Furthermore, the synthetic hydrographs can be specified to directly compare different climatic controls without the confounding variables traditionally associated with real watersheds. For these purposes, the specifications of the synthetic hydrographs were chosen to explore the effects of the magnitudes and

frequency of recharge events on the recession analysis parameters from collective vs. individual recessions.

The falling limb of the hydrograph is assumed to follow a power law following Equation (13) (Dewandel et al., 2003; Drogue, 1972; Rupp and Woods, 2008).

$$Q(t) = Q_o \left(\frac{t}{\tau} + 1\right)^{-w} \tag{13}$$

where Q is the discharge, Q_o the initial discharge prior recession at t=0, t is the time in days since the recession started, τ is a characteristic timescale, and w is the dimensionless power-law decay exponent. Equation (13) can be expressed as Equation (12) with $a=w/(\tau Q_o^{1/w})$ and $b = (1+w)/w$.

Holding τ constant and varying the initial condition Q_o, results in a hysteretic relationship of $-dQ/dt$ vs. Q, in contrast to a constant a value which produces a single non-hysteric relationship. Defining a as a function of initial conditions has both theoretical (e.g., Rupp and Selker, 2006b) and empirical (e.g., Bart and Hope, 2014) support. The constancy of τ is not well established, but we assume it is constant for the scenarios examined here. Consequentially, a constant τ results in a variable value for a that is inversely proportional to the initial discharge. An inverse relationship is consistent with theoretical expectations for non-linear aquifers ($b > 1$), where Q_o increases with increasing initial saturated thickness (see Figs. 2 and 3 in Rupp et al., 2006b). Though the particular timescale is not important to our objectives, we chose it to be 45 days. Brutsaert (2008) noted a tendency for τ to be near 45 days across a large number of basins when fitting Equation (12) with b =1 to point cloud data. It remains to be seen whether a similarly narrow distribution of τ occurs for b not equal to 1.

A pulse recharge amount corresponding to a given Q_o can be calculated by integrating Equation (13) from $t = 0$ to $t = \infty$. For $w > 1$ ($b < 2$), the recharge volume is expressed in Equation (14).

$$V = DA = \tau Q_o/(w - 1) \tag{14}$$

where D is the depth of recharge and A is the aquifer area. For w <=1 (b >= 2), integrating Eq. (2) results in an infinite volume, so $b > 2$ can only be sustained over a finite part of any recession. Values of $b > 2$ have been derived from the physical theory for the early portion of a recession (Brutsaert and Nieber, 1977; Rupp and Selker, 2005) or can be obtained from recession curves over a finite time period while retaining physical realism by combining discharge from multiple linear ($b = 1$) or non-linear ($1 < b < 2$) reservoirs (e.g., McMillan et al., 2011). The effect on b of combining linear reservoirs in parallel (e.g., Clark et al., 2009; Gao et al., 2017; Harman et al., 2009) and series (e.g., Rupp et al., 2009; Wang, 2011) has received much more attention.

We compared three hypothetical time series generated with different assumptions about the distribution of the magnitudes and inter-arrival times of recharge events and the superposition of recession events (Table 1). The inter-arrival times are distributed log-normally (Cases 1 and 3) or uniformly (Case 2). Event magnitudes (as defined given by Q_o) are either distributed log-normally (Cases 1 and 3) or have constant magnitude (Case 2). Events are either independent of antecedent conditions (Case 1) or events are superimposed on antecedent conditions (Cases 2 and 3) (Table 1 and Figure 10).

To generate the time series for Cases 1 and 3, independent recessions were created using a random-number generator for a log-normal distribution for event peak magnitude and duration for a total of 10 years of time series data. The log-normal distributions for event magnitude and duration are chosen for the synthetic hydrographs because the distributions for Lookout Creek are skewed right and roughly log-normal (Figure S1), which is also consistent with other skewed-right precipitation distributions in previous studies (Begueria et al., 2009; Selker and Haith, 1990). Recharge events were created with log-normally distributed inter-arrival times ($\mu = 2.5$, $\sigma = 1$) and event magnitudes ($\mu = 1$ day, $\sigma = 1$) where both values are normalized by timescale and the unit hydrograph respectively, resulting in dimensionless quantities. These values of μ and σ result in event lengths with a mean of 20 days and an average of 18 events per year. This value was chosen to be comparable to the 19 events per year identified in

the Lookout Creek example. The distributions of both the inter-arrival times and event magnitudes are skewed right, representing the high frequency of smaller events and less frequent large events. Changing μ and σ will modify the amount of variability in individual recessions and could be further explored with different distributions in future research regarding the resulting variability in b. Case 2 assumes a constant event inter-arrival time ($\mu = 450/\tau$) and magnitudes ($\mu = 1$). The mean inter-arrival time of 10 days is intended to be comparable with the 19 events per year identified in the Lookout Creek example.

For Case 1, the individual recessions were combined to make a time series such that each event was concatenated onto the last event disregarding the antecedent flows. For Cases 2 and 3, individual recessions were superimposed on antecedent flows, appealing to the simplest model presented by the instantaneous unit hydrograph method (Dooge, 1973). We acknowledge that the framework for the instantaneous unit hydrograph as described in Dooge (1973) does not consider non-linear reservoirs, but we use it as a simple representation to produce variability between recessions. We discuss the implicit assumptions of this model in the Discussions and Conclusions section. From Figure 10, the baseflow from the first event, Q_B, is a simple continuation of the first recession. The underlying second event, Q_C, is defined by the second event's initial magnitude (constant in Case 2 and randomly generated in Case 3). The resulting flow, Q_D, is the sum of Q_B and Q_C.

As a result, Case 1 looks specifically at a time series events where the falling limb of each event maintains the same decay constant and the effect of having no antecedent baseflow influence on streamflow. By including baseflow to Case 2 but maintaining equal inter-arrival times and event magnitudes, we look specifically at the effect of antecedent conditions on individual recessions and the point cloud. Case 3 combines the distribution of event inter-arrival times and magnitudes of Case 1 with the baseflow conditions of Case 2, best representing the variability and inter-arrival times of individual recession events seen in Figure 9 for data from Lookout Creek.

Each case will address how the controls on the hydrograph affect the recession analysis plot and the estimates of *a* and *b*.

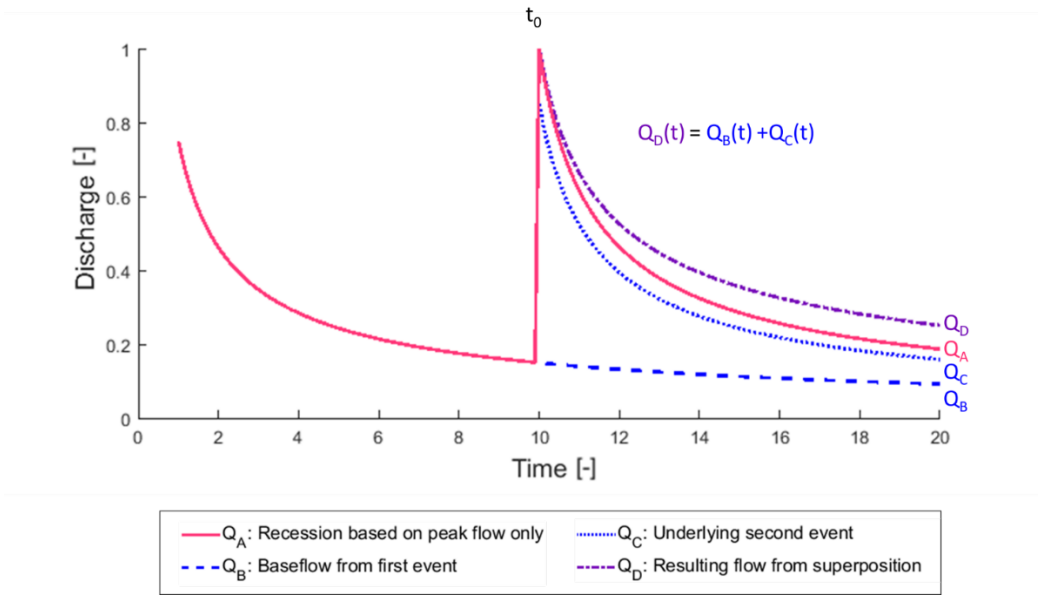

Figure 10. Conceptual model of identical recession events only dependent on the initial dimensionless flow (Q_A representing Case 1) and superposition of events to include antecedent conditions (summation of the blue-dotted line -Q_C and blue-dashed line-Q_B resulting in the superposition of the flow in the purple dash-dot line-Q_D representing Cases 2 and 3). By superimposing the antecedent flows (Q_B) on the underlying event (Q_C), the effective falling limb (Q_D) is less steep than the non-superimposed falling limb (Q_A). Time is expressed in dimensionless units and arbitrary values.

Table 1. Synthetic hydrograph scenarios

	Event Magnitudes	**Event Inter-Arrival Time**	**Superposition of antecedent flow?**
Case 1	Log-normal	Log-normal	No
Case 2	Constant	Constant	Yes
Case 3	Log-normal	Log-normal	Yes

3.3.2 Recession Extraction Method

Recession extraction from observed hydrographs and the associated sensitivities to different criteria have been explored by Dralle et al. (2017), including minimum recession length, and the definition of the beginning and the end of the event. For Lookout Creek, we used extraction criteria similar to those of other studies (e.g., Chen and Krajewski, 2016; Dralle et al., 2017; Stoelzle et al., 2013) and applied the same criteria prior to all fitting methods presented in Section 2.3 to isolate differences in calculated *b* values due to the fitting method only. An individual recession event duration must be longer than 5 days. Rainfall data can be used to identify non-interrupted recessions, but rainfall data will not available in all cases, so we rely on the hydrograph only. The start of the recession is defined as one day after the discharge peak to account for the presence of overland flow. The end of the recession occurs at the minimum discharge prior to an increase in discharge greater than the error associated with instrument precision for stage height of ~0.5 cm, which translates into errors in discharge from ~0.01-0.1 m3/s, depending on the rating curve and the discharge level (Thomas et al., 2015).

For the synthetic hydrographs used in Section 3.4.2, events of any length were included, the recession start was selected at peak discharge because overland flow was not a factor, and the end of the recession was chosen as the time immediately before the next generated discharge peak.

3.3.3 Parameter Estimation Methods

Four methods of estimating representative recession parameters were evaluated: lower envelope (LE), central tendency (CT), binning average (BA; Kirchner, 2009), and median of individual recessions (MI) (Roques et al., 2017). Linear regression in bi-logarithmic space was used with each method for consistency across methods.

Because a change of hydraulic regime was suggestive in Figure 9 between high-flow ranges and low-flow ranges, recession analysis parameters were estimated for two

flow ranges, early-time and late-time. Early-time and late-time describe a theoretical transition of flow regimes between high-flow and low-flow ranges (Brutsaert and Nieber, 1977). To reduce the subjectivity of distinguishing between high and low flows, a breakpoint in discharge separating high- from low-flow behavior was optimized to best represent the analytical solution. By separating the data into two subgroups, either smaller or larger than a defined breakpoint discharge, the best-fit line was determined for each subgroup. The location of the breakpoint is defined so the error between the observed ratio of *b* for the two subgroups and the theoretical ratio (b=3 for early and 1.5 for late give a ratio of 2) is minimized, theoretically defining the subgroup above the breakpoint as early-time and the subgroup below the breakpoint at late-time. \

For each of the four estimated methods, parameters were estimated for the early-time and late-time behavior separately. For the LE method, *b* was fixed to 3 and 1.5 for early and late-time, respectively, following Brutsaert and Nieber (1977) and *a* was chosen such that 5% of points were below the lower envelope (Brutsaert, 2008; Troch et al., 1993; Wang, 2011). It should be noted that using these values for *b* assumes that the groundwater discharge behaves like discharge from a single, initially saturated, and homogenous Boussinesq aquifer. An alternative method to fitting the lower envelope without a predefined value of *b* was introduced by Thomas et al. (2015) using quantile regression to estimate both *a* and *b*, but it was not used in this study. For the CT method, the fit included all points of $-dQ/dt$ vs Q as unweighted (Vogel and Kroll, 1992). For the BA method, bins spanned at least 1% of the logarithmic range, and a line, instead of the polynomial suggested by Kirchner (2009), was fit to the binned data. We dispensed with the inverse-variance bin weighting used by Kirchner (2009) to account for data noise when we applied the method to the synthetic recessions because some bins contained few points with very low variance and therefore were weighted excessively. For the MI method, parameters were estimated for individual recessions following Roques et al. (2017), and the medians of a and *b* were calculated. In all cases, the time derivative of $-dQ/dt$ was computed using the exponential-time-step (ETS) method proposed by Roques et al. (2017).

3.4 Results

3.4.1 Parameter Estimation for Observed Recessions (Lookout Creek)

In Figure 11 we display the recession plot stacking all individual recessions resulting in the formation of the point cloud. The different fitting strategies revealed that the LE, CT, and BA methods all fit to the point cloud and result in different values of *b* when applied to the observed daily averaged streamflow for Lookout Creek: early-time values of *b* are over 50% larger for LE (fixed at 1.5) than CT and BA, and late-time values of *b* are 50% and 25% larger for LE than CT and BA, respectively (Figure 11 and Table 2). The CT and BA methods are fairly consistent with each other for both early and late-time, whereas the pre-defined theoretical *b* values for the LE appear to provide poorer fits to the point cloud.

More importantly, parameter estimation differs greatly whether the point cloud or individual recessions are used. The late-time *b* value which defines the low-flow baseflow regime is 6 times greater for MI than CT (Table 2). Using the MI method, the *b* value is larger than any other method for both early and late time.

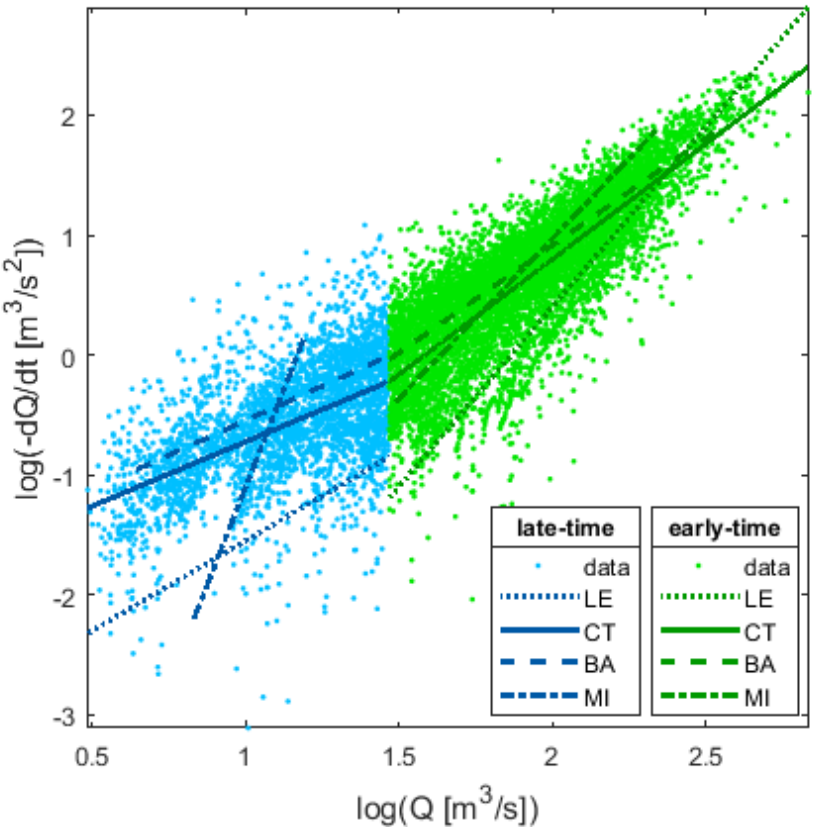

Figure 11. Recession analysis for Lookout Creek to aid in the comparison of four different fitting methods and the dependency on parameter estimation shown visually (lower envelope-LE, central tendency-CT, binning average-BA) and individual recessions parameters (median individual recession-MI). Depending on the fitting method, the parameter estimation for *a* and *b* will be different.

Table 2. Comparison of recession analysis parameters *a* and *b* for Lookout Creek between different methods: lower envelope (LE), central tendency (CT), binning average (BA), and the median individual recession (MI). Each value is represented as a ratio of parameter estimation for early to late time. Depending on the fitting method, the parameter estimation for *a* and *b* will be different. s

	log(a **[$s^{-1}\cdot(m^3\cdot s^{-1})^{1-b}$])**		***b*** **[-]**	
	Early	**Late**	**Early**	**Late**
LE	-5.6	-3.0	3.0	1.5
CT	-3.0	-1.8	1.9	1.0

BA	-2.6	-1.6	1.8	1.2
MI	-3.9	-8.1	2.7	6.4

3.4.2 Synthetic Hydrograph Results

Based on the similar results from BA and CT methods discussed above, and the questionable practice of setting an early- and late-time *b* a priori as we did in the LE method, hereafter we use the BA method to represent to point cloud recession parameter estimation when comparing to the MI method using individual recessions.

The recession decay exponent *w* in Equation (13) was set to 1.2; distinct values of *w* were not used for early and late time. This value for *w* results in $b = 1.8$ for an individual synthetic recession, which is near the reported median of individual *b* values of 2.0 in Biswal and Marani (2010), and 2.1 in Shaw and Riha (2012) and Roques et al. (2017), though less than the median individual *b* of 2.8 for Lookout Creek.

The *b* values and the offset of individual recessions resulting from Equation (12) are both functions of *w*. A larger *b* value indicates a more stable baseflow discharge (a slower decline rate for given discharge). For a given value of *b* and τ, *a* varies inversely with $Q_o^{1/(b-1)}$. Decreasing *w* results in larger values of *b* while also increasing the offset between individual recessions, resulting in a larger range of *a* values and a more scattered point cloud. In contrast, as *w* approaches infinity, the offset is minimized as *b* goes to 1, resulting in an exponential falling-limb recession in time (Rupp and Woods, 2008). In this special case, all of the individual recessions overlap with constant *a* (i.e., there is no offset among individual recessions lines). While $b=1$ is interpreted as a linear reservoir according to traditional theory and is a convenience often assumed, this result suggests that a condition where $b=1$ and *a* is a constant is not consistent with the existence of a point cloud, except to the degree at which observation error introduces noise into the recession hydrograph or other pathways (e.g., overland flow) contribute to the flow in the stream. In summary, the more linear the response is (the closer *b* is to 1), the smaller the offset is, whereas the more non-linear the response (the larger the b) is, the greater the offset and thus the more different the parameter

estimations between the point cloud and individual recession methods will be. The three following cases using synthetic hydrographs are intended to highlight the offset of the individual recession curves.

3.4.2.1 Case 1

Recession analysis of a hydrograph with log-normally distributed event inter-arrival times and peak discharge with a constant falling-limb decay constant (no baseflow represented) results in individual recession events with the same b, horizontally shifted based on the initial discharge (Figure 12). In this case, the peak flow of the event is the only source of variability in the recession parameter a. The variable event magnitudes result in individual events located over a range of ln(Q) values, whereas if the same flow magnitude was preserved for each event, each individual recession would plot on top of one another creating a single line without a point cloud. The variable event inter-arrival times change the duration of an event, with longer events occurring over a greater range on the y-axis. In this simple hydrograph, parallel individual recessions are present, and all have b = 1.8, as expected. The value of b is estimated at 1.3 considering the point cloud, which appears to be significantly less than imposed individual b value of 1.8. This underestimation results from the offset between individual recessions based on the range of initial discharges.

To examine the sensitivity of parameter estimation to recession extraction criteria, we evaluated how choosing the start of the recession (i.e., the time elapsed since peak discharge) affects the value of a when using the point cloud method. Whether we chose 0, 1, or 2 days following peak discharge, a from the point cloud a was 0.17 [-] and b was 1.3 [-].

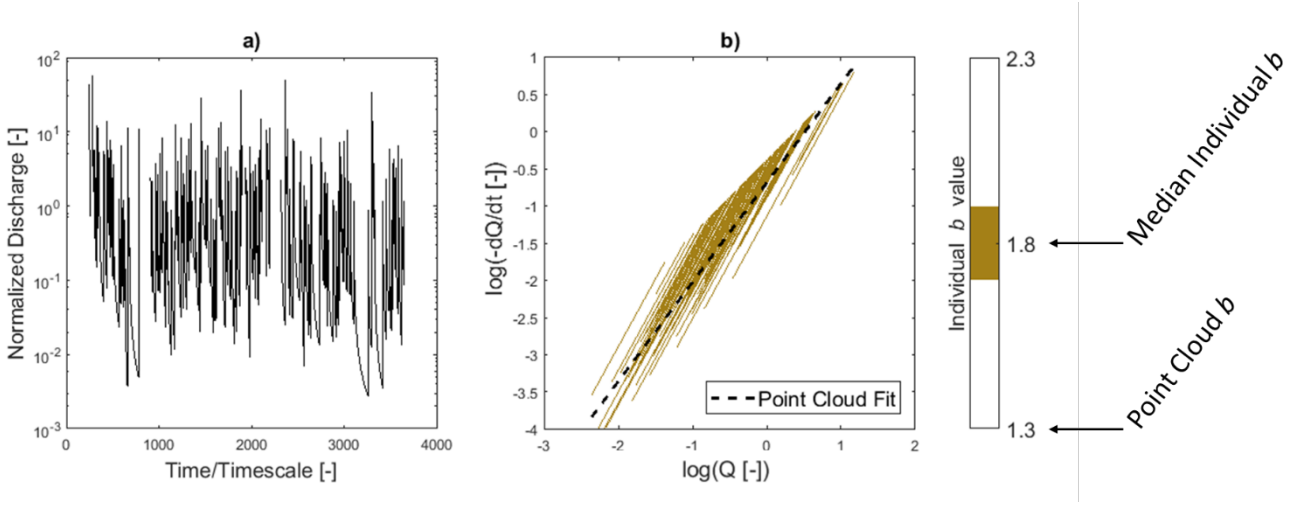

Figure 12. a) Hydrograph with log-normally distributed event inter-arrival times and peak magnitudes with each event maintaining a constant falling-limb decay constant and b) recession analysis with resulting parallel individual recessions having a constant *b* value (MI *b* = 1.8) compared to the point cloud fit (black dotted line), which results in *b* = 1.3. Discharge and time are normalized, resulting in dimensionless quantities. Gaps in the hydrograph are a result of individual event magnitudes that are smaller than the streamflow that precedes the event start. The individual recessions are offset, which when viewed collectively, results in the point cloud.

3.4.2.2 Case 2

The superposition of recession events accounts for the effects of antecedent baseflow. The superposition changes the effective *w* of the falling limb of the hydrograph as the event recession is added to the antecedent events, resulting in a variable *b* value across the individual recessions (Figure 13). The median *b* value represented is 3.25 with a range of 2.56 to 3.41 (quantile range represented in the color bar of Figure 13). The point cloud *b* value of 2.35 falls outside of the range of *b* values for individual recessions. Superposition results in a larger *b* value than what would arise from non-superposition. Steeper recessions (higher *b* value) are associated with events with higher baseflow contribution given the same addition of flow. By including antecedent-flow conditions, neither *a* nor *b* is preserved between individual recessions.

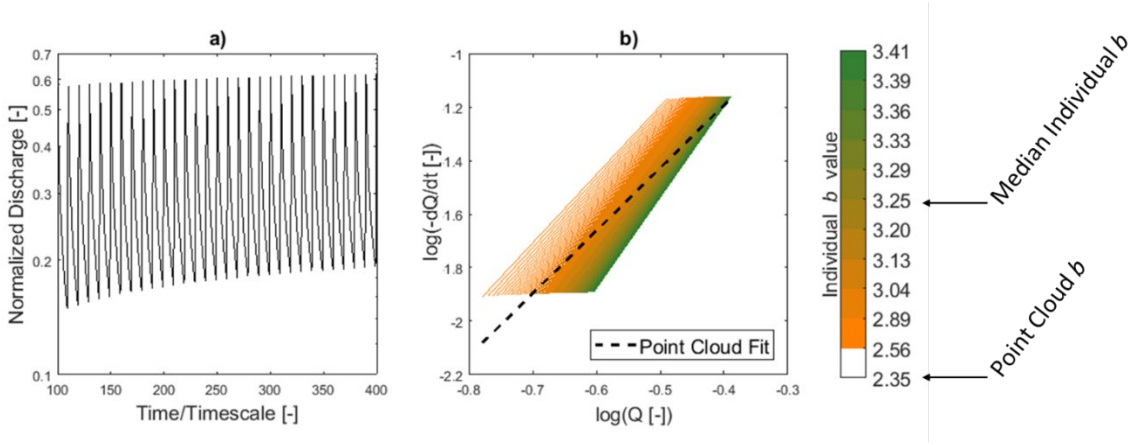

Figure 13. a) Hydrograph of equally spaced recharge events with each underlying equal magnitude recession event superimposed on previous ones resulting in varying falling-limb decay constants (x-axis zoomed in to show detail) and b) recession analysis plot showing a range of *b* values of individual recessions (MI *b* = 3.25), with steeper recessions associated with events with a higher baseflow contribution, compared to the point cloud fit (black dotted line- BA; *b* = 2.35). The color bar is divided into 10 ranges based on the individual *b* value; each range contains 10% of individual recessions, and the lowest range is in white for comparison to the point cloud range.

3.4.2.3 Case 3

A hydrograph more representative of real-case conditions includes variable inter-arrival times and event magnitudes from Case 1 and baseflow antecedent conditions from Case 2 (Figure 14a). These complexities result in a recession plot where the individual recessions represent the variability in watershed response represented by the hydrograph (Figure 14b), where *a* and *b* are different between individual recessions. As with Cases 1 and 2, the median individual *b* value (3.3) is greater than the point cloud *b* value (2.0) The minimum individual *b* is 1.9 with a maximum of 8.5, while the point cloud *b* is near the low end of the range of individual *b* values (see the color bar of Figure 14). The similarity of features of Figure 14b and Figure 9 are noteworthy. Though many of the observed recessions in Figure 9 are slightly curvilinear (in the log-log space), the synthetic recessions are power laws; in both cases there is a tendency for recessions with lower initial discharges to have higher

values of *b*, yet still many instances of recessions have similar initial discharges but different values of *b*.

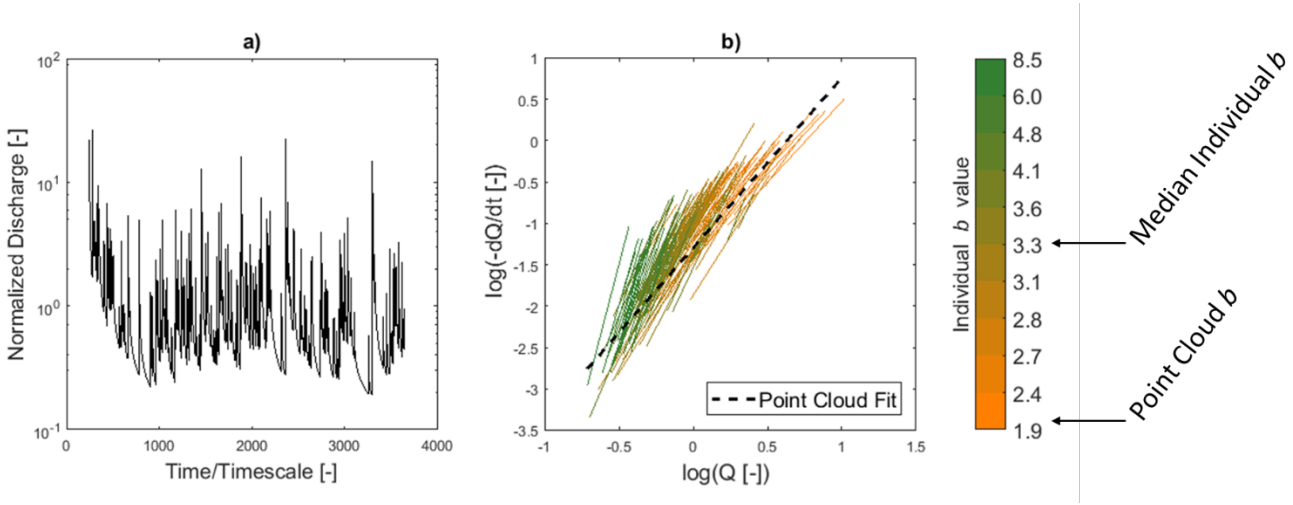

Figure 14. a) Hydrograph with a log-normal distribution in recharge event inter-arrival times and magnitudes and b) recession analysis plot showing a large range of b values (with the median of b = 3.3), compared to the point cloud fit (black dotted line-BA; b = 2.0). The color bar is divided into deciles in the distribution of b values compared to the point cloud range.

3.5 Discussion and Conclusions

In the 42 years since Brutsaert and Nieber (1977) proposed their recession analysis, it has provided a seemingly simple analytical method for estimating basin-scale hydrologic properties. However, recent studies have highlighted the sensitivity to estimation methods on the recession parameter values and to the resulting interpretation of average watershed behavior. This paper explores the effect of the distribution (in time and in magnitude) of individual recessions on parameter estimation and compares that to the parameter estimation from collective recessions (i.e., the point cloud). The four estimation methods considered were the lower envelope, central tendency, binning, and individual recession method. Because of the poorer apparent fit and problems pointed out from previous studies when using the lower envelope and central tendency methods, we chose to use the binning method to compare with results from the individual recessions method for a set of synthetic case studies.

We hypothesize that the climate controls the distribution of individual recessions in bi-logarithmic plots of $-dQ/dt$ vs. Q. This distribution can be related to the variability in recession analysis parameters. Using the three synthetic case studies, we examine the effects of event inter-arrival time, magnitude, and antecedent conditions on the distribution of individual recession events that comprise the pattern of collective recessions.

We conclude that recession analysis performed on collective recessions does not capture average watershed behavior, regardless of the fitting method. The point cloud is an artifact of the variability of the individual recessions, including the event inter-arrival times and distribution of magnitudes. Individual recessions with the same b but different a values can be produced by varying the initial discharges (Case 1); variability of b for individual recessions can be produced by superimposing events on antecedent-flow conditions (Case 2); and different recession event lengths with different b values can be produced by including variable event inter-arrival times and magnitudes (Case 3).

For Case 1, the recession analysis parameter a is equal to $w/(\tau Q_o^{1/w})$, and thus the intercept of the individual recession curves will scale with Q_o. The result is a collection of individual recession curves that are horizontally offset based on the initial discharge, producing a smaller b value for the point cloud compared to the individual recessions. Case 1 illustrates that the slope of individual recession events can be greater than the best-fit line through the point cloud, consistent with previous studies (Biswal and Marani, 2010; Mutzner et al., 2013; Shaw and Riha, 2012). However, the point cloud in Case 1 is generated by a collection of multiple individual recessions, all with the same slope, and does not have the variability in b values presented in these previous studies and shown for Lookout Creek in Figure 9. Cases 2 and 3 use superposition of antecedent-flow events that consequentially changes the individual b values, providing a possible explanation for the variability in b values for individual recessions. For Case 2, the superposition of events takes account of antecedent conditions which results in a distribution of individual b values despite the decay exponent w being fixed. For Case 3, the horizontal offset of individual recessions from Case 1 and the effects of

antecedent conditions from Case 2 result in the recessions with variable individual *b* values that are horizontally offset to create a pattern similar to that observed in a real watershed.

While the mean *b* for individual recessions in Case 1 is a direct consequence of the value of w used in Equation (13), this is not true when the discharge from each application of Equation (13), which we call an event, is superimposed on the antecedent flow, as in Cases 2 and 3. This superposition of events results in a range of individual recession *b* as often observed in the literature (Basso et al., 2015; Biswal and Marani, 2010; McMillan et al., 2014; Mutzner et al., 2013; Shaw and Riha, 2012); thus it appears that the straightforward superposition of events can recreate the watershed behavior. However, there is a key underlying assumption of this superposition that is inconsistent with a real watershed. To help describe this inconsistency, we can compare two distinctly different conceptual models of watersheds. The first, and very frequently used, model is a single bucket with an outlet near the bottom. The bucket contains a porous medium whose properties may vary with depth to create a variety of non-linear outflows. Each new recharge event adds to the pre-existing storage of water in the bucket. The second model is the one used for Cases 2 and 3: each new event adds water to a new and independent bucket, and the outflows from all buckets are aggregated. Both conceptual models have components that are patently unrealistic when applied to natural watersheds, but, remarkably, the latter model produces a distribution of recession events in the space of $-dQ/dt$ vs. Q that is more like what is observed in the Lookout Creek basin and others (Mutzner et al., 2013; Shaw and Riha, 2012). This finding reveals key information about the subsurface plumbing system of the basin and its dynamics that could be explored with models with a higher degree of realism. We acknowledge that there are other ways to create watershed memory that would also generate variability in apparent recession parameters and would be worthwhile to consider. For example, following previous works that have shown that multiple linear reservoirs can generate power law recessions (Clark et al., 2009; Harman et al. 2009), one could explore combinations of parallel linear reservoirs with varying sizes and recession constants under time-varying recharge. However, based on the results of

Harman et al. (2009) using periodic recharge events, it is not clear that this would lead to a distribution of recession curves of varying b values like what is seen in Figure 9. A similar, albeit more complicated, exercise could also be done with combinations of parallel non-linear reservoirs with distinct recession parameters.

An additional important simplifying assumption of this study is the use of a constant timescale τ for each individual event. Previous studies that have examined timescales across basins by setting $b = 1$ and estimating τ from the point cloud (Brutsaert, 2008; Lyon et al., 2015). However, given the questionable of the validity of the point cloud estimation methods, additional studies of the variability of the timescale among individual recession events and across the basin should be done.

We show how the point cloud pattern does not arise from watershed properties alone. The consequence is that parameters estimated from the point cloud do not represent watershed properties. In all three synthetic-hydrograph representations, the median individual recession b is significantly greater than b from the point cloud. Additionally, it is possible for the point cloud b to be smaller than the minimum individual recession b indicating the point cloud fit represents a behavior outside the range of watershed responses represented by individual recession events. In contrast to the point cloud, individual recession analysis provides insights into the average and variability of watershed responses which is highly dependent on the memory effect of the watershed. The variability in individual responses gives insight into watershed complexities including heterogeneity in topography, geology, and climate. Watersheds may present large variability in geology and so hydrogeological conditions such as unconfined or confined aquifers, inter-basin groundwater flows, high spatial hydraulic conductivity variability, depth-dependent hydraulic conductivity, or large-scale discontinuities. As a result, there are still opportunities to further characterize the variability in watershed responses and the associated variability in individual b values to improve streamflow prediction using recession analysis.

A strength of the critical-zone community is the ability to create a global analysis by comparing across studies (Brooks et al., 2015; Fan et al., 2019). However, a lack of consensus for a standard method for recession analysis procedures exists and thus inhibits recession analysis studies from being widely compared. If streamflow analysis is to be included in a global analysis, results need to be comparable across scales and observatories. There is a need for a common method employed to compare the average and variability in watershed responses. Because estimated parameters may differ greatly by estimation **method**, misinterpretation of hydrological properties and incorrect predictions within the critical zone are possible. When using the point cloud in particular, a smaller recession parameter *b* at late time could be, and has been, interpreted to imply greater basin vulnerability to drought (Berghuijs et al., 2014, 2016; Yeh and Huang, 2019). However, a more stable baseflow is implied by the distribution of *b* values from the individual recessions and its median *b* value, which can be much larger than what is estimated from the point cloud. We suggest that the use of collective recession analysis should be avoided in favor of individual recession analysis as the standard to describe the average and variability in watershed response. The methods employed for recession analysis certainly require more attention. Correct methods are critical to understand the underlying hydrology and thus the interpretation of a watershed's vulnerability to climate change.

Code and Data Availability

Streamflow record for Lookout Creek is freely available from the USGS website (USGS, 2019). Source code for the exponential time-step method is available by request (Roques *et al.*, 2017). Randomly generated log-normal event magnitudes and inter-arrival times presented in this paper for Cases 1 & 3 are available at: http://www.hydroshare.org/resource/e3c159631acd470cbeef5fa1abe0142e.
Respective codes can be obtained from the corresponding author.

Supplement

The supplement related to this article is available online at: https://doi.org/10.5194/hess-24-1-2020-supplement.

Financial support

This work was supported by the National Science Foundation awards to the Center for Transformative Environmental Monitoring Programs (nos. 1551483 and 1440506).

References

Bart, R. and Hope, A.: Inter-seasonal variability in baseflow recession rates: The role of aquifer antecedent storage in central California watersheds, J. Hydrol., 519(PA), 205–213, doi:10.1016/j.jhydrol.2014.07.020, 2014.

Basso, S., Schirmer, M. and Botter, G.: On the emergence of heavy-tailed streamflow distributions, Adv. Water Resour., 82, 98–105, doi:10.1016/j.advwatres.2015.04.013, 2015.

Begueria, S., Vicente-Serrano, S. M., Lopez-Moreno, J. I. and Garcia-Ruiz, J. M.: Annual and seasonal mapping of peak intensity, magnitude and duration of extreme precipitation events across a climatic gradient, northeast Spain, Int. J. Climatol., 29, 1759–1779, doi:10.1002/joc.1808, 2009.

Berghuijs, W. R., Sivapalan, M., Woods, R. A. and Savenije, H. H. G.: Patterns of similarity of seasonal water balances: A window into streamflow variability over a range of time scales, Water Resour. Res., 50(7), doi:10.1002/2014WR015692, 2014.

Berghuijs, W. R., Hartmann, A. and Woods, R. A.: Streamflow sensitivity to water storage changes across Europe, Geophys. Res. Lett., 43, 1980–1987, doi:10.1002/2016GL067927, 2016.

Biswal, B. and Marani, M.: Geomorphological origin of recession curves, Geophys. Res. Lett., 37(24), 1–5, doi:10.1029/2010GL045415, 2010.

Brooks, P., Chorover, J., Fan, Y., Godsey, S. E., Maxwell, R. M., McNamara, J. and Tague, C.: Hydrological partitioning in the critical zone: Recent advances and opportunities for developing transferable understanding of water cycle dynamics, Water Resour. Res., 51, 6973–6987, doi:10.1002/2015WR017039, 2015.

Brutsaert, W.: Long-term groundwater storage trends estimated from streamflow records: Climatic perspective, Water Resour. Res., 44(2), 1–7, doi:10.1029/2007WR006518, 2008.

Brutsaert, W. and Nieber, J. L.: Regionalized drought flow hydrographs from a mature glaciated plateau, Water Resour. Res., 13(3), 637–643, doi:10.1029/WR013i003p00637, 1977.

Buttle, J. M.: Mediating stream baseflow response to climate change: The role of basin storage, Hydrol. Process., 32(3), 363–378, doi:10.1002/hyp.11418, 2018.

Chen, B. and Krajewski, W.: Analysing individual recession events: sensitivity of parameter determination to the calculation procedure, Hydrol. Sci. J., 61(16), 2887–2901, doi:10.1080/02626667.2016.1170940, 2016.

Chen, X., Kumar, M., Basso, S. and Marani, M.: On the effectiveness of recession analysis methods for capturing the characteristic storage-discharge relation: An intercomparison study, Hydrol. Earth Syst. Sci. Discuss., (February), 1–30,

doi:10.5194/hess-2018-65, 2018.

Clark, M. P., Rupp, D. E., Woods, R. A., Tromp-van Meerveld, H. J., Peters, N. E. and Freer, J. E.: Consistency between hydrological models and field observations: Linking processes at the hillslope scale to hydrological responses at the watershed scale, Hydrol. Process., 23, 311–319, doi:10.1002/hyp.7154, 2009.

Dewandel, B., Lachassagne, P., Bakalowicz, M., Weng, P. and Al-Malki, A.: Evaluation of aquifer thickness by analysing recession hydrographs. Application to the Oman ophiolite hard-rock aquifer, J. Hydrol., 274(1–4), 248–269, doi:10.1016/S0022-1694(02)00418-3, 2003.

Dooge, J. C. I.: Linear Theory of Hydrologic Systems: Technical Bulletin No. 1468, Agricultural Research Service: United States Department of Agriculture, Washington, D.C., 1973.

Dralle, D., Karst, N. and Thompson, S. E.: A, b careful: The challenge of scale invariance for comparative analyses in power law models of the streamflow recession, Geophys. Res. Lett., 42(21), 9285–9293, doi:10.1002/2015GL066007, 2015.

Dralle, D. N., Karst, N. J., Charalampous, K., Veenstra, A. and Thompson, S. E.: Event-scale power law recession analysis: Quantifying methodological uncertainty, Hydrol. Earth Syst. Sci., 21(1), 65–81, doi:10.5194/hess-21-65-2017, 2017.

Drogue, C.: Analyse statistique des hydrogrammes de decrues des sources karstiques statistical analysis of hydrographs of karstic springs, J. Hydrol., 15(1), 49–68, 1972.

Fan, Y., Clark, M., Lawrence, D., Swenson, S., Band, L. E., Brantley, S., Brooks, P., Dietrich, W., Flores, A., Grant, G., Kirchner, J., Mackay, D., McDonnell, J., Milly, P., Sullivan, P., Tague, C., Ajami, H., Chaney, N., Hartmann, A., Hazenberg, P., McNamara, J., Pellet, J., Volk, J. and Yamazaki, D.: Hillslope Hydrology in Global Change Research and Earth System Modeling, Water Resour. Res. AGU Centen. Vol. Gd. CHALLENGES EARTH Sp. Sci., 1737–1772, doi:10.1029/2018WR023903, 2019.

Gao, M., Chen, X., Liu, J., Zhang, Z. and Cheng, Q.-B.: Using Two Parallel Linear Reservoirs to Express Multiple Relations of Power-Law Recession Curves, J. Hydrol. Eng., 22(7), 1–12, doi:10.1061/(asce)he.1943-5584.0001518, 2017.

Harman, C. J., Sivapalan, M. and Kumar, P.: Power law catchment-scale recessions arising from heterogeneous linear small-scale dynamics, Water Resour. Res., 45(9), 1–13, doi:10.1029/2008WR007392, 2009.

Johnson, S. and Rothacher, J.: Stream discharge in gaged watersheds at the Andrews Experimental Forest, 1949 to present., Long-Term Ecol. Res. For. Sci. Data Bank [Database], doi:10.6073/pasta/c85f62e9070a4ebe5e455190b4879c0c, 2019.

Karlsen, R. H., Bishop, K., Grabs, T., Ottosson-Löfvenius, M., Laudon, H. and Seibert, J.: The role of landscape properties, storage and evapotranspiration on variability in streamflow recessions in a boreal catchment, J. Hydrol., 570, 315–328, doi:10.1016/j.jhydrol.2018.12.065, 2019.

Kirchner, J. W.: Catchments as simple dynamical systems: Catchment characterization, rainfall-runoff modeling, and doing hydrology backward, Water Resour. Res., 45(2), 1–34, doi:10.1029/2008WR006912, 2009.

Liu, J., Han, X., Chen, X., Lin, H. and Wang, A.: How well can the subsurface storage–discharge relation be interpreted and predicted using the geometric factors in headwater areas?, Hydrol. Process., 30(25), 4826–4840, doi:10.1002/hyp.10958, 2016.

Lyon, S. W., Koutsouris, A., Scheibler, F., Jarsjö, J., Mbanguka, R., Tumbo, M., Robert, K. K., Sharma, A. N. and van der Velde, Y.: Interpreting characteristic drainage timescale variability across Kilombero Valley, Tanzania, Hydrol. Process., 29(8), 1912–1924, doi:10.1002/hyp.10304, 2015.

McMillan, H., Gueguen, M., Grimon, E., Woods, R., Clark, M. and Rupp, D. E.: Spatial variability of hydrological processes and model structure diagnostics in a 50km2catchment, Hydrol. Process., 28(18), 4896–4913, doi:10.1002/hyp.9988, 2014.

McMillan, H. K., Clark, M. P., Bowden, W. B., Duncan, M. and Woods, R. A.: Hydrological field data from a modeller's perspective: Part 1. Diagnostic tests for model structure, Hydrol. Process., 25(4), 511–522, doi:10.1002/hyp.7841, 2011.

Meriö, L., Ala-aho, P., Linjama, J., Hjort, J., Kløve, B. and Marttila, H.: Snow to Precipitation Ratio Controls Catchment Storage and Summer Flows in Boreal Headwater Catchments, Water Resour. Res., 55, 4096–4109, doi:10.1029/2018WR023031, 2019.

Mutzner, R., Bertuzzo, E., Tarolli, P., Weijs, S. V., Nicotina, L., Ceola, S., Tomasic, N., Rodriguez-Iturbe, I., Parlange, M. B. and Rinaldo, A.: Geomorphic signatures on Brutsaert base flow recession analysis, Water Resour. Res., 49(9), 5462–5472, doi:10.1002/wrcr.20417, 2013.

Ploum, S. W., Lyon, S. W., Teuling, A. J., Laudon, H. and van der Velde, Y.: Soil frost effects on streamflow recessions in a sub-arctic catchment, Hydrol. Process., 33, 1304–1316, doi:10.1002/hyp.13401, 2019.

Roques, C., Rupp, D. E. and Selker, J. S.: Improved streamflow recession parameter estimation with attention to calculation of − dQ/dt, Adv. Water Resour., 108, 29–43, doi:10.1016/j.advwatres.2017.07.013, 2017.

Rupp, D. E. and Selker, J. S.: Drainage of a horizontal Boussinesq aquifer with a power law hydraulic conductivity profile, Water Resour. Res., 41(11), 1–8, doi:10.1029/2005WR004241, 2005.

Rupp, D. E. and Selker, J. S.: Information, artifacts, and noise in dQ/dt - Q recession analysis, Adv. Water Resour., 29(2), 154–160, doi:10.1016/j.advwatres.2005.03.019, 2006a.

Rupp, D. E. and Selker, J. S.: On the use of the Boussinesq equation for interpreting recession hydrographs from sloping aquifers, Water Resour. Res., 42(12), 1–15, doi:10.1029/2006WR005080, 2006b.

Rupp, D. E. and Woods, R. A.: Increased flexibility in base flow modelling using a power law transmissivity profile, Hydrol. Process., 22, 2667–2671, doi:10.1002/hyp.6863, 2008.

Rupp, D. E., Schmidt, J., Woods, R. A. and Bidwell, V. J.: Analytical assessment and parameter estimation of a low-dimensional groundwater model, J. Hydrol., 377(1–2), 143–154, doi:10.1016/j.jhydrol.2009.08.018, 2009.

Sánchez-Murillo, R., Brooks, E. S., Elliot, W. J., Gazel, E. and Boll, J.: Baseflow

recession analysis in the inland Pacific Northwest of the United States, Hydrogeol. J., 23(2), 287–303, doi:10.1007/s10040-014-1191-4, 2015.

Santos, A. C., Portela, M. M., Rinaldo, A. and Schaefli, B.: Estimation of streamflow recession parameters: New insights from an analytic streamflow distribution model, Hydrol. Process., 33, 1595–1609, doi:10.1002/hyp.13425, 2019.

Selker, J. S. and Haith, D. A.: Development and Testing of Single-Parameter Precipitation Distributions, Water Resour. Res., 26(11), 2733–2740, doi:10.1029/WR026i011p02733, 1990.

Shaw, S. B. and Riha, S. J.: Examining individual recession events instead of a data cloud: Using a modified interpretation of dQ/dt-Q streamflow recession in glaciated watersheds to better inform models of low flow, J. Hydrol., 434–435, 46–54, doi:10.1016/j.jhydrol.2012.02.034, 2012.

Stewart, M. K.: Promising new baseflow separation and recession analysis methods applied to streamflow at Glendhu Catchment, New Zealand, Hydrol. Earth Syst. Sci., 19(6), 2587–2603, doi:10.5194/hess-19-2587-2015, 2015.

Stoelzle, M., Stahl, K. and Weiler, M.: Are streamflow recession characteristics really characteristic?, Hydrol. Earth Syst. Sci., 17(2), doi:10.5194/hess-17-817-2013, 2013.

Szilagyi, J., Gribovszki, Z. and Kalicz, P.: Estimation of catchment-scale evapotranspiration from baseflow recession data: Numerical model and practical application results, J. Hydrol., 336(1–2), 206–217, doi:10.1016/j.jhydrol.2007.01.004, 2007.

Tashie, A., Scaife, C. I. and Band, L. E.: Transpiration and Subsurface Controls of Streamflow Recession Characteristics, Hydrol. Process., 33, 2561–2575, doi:10.1002/hyp.13530, 2019.

Thomas, B. F., Vogel, R. M. and Famiglietti, J. S.: Objective hydrograph baseflow recession analysis, J. Hydrol., 525, 102–112, doi:10.1016/j.jhydrol.2015.03.028, 2015.

Troch, P. A., de Troch, F. P. and Brutsaert, W.: Effective Water Table Depth to Describe Initial Conditions Prior to Storm Rainfall in Humid Regions, Water Resour. Res., 29(2), 427–434, 1993.

USGS: National Water Information System, [online] Available from: https://waterdata.usgs.gov/nwis, 2019.

Vannier, O., Braud, I. and Anquetin, S.: Regional estimation of catchment-scale soil properties by means of streamflow recession analysis for use in distributed hydrological models, Hydrol. Process., 28(26), 6276–6291, doi:10.1002/hyp.10101, 2014.

Vogel, R. M. and Kroll, C. N.: Regional Geohydrologic-Geomorphic Relationships for the Estimation of Low-Flow Statistics, Water Resour., 28(9), 2451–2458, 1992.

Wang, D.: On the base flow recession at the Panola Mountain Research Watershed, Georgia, United States, Water Resour. Res., 47(3), 1–10, doi:10.1029/2010WR009910, 2011.

Yeh, H. and Huang, C.: Evaluation of basin storage–discharge sensitivity in Taiwan using low-flow recession analysis, Hydrol. Process., 1–14, doi:10.1002/hyp.13411, 2019.

Chapter 4. A New Angle on Hillslope Drainage Modeling

Elizabeth R. Jachens[1], Clément Roques[2], David E. Rupp[3], John S. Selker[1]

[1]Department of Biological and Ecological Engineering, Oregon State University, USA.

[2]Department of Earth Sciences, ETH Zürich, Switzerland.

[3]Oregon Climate Change Research Institute, College of Earth, Oceanic and Atmospheric Sciences, Oregon State University, USA.

For Submission to:

Undecided

Status: NA

4.1 Abstract

Hillslope drainage into a stream can be described by the Boussinesq equation. Fundamentally, the classically employed analytical solutions to the 2-D Boussinesq equation embeds an assumption that the stream slope does not play a role in the drainage time series. This is equivalent to assuming that water drains from the hillslope perpendicularly to the stream. However, real watersheds have non-zero stream slope that increasingly contributes to the gradient of flow as the hillslope drains. The result is a 3D drainage path of the streamlines are oriented in a time-dependent vector which has down hillslope and stream slope components. Generally, the drainage network will shift from primarily stream perpendicular to stream parallel as the aquifer drains. The resulting path length grows in time, always longer than the 2D solution, and thus has increasing travel time to the stream. We show that modeling hillslope drainage in 3D is required to accurately describe the timing and magnitude of summer streamflow in response to drought. This study presents preliminary analysis exploring the theoretical framework of hillslope drainage resulting in the fundamental changes in the driving gradient for flow using a conceptual book model and a mathematical model.

4.2 Introduction

Traditionally, shallow groundwater drainage in a hillslope has been calculated assuming water flows down the hillslope in a pathway perpendicular to the stream. This is based on classical theory, where the outflow of a hillslope aquifer into a steam is described by the Boussinesq equation (Brutsaert and Nieber, 1977). This model assumes a homogenous rectangular aquifer with perfect stream-wide symmetry, implicitly suggesting the water flows perpendicularly in the hillslope to the stream. Further, the representation requires that vertical velocity can be neglected based on the Dupuit-Forchheimer assumption of groundwater flow in an unconfined aquifer where the flow is parallel to the bed (Boussinesq, 1877). A limited number of exact solutions to this formulation exist for horizontal and sloping aquifers (Boussinesq, 1877; Polubarinova-Kochina, 1962; Rupp and Selker, 2006b). For both horizontal and sloping aquifers, the two-dimensional representation of the aquifer assumes negligible contribution to hillslope flow in the down-river direction. As a result of the hydraulic

gradient between the aquifer and the stream, water flows from the hillcrest to the stream in the aquifer in a path that is perpendicular to the stream.

While the assumption for perpendicular flow is valid when the streambed slope is negligible, as for flat streams where the aquifer width is constant in space, it is not valid in watersheds where the stream has slope of the same order of magnitude as the slope of the free-surface of the aquifer. By simplifying a headwater watershed to fit the 2D representations, we neglect the stream slope as a driving factor for flow and mischaracterize the flow path length and the residence time (Leapold and Dunne, 1979; McDonnell *et al.*, 1996). In contrast to the 2D solutions, a watershed with stream slope will drain at an angle in the downstream and downhill directions based on the steepest gradient. The resulting drainage path is 3D, just like the watershed, not the perpendicular to stream flow paths described by 2D models. The changes in drainage patterns will be consequential for the timing and magnitude of summer baseflow during drought as the aquifer drains and the driving gradient of flow is shifted to the downstream direction, thus increasing the drainage path length. Using the existing 2D models and analytical solutions, the temporal and spatial patterns of streamflow during drought are not being captured, leading to models that incorrectly predict summer streamflow. Water managers need accurate streamflow predictions to effectively manage water resources within a basin, but this can't be met if models are not capturing the temporal evolution of hillslope drainage and streamflow during drought.

Previous studies have documented the 3D nature of shallow groundwater flow in hillslopes at angles pointing downstream of stream perpendicular (van Meerveld *et al.*, 2015; Rodhe and Seibert, 2011). Rodhe and Seibert (2011) observe the greatest change in flow direction occurs at the foot of the hillslope. At the foot of the hillslope close to the stream, the flow direction changed from towards the stream to parallel with the stream by 25–30° relative to stream perpendicular. They also concluded that there are negative relationships between the variation in flow direction and the slope of the ground surface and the groundwater table surface. While these studies captured spatial and temporal changes in groundwater flow patterns, the discrete measurements of the groundwater table were not enough the capture the evolution of flow under extended

drying periods. Thus, there is an opportunity to capture the full temporal and spatial extents of shallow aquifer flow patterns with an increased resolution that is necessary to describe how the flow patterns change during a severe drought. Consequently, developing a 3D hillslope drainage model for alpine catchments that incorporates both hillslope and stream slope relief to gain a more complete understanding of streamflow response to drought.

Other studies have also analyzed drainage flow and attributed drainage patterns to various factors including the gradient in moisture content (Lu *et al.*, 2011), hydraulic conductivity with depth (Ameli, McDonnell, *et al.*, 2016; Ameli, Amvrosiadi, *et al.*, 2016), bedrock slope and weather (Camporese *et al.*, 2019; Harman and Cosans, 2019), and the geometry of the hillslope using Peclet number (Lyon and Troch, 2007) and the Brutsaert hillslope number (Berne *et al.*, 2005; Brutsaert, 1994). However, many studies use 2D representations of hillslope drainage. As a result, representing an alpine catchment in 2D by ignoring the stream slope angle will consequently change the driving gradient for flow (Goode and Konikow, 1990; Y. Fang, P. Broxton, D. Gochis, G.-Y. Niu, J. D. Pelletier, P. A. Troch, and X. Zeng, 2015).

Studies have acknowledged the problematic nature of using the simplified representation hillslope drainage of 2D, and suggested improvements by including soil water storage (Troch *et al.*, 2003) or lateral flow (Kong *et al.*, 2016). However, the 2D simplification have been acknowledged to systematically reduce the accuracy of our models as heterogeneity and watershed complexity is simplified (McDonnell *et al.*, 2007; Mirus *et al.*, 2016; Weiler and McDonnell, 2007). It is understandable that in the past the 2D simplifying assumption has been used to reduce a complex 3D watershed into 2D models and numeric solutions, but with the current resources available and the increased importance of predicting system response, there is a need for more refined solutions. Additionally, since alpine watersheds disproportionately control both timing and magnitude of streamflow to downstream communities in natural systems, consisting of a small area but most of the precipitation origin, there is a need for research focus emphasizing the understanding alpine systems in drought (Markovich *et al.*, 2016). Recently, there have been three studies utilizing models that include 3D

drainage (Carlier *et al.*, 2019; Fan *et al.*, 2019; Y. Fang, P. Broxton, D. Gochis, G.-Y. Niu, J. D. Pelletier, P. A. Troch, and X. Zeng, 2015). However, we do not know of a study that quantifies the 3D approach to address hillslope drainage and compares the errors in path length and retention time compared to 2D hillslope drainage.

Headwaters with 1st and 2nd order streams account over two thirds of total stream length of a river network (Leapold *et al.*, 1964). Because headwaters have significant contributions water resources management including water quality (Alexander *et al.*, 2007), biodiversity (Meyer *et al.*, 2007), and hydrologic connectivity (Nadeau and Rains, 2007) it is important to correctly describe hillslope drainage paths, path length, and residence times. For 2D models that only account for water flow perpendicular to the stream, calculating path length and mean transit time also implicitly follow this assumption. The residence time is the average time a parcel of water is in a watershed between entering and exiting the watershed. The concept is essential for groundwater management decisions that require quantification of aquifer properties including storage capacity, mixing processes, and subsurface flow paths. The residence time of groundwater is often calculated using tracer analysis from surface water samples (Gilmore *et al.*, 2016; Maloszewski and Zuber, 1982; McGuire *et al.*, 2005; McGuire and McDonnell, 2006). Knowing the path of hillslope drainage is crucial for estimating the residence time of a draining aquifer (Ameli, Amvrosiadi, *et al.*, 2016; Hale *et al.*, 2016).

The objective of this paper is to provide a conceptual framework for describing hillslope drainage in 3D watersheds and to illustrate the consequences in a changing path length and residence time as streamlines rotate due to a declining water table.

4.3 Methods

This paper explores hillslope drainage for a 3D aquifer compared to a 2D aquifer using a conceptual model, mathematical model, and a numerical model. Nine models with different geometries are compared for drainage path length, residence time, and drainage angle using the mathematical model and the numerical model.

4.3.1 Conceptual Model

The dynamic geometry of a hillslope and stream system can be visualized as a book, with the spine representing the stream and the free-surface of the hillslopes aquifer being represented by the pages (Figure 16). The aquifer gradient can be envisioned by holding the book with the pages splayed open and the spine resting in your palm. With the book spine parallel with the floor, consider the gradients as you close the book partially. In this configuration, we see that water would flow along the lines of text towards the spine (perpendicular to the stream). This is the classical representation of a 2D hillslope drainage model.

If the book spine is tilted, the aquifer is necessarily 3D. The flow paths are no longer perpendicular to the spine: flow paths are dependent on the angle of the spine *and* of the slope of the pages. In cases where the spine is steeper than the pages, the direction of flow will be dominantly in the downstream direction, while when the page-angle is more severe than the spine, flow will dominantly be in the hillslope direction. Thus, as the aquifer drains, the flow vector rotates from being largely perpendicular to the stream when the hillslope-oriented gradient is large, toward more stream-parallel as the "pages" lay ever flatter as the book opens (the free surface becomes more level as it drains). While 2D hillslope models only allow for hillslope drainage in the x-z direction perpendicular to the stream, the 3D hillslope is represented in the x-y-z directions with the drainage path influenced by the combination of the aquifer gradient in both the hillslope and the streamwise directions (Figure 15).

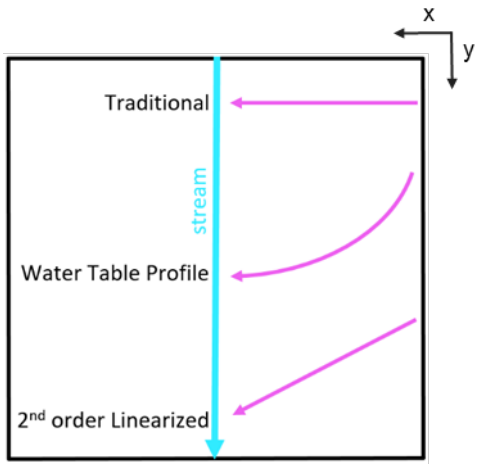

Figure 15. Plan view of flow paths of hillslope drainage

A first-order estimate of transit time can be calculated using Darcy's Law (Darcy, 1856) where specific discharge (L/T) is the negative hydraulic conductivity times the hydraulic gradient. The mean transit time is dependent on the Darcy velocity, specific discharge divided by porosity. This simple calculation will be used in the following text to approximate the mean transit time for a parcel of water draining from the hillcrest to the stream in the hillslope's aquifer to compare again model results. As a further simplification, Equation (15) uses a constant gradient along the flow path as in the linearized water table to approximate the path length.

$$T = \frac{L \cdot n}{-K \cdot \nabla H} \tag{15}$$

Where T is the travel time, L is the path length through soil, n is the porosity, K is the hydraulic conductivity, and ∇H is the hydraulic gradient.

Without added percolation, in time the aquifer will drain and the water table will lower. In the book metaphor, the pages become less steep over time, increasingly oriented in the downstream direction, resulting in an increasing path length and decreasing gradient along the streamline in time. The water flow represented in vectors will rotate from being hillslope driven perpendicular to the stream to stream angle driven and more parallel to the stream. Figure 16 shows how the drainage vectors will change across time as the aquifer drains and the water table lowers.

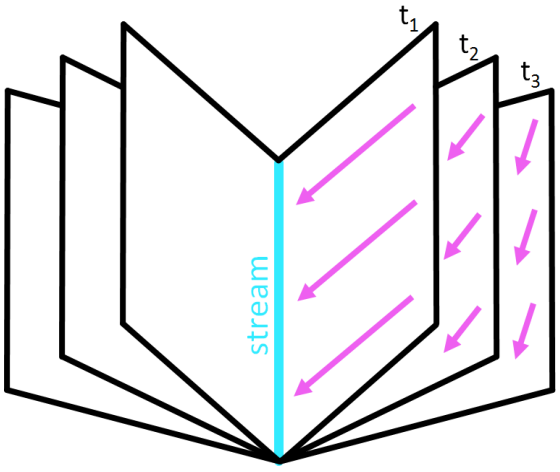

Figure 16. Book conceptualization of hillslope drainage illustrating flow vector rotation towards stream-parallel as the aquifer drains in time (t1, t2, and t3 being successive snapshots of the aquifer).

4.3.2 Mathematical Model

The model geometry is based on the classical representation of an aquifer, with homogeneous soil properties, a fully penetrating stream, and no-flux boundaries on the other surfaces to represent the aquifer boundary extents. The aquifer is initially saturated and allowed to drain along the stream face (a seepage plane with zero pressure head). The downstream edge of the hillslope is a seepage face with low hydraulic conductivity, representing a continuing hillslope. All other planes are no-flow boundaries. Hillslope geometry in the model is based on a parallelogram aquifer, with a hillslope length of 10 m, aquifer thickness of 3 m, and a stream length of 50 m (Figure 17). The hillslope angle and the stream angle vary for different trails. The aquifer drains for a total of 120 days, or until the water content reaches the residual water content. Soil characteristics are classified using the residual water content, saturated water content, empirical coefficients in the soil water retention function, saturated hydraulic conductivity (ks=5E-6 m/s), and the pore connectivity to tortuosity.

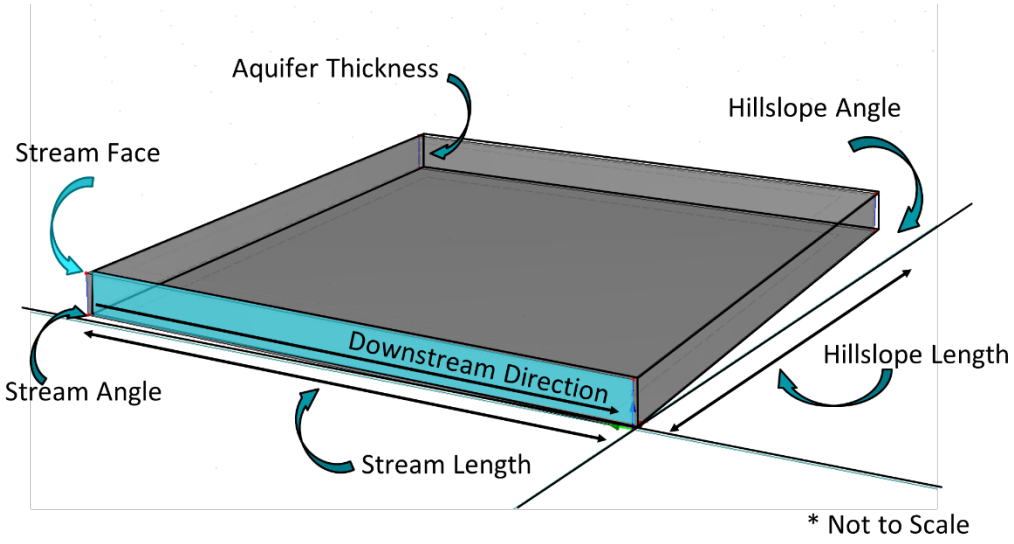

Figure 17. The geometry of the conceptualized aquifer

The geometry of a hillslope aquifer dictates how the travel path of water changes from the hillcrest to the stream. The angle of drainage in 3D can be compared

to the perpendicular 2D drainage using the difference in where a droplet of water would intersect the stream when starting at the same point of the hillslope. Using the 2nd order linearization of the Boussinesq Equation, a hillslope drainage model can be used to demonstrate the proof of concept of the displacement drainage vector. Considering only the right-hand side of the book, the angle of the spine compared to horizontal is the stream slope angle, the angle of the book pages compared to horizontal is the hillslope angle. The stream angle, γ, and the hillslope angle, β, can be identified in Figure 18. The stream angle and the hillslope angle are independent, each describing the angle compared to horizontal in the y or x directions respectively. It should be noted that the hillslope angle, β, is not the same as the ground surface slope which is often larger. The height of the water table at the crest, h, is perpendicular to the length of the hillslope, w. The stream is located along the length of the hillslope and is sufficiently long enough such that the flow from the aquifer to the stream is constant along its length. The depiction in Figure 18 shows the water table to be linear, while it may well be curved it would not materially change the results obtained here because the distance traveled along the stream would remain the same. The distance of the hillslope drainage in the horizontal stream-wise direction is referred to as the displacement vector, y.

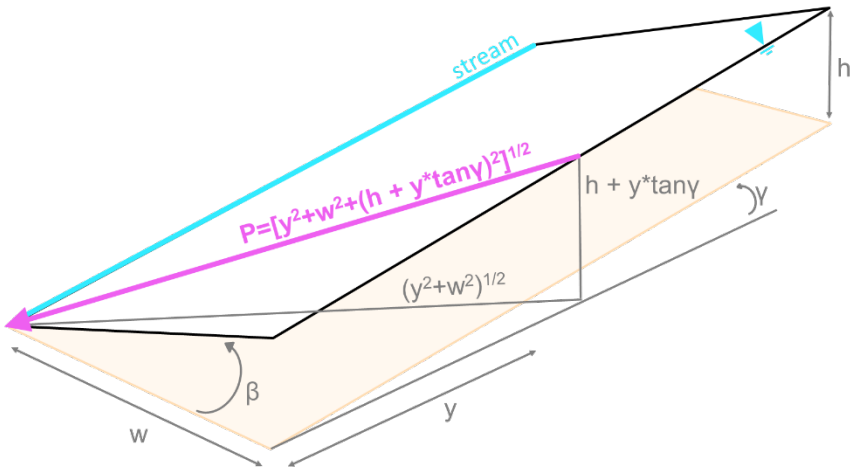

Figure 18. Geometric representation of hillslope drainage for the mathematical model

If the height of the water table is zero (h=0) then the angle aquifer is also zero (β =0), thus the slope of the water table would be zero and flow would be parallel to

the stream. This holds true for when the height of the water table is very small: when *h* is very small or zero, the flow in the aquifer is stream parallel. In this scenario, flow is perpendicular to the stream and the path length is minimized. In the other extreme, if the slope of the stream is very small or zero (γ=0) then the angle of the water table is large and the slope of the water table would be greatest perpendicularly to the stream and negligible parallel to the stream, resulting in aquifer flow that would be entirely perpendicular to the stream. In this scenario, flow parallel to the stream will result in an infinitely long flow path as the water remains in the aquifer never enters the stream.

The length of the flow path is designated by the variable *P* from Figure 18. This depiction assumes that flow paths are parallel within the hillslope. The vectors will shift between stream parallel and stream perpendicular depending on the relative magnitudes for *h* and γ. When γ=o and the stream is infinitely long, the path of hillslope drainage be easily solved for the purely 2-dimensional flow along the vector P, but this rationale is often used even with the assumption of no stream slope is not valid. In the case where stream slope is not zero but the purely 2-dimensional flow is analyzed, there will be errors associated with the underestimation of the flow path length and thus the streamflow contribution will be incorrect. Fortunately, it is not particularly difficult or confusing to obtain the magnitude and direction of P for a 3-dimensional flow when the stream slope is not zero. The magnitude of P can be calculated using the Pythagoreans theorem, shown in Figure 18. The direction of P is expressed as the displacement vector, y, which is the stream-parallel displacement of the up-slope end of P relative to the point where P enters the stream. Since water flows is controlled the steepest gradient, the displacement vector is solved such that the slope of P is maximized to retain the expected limit behavior of the slope (γ at *h* = 0 and β when y= 0) shown in Equation (16).

$$slope(P) = tan^{-1}\left[\frac{h + y * tan\gamma}{(y^2 + w^2)^{\frac{1}{2}}}\right] \tag{16}$$

Since the arctangent is a monotonic function with a positive slope as a function of its argument in the range of 0 to 1, the maximum slope of Equation (16) is solved for by finding the value of y at which the derivative to zero shown in Equation (17).

$$\frac{d}{dy}\left[\frac{h + y * tan\gamma}{(y^2 + w^2)^{\frac{1}{2}}}\right] = 0 \tag{17}$$

By applying the product rule and the chain rule while taking the derivative of the function in Equation (17), the yielding equation can be simplified and expressed as the displacement vector, y, shown in Equations (19) and (19).

$$-y * \frac{h + y * tan\gamma}{(y^2 + w^2)^{\frac{3}{2}}} + \frac{tan\gamma}{(y^2 + w^2)^{\frac{1}{2}}} = 0 \tag{18}$$

$$y = w^2 * \frac{tan\gamma}{h} \tag{19}$$

Based on Equation (19), the drainage angle will be greater for smaller water table heights. For a steep hillslope angle, $\beta=\tan^{-1}(h/w)$, the drainage path will be driven by β such that the flow will be primarily perpendicular to the stream. This trend is the same as shown in the conceptual model using the book analogy from the previous section. In gradually sloped hillslopes, the displacement vector will be larger and the flow will be driven by γ and be parallel to the stream. Alternatively, the displacement can be written as a function of the ratio between the stream and aquifer slopes. Equation (20) shows that the displacement vector is a function of the stream angle, hillslope angle, and the distance from the hillslope crest to the stream. As a result, the path length P can be expressed using only the variables of hillslope length, stream angle, and hillslope angle in Equation (21).

$$y = w * \frac{tan\gamma}{tan\beta} \tag{20}$$

$$P = \sqrt{\left(w \cdot \frac{tan\gamma}{tan\beta}\right)^2 + w^2 + \left(w \cdot \tan\beta + \left(w \cdot \frac{tan\gamma}{tan\beta}\right)\tan\gamma\right)^2} \quad (21)$$

An aquifer with gradient in the direction of the hillslope of 5º and a stream slope of 1º and hillslope distance from stream to the crest of 10 m will have an initial displacement of 2 m. Traditional modeling would have a flow path length of 10.0 meters (purely perpendicular to the stream), but the 3-dimensional linearized flow path is 10.2 m (11.3 º from stream perpendicular) and a transit time of 21.2 d. After the water table drains, the aquifer slope may decrease to 2.5º and the displacement vector will increase to 4 m and the total path length increases to 10.8 m (21.8 º from stream perpendicular) and a transit time of 25.0 d.

The geometry of the system is important to evaluate when determining if the assumption of a stream perpendicular streamflow is valid. Fundamentally, the stream angle must have a non-zero slope in order to produce a non-zero displacement vector. In general, conditions where the sweeping drainage vectors may occur are shallow slopes with deep soil columns. A deep soil column or permeable bedrock is needed in order for drainage to occur such that the water table lowers enough to change the driving gradient. In shallow soil columns, the water table change would not be significant enough to change the driving gradient of flow. The hillslope height, h, that is less than the soil column depth can drain enough so that the relative change in water table height is significant compared to the initial water table angle. When the hillslope angle is larger than the stream slope angle, a saturated soil column will be dominated by hillslope drainage but as the hillslope drains then drainage can rotate to the streamwise direction. In order to maintain the Dupuit-Forchheimer assumption of a negligible vertical gradient, the stream elevation change should not be significantly larger than the soil thickness.

Watersheds with low angle and moderate soil column depths can result in sweeping drainage vectors that change the drainage path, path length, and residence times. In contrast, watersheds with very steep hillslopes or thin soil depths will not experience a significant change in the driving gradient as the hillslope drains and thus

a rotation of flow vectors is not pronounced. These comparisons of the aquifer geometry can help qualitatively determine when rotating vectors would arise and have the potential to change the flow path and residence time of a draining hillslope.

A total of nine model geometries are analyzed: one representing a horizontal Boussinesq aquifer, two which represented a sloping aquifer with the 2D flow, four with both a hillslope angle and stream angle representing the 3D flow case, and two which only had a stream slope angle with no hillslope angle (Table 3). The ratio of slopes from Equation 6 describes the displacement vector, with higher slope ratios corresponding to greater displacement vectors, path lengths, and transit times.

Table 3. Nine model configurations

Model #	**Model Description**	**Stream Angle (%)**	**Hillslope Angle (%)**	**Slope Ratio**
1	Horizontal Aquifer	0	0	0
2	Sloping Aquifer	0	0.1	0
3	Sloping Aquifer	0	0.2	0
4	3D	0.05	0.1	0.5
5	3D	0.05	0.2	0.25
6	3D	0.1	0.1	1
7	3D	0.1	0.2	0.5
8	w/o hillslope	0.05	0	-
9	w/o hillslope	0.1	0	-

4.4 Results

For each of the nine model configuration, the displacement vector and path length can be calculated using the mathematical model (Table 4). The transit time is approximated from Equation (16). For the horizontal aquifer, the initial path length is 10 m, the same as the hillslope length. For both the horizontal aquifer and sloping aquifer cases, there is no initial displacement vector as these cases represent the 2D drainage cases. The initial displacement vector increases when the ratio of stream angle to stream slope increases, whereas the initial path length is proportional to both the stream angle and hillslope angle. For the two geometries that have a stream angle but no hillslope angle, the water would flow parallel to the stream, and assuming an infinity long hillslope, the path length and transit time would be theoretically infinite.

For very small values for the stream angle and hillslope angle, the small-angle approximation can be invoked where the $\tan(\theta) \approx \theta$ and thus the displacement vector calculated in Equation (20) can be approximated by the ratio of the stream slope to the hillslope multiplied by the hillslope width using Equation (22).

$$y \approx w * \frac{\gamma}{\beta} \tag{22}$$

Table 4. Calculated initial displacement vector, path length, and flow path angle using the mathematical model for seven of the model geometries. Models with greater slope ratios have longer path lengths and residence times compared to models with smaller slope ratios. Models 8 & 9 have infinite or not defined initial displacement, initial path length, and transit time because the flow path is parallel to the stream.

Model #	Stream Angle (%)	Initial Hillslope Angle (%)	Initial Displacement (m)	Initial Path Length (m)	Transit time (d)	Angle from Perpendicular (º)
1	0	0	0	10.0	23.1	0

2	0	0.1	0	10.0	18.3	0
3	0	0.2	0	10.0	15.1	0
4	0.05	0.1	5.0	11.2	21.8	26.6
5	0.05	0.2	2.5	10.3	15.7	14.1
6	0.1	0.1	10	14.1	30.4	45.2
7	0.1	0.2	5.0	11.2	17.4	26.8
8	0.05	0	-	-	-	90.0
9	0.1	0	-	-	-	90.0

As the aquifer drains and the water table lowers, the hillslope angle decreases. Table 5 shows the scenario where the path length and transit time when the water table lowers such that the saturated aquifer thickness decreases by a factor of two. For the horizontal and sloping aquifers, the change in the water table level has no effect of the displacement vector but slightly decreases the path length and transit time. For the four 3D models with both a stream slope and hillslope angle, lowering the water table changes the driving gradients for flow, increasing both the path length and transit time Figure 19. Model 6 has the largest increase in path length with the lowered water table, consistent with expectations because the model has the highest stream slope to the hillslope ratio. Initially, Model 6 has a stream slope and hillslope angle of 0.1% and when the aquifer drains the stream angle is 2X greater than the hillslope angle and is the only model where the hillslope angle is less than the steam angle but non-zero. The slope ratio is proportional to an increase of path length, transit time, and flow angle. The increase in the stream slope corresponds to an increased path length when the hillslope angle decreases corresponding with the lowering of the water table. For all

four 3D models, the streamflow angle rotated to be more stream parallel as the water table lowered (Figure 20).

Table 5. The change in path length, transit time, and flow path angle when the water table lowers such that the saturated aquifer thickness decreases by a factor of two, representing an aquifer that has drained and the resulting water table has lowered. Models is greater slope ratios have longer path lengths and transit times. Models 8 & 9 have infinite or not defined initial displacement, initial path length, and transit time because the flow path is parallel to the stream.

Model #	Stream Angle (%)	Final Hillslope Angle (%)	Final Displacement (m)	Final Path Length (m)	Transit time (d)	Angle from Perpendicular (°)
1	0	0	0	10.0	23.1	0
2	0	0.05	0	10.0	20.5	0
3	0	0.1	0	10.0	18.5	0
4	0.05	0.05	10.0	14.2	36.8	45.0
5	0.05	0.1	5.0	11.2	21.9	26.6
6	0.1	0.05	20.0	22.5	70.6	63.6
7	0.1	0.1	10.0	14.2	30.7	45.2
8	0.05	0	-	-	-	90.0
9	0.1	0	-	-	-	90.0

Figure 19. Percent change in path length (orange circles) and transit time (blue diamonds) compared to the initial ratio of slopes defined as tan(γ)/tan(β) for Models 1-7. For models with a zero stream slope or hillslope, the path length decreases slightly as the water table lowers. For the four models 3D models, lowering the water table changes the driving gradients for flow, increasing the path length and transit time.

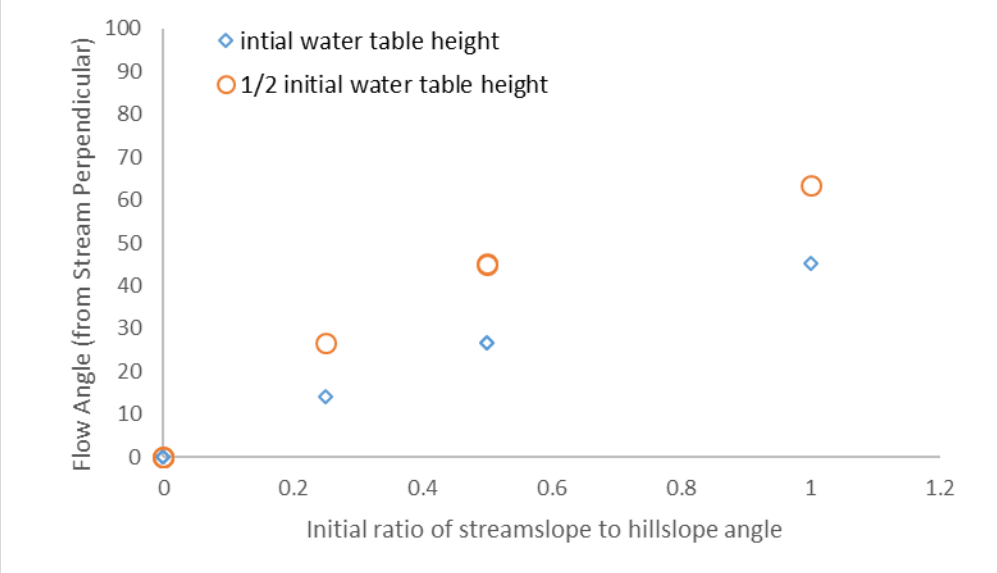

Figure 20. The flow vector angle from stream perpendicular for a lowering water table. For all four 3D models, the streamflow angle rotated to be more stream parallel as the water table lowered. Models 8 & 9 have flow lines parallel to the stream because there is no hillslope angle and thus the result is a flow angle 90 degrees from stream perpendicular.

4.5 Conclusions

An aquifer draining into a stream is described by the Boussinesq equation and characterizes hillslope drainage. Fundamentally, the Boussinesq equation and its analytical solutions use a 2D aquifer where the stream has no slope. As a result, water drains the hillslope from the aquifer perpendicularly to the stream because the hillslope angle dominates flow direction. However, real watersheds have a stream slope that is often not negligible, and that nonzero stream slope will contribute to the gradient of flow. The result is a 3D drainage path of the hillslope. This paper uses a conceptual book model used for visualization, a mathematical model, and a numerical model to describe hillslope drainage of a 3D aquifer.

The mathematical model uses a linearized water table to calculate the length of the drainage path based on the hillslope angle and the stream slope angle. The distance of the hillslope drainage in the horizontal stream-wise direction is referred to as the displacement vector as is based on the ratio of the tangents for the stream angle and hillslope angle. The path length, mean transit time, flow path angle estimates can also be calculated. For 3D watersheds, hillslope drainage starts as primarily perpendicular to the stream and as the water table lowers the drainage vectors rotate and become more stream parallel. The result is a rotation of the flow paths going farther away from perpendicular to the stream, becoming longer and having a lower gradient. This rotation will result in an increased path length and transit time.

When considering a 3D hillslope, hillslope drainage is controlled by both the hillslope angle and the stream angle. The hillslope drains diagonally downstream and downslope with a path length longer than the perpendicular to the stream flow path in 2D drainage paths. This study presents preliminary analysis exploring the theoretical framework of hillslope drainage resulting in the fundamental changes in the driving gradient for flow. The driving gradient is determined by the ratio of the stream angle to the hillslope angle, thus the driving gradient controlled by the downslope direction for very large hillslope angles compared to the driving gradient of downstream for comparatively large stream angles. While the geometry of the watershed does not change, the effective hillslope angle decreases as the aquifer drains, thus transitioning

from a driving gradient of down hillslope to streamwise corresponding to streamlines rotating from stream perpendicular to stream parallel. This results in the path of steepest descent that the water will drain, shifting the actual flow lines from being primarily perpendicular to the stream rotating until they are stream parallel, resulting in a longer the path length and residence time of hillslope drainage.

References

Alexander, R.B., E.W. Boyer, R.A. Smith, G.E. Schwarz, and R.B. Moore, 2007. The Role of Headwater Streams in Downstream Water Quality. Journal of the American Water Resources Association 43:41–59.

Ameli, A.A., N. Amvrosiadi, T. Grabs, H. Laudon, I.F. Creed, J.J. McDonnell, and K. Bishop, 2016. Hillslope Permeability Architecture Controls on Subsurface Transit Time Distribution and Flow Paths. Journal of Hydrology 543:17–30.

Ameli, A.A., J.J. McDonnell, and K. Bishop, 2016. The Exponential Decline in Saturated Hydraulic Conductivity with Depth: A Novel Method for Exploring Its Effect on Water Flow Paths and Transit Time Distribution. Hydrological Processes 30:2438–2450.

Berne, A., R. Uijlenhoet, and P.A. Troch, 2005. Similarity Analysis of Subsurface Flow Response of Hillslopes with Complex Geometry. Water Resources Research 41:1–10.

Boussinesq, J., 1877. Essai Sur La Theorie Des Eaux Courantes. Mem. Acad. Sci. Inst. Fr. 31:252–260.

Brutsaert, W., 1994. The Unit Response of Groundwater Outflow from a Hillslope. Water Resour. Res. 30:2759–2763.

Brutsaert, W. and J.L. Nieber, 1977. Regionalized Drought Flow Hydrographs from a Mature Glaciated Plateau. Water Resources Research 13:637–643.

Camporese, M., C. Paniconi, M. Putti, and J.J. Mcdonnell, 2019. Supporting Information for " Fill and Spill Hillslope Runoff Representation with a Richards Equation- Based Model ." Water Resources Research:2–4.

Carlier, C., S.B. Wirth, F. Cochand, D. Hunkeler, and P. Brunner, 2019. Exploring Geological and Topographical Controls on Low Flows with Hydrogeological Models. Groundwater 57:48–62.

Fan, Y., M. Clark, D. Lawrence, S. Swenson, L.E. Band, S. Brantley, P. Brooks, W. Dietrich, A. Flores, G. Grant, J. Kirchner, D. Mackay, J. McDonnell, P. Milly, P. Sullivan, C. Tague, H. Ajami, N. Chaney, A. Hartmann, P. Hazenberg, J. McNamara, J. Pellet, J. Volk, and D. Yamazaki, 2019. Hillslope Hydrology in Global Change Research and Earth System Modeling. Water Resources Research, AGU Centennial Volume on GRAND CHALLENGES IN THE EARTH AND SPACE SCIENCES:1737–1772.

Gilmore, T.E., D.P. Genereux, D.K. Soloman, and J.E. Solder, 2016. Groundwater Transit Time Distribution and Mean from Streambed Sampling in an Agricultural Coastal Plain Watershed, North Carolina, USA. Water Resources Research 52:2025–2044.

Goode, D.J. and L.F. Konikow, 1990. Apparent Dispersion in Transient Groundwater Flow. Water Resources Research 26:2339–2351.

Hale, V.C., J.J. Mcdonnell, M.K. Stewart, D.K. Solomon, J. Doolitte, G.G. Ice, and R.T. Pack, 2016. Effect of Bedrock Permeability on Stream Baseflow Mean Transit Time Scaling Relationship. :1375–1397.

Harman, C.J. and C.L. Cosans, 2019. A Low-Dimensional Model of Bedrock Weathering and Lateral Flow Coevolution in Hillslopes: 2. Controls on Weathering and Permeability Profiles, Drainage Hydraulics, and Solute Export Pathways. Hydrological Processes 33:1168–1190.

Kong, J., C. Shen, Z. Luo, G. Hua, and H. Zhao, 2016. Improvement of the Hillslope-Storage Boussinesq Model by Considering Lateral Flow in the Unsaturated Zone. Water Resources Research 52:2965–2984.

Leapold, L.B. and T. Dunne, 1979. Water in Environmental Planning. W.H. Freeman, New York, NY.

Leapold, L.B., M.G. Wolman, and J.P. Miller, 1964. Fluvial Processes in Geomorphology. Dover Publications, Inc., New York, NY.

Lu, N., B.S. Kaya, and J.W. Godt, 2011. Direction of Unsaturated Flow in a Homogeneous and Isotropic Hillslope. Water Resources Research 47:1–15.

Lyon, S.W. and P.A. Troch, 2007. Hillslope Subsurface Flow Similarity: Real-World Tests of the Hillslope Péclet Number. Water Resources Research 43:1–9.

Maloszewski, P. and A. Zuber, 1982. Journal of Hydrology, 57 (1982) 207--231. 57:207–231.

Markovich, K.H., R.M. Maxwell, and G.E. Fogg, 2016. Hydrogeological Response to Climate Change in Alpine Hillslopes. Hydrological Processes. doi:10.1002/hyp.10851.

McDonnell, J.J., J. Freer, R. Hooper, C. Kendall, D. Burns, K. Beven, and J. Peters, 1996. New Method Developed for Studying Flow on Hillslopes. EOS Transactions American Geophysical Union 77:465–472.

McDonnell, J.J., M. Sivapalan, K. Vaché, S. Dunn, G. Grant, R. Haggerty, C. Hinz, R. Hooper, J. Kirchner, M.L. Roderick, J. Selker, and M. Weiler, 2007. Moving beyond Heterogeneity and Process Complexity: A New Vision for Watershed Hydrology. Water Resources Research 43:1–6.

McGuire, K.J. and J.J. McDonnell, 2006. A Review and Evaluation of Catchment Transit Time Modeling. Journal of Hydrology 330:543–563.

McGuire, K.J., J.J. McDonnell, M. Weiler, C. Kendall, B.L. McGlynn, J.M. Welker, and J. Seibert, 2005. The Role of Topography on Catchment-Scale Water Residence Time. Water Resources Research 41:1–14.

van Meerveld, H.J., J. Seibert, and N.E. Peters, 2015. Hillslope-Riparian-Stream Connectivity and Flow Directions at the Panola Mountain Research Watershed. Hydrological Processes. doi:10.1002/hyp.10508.

Meyer, J.L., D.L. Strayer, J.B. Wallace, S.L. Eggert, G.S. Helfman, and N.E. Leonard, 2007. The Contribution of Headwater Streams to Biodiversity in River Networks. Journal of the American Water Resources Association 43:86–103.

Mirus, B., J. Smith, J. Godt, and R. Baum, 2016. Simulated Effect of Topography and Soil Properties on Hydrologic Response and Landslide Potential under Variable

Rainfall Conditions in the Oregon Coast Range,. Landslides and Engineered Slopes:1431–1439.

Nadeau, T.L. and M.C. Rains, 2007. Hydrological Connectivity between Headwater Streams and Downstream Waters: How Science Can Inform Policy. Journal of the American Water Resources Association 43:118–133.

Polubarinova-Kochina, P.Y., 1962. Theory of Ground Water Movement. Princeton Univ. Press, Princeton, N.J.

Rodhe, A. and J. Seibert, 2011. Groundwater Dynamics in a till Hillslope: Flow Directions, Gradients and Delay. Hydrological Processes. doi:10.1002/hyp.7946.

Rupp, D.E. and J.S. Selker, 2006. On the Use of the Boussinesq Equation for Interpreting Recession Hydrographs from Sloping Aquifers. Water Resources Research 42:1–15.

Troch, P.A., C. Paniconi, and E. Emiel van Loon, 2003. Hillslope-Storage Boussinesq Model for Subsurface Flow and Variable Source Areas along Complex Hillslopes: 1. Formulation and Characteristic Response. Water Resour. Res. 39:1316.

Weiler, M. and J.J. McDonnell, 2007. Conceptualizing Lateral Preferential Flow and Flow Networks and Simulating the Effects on Gauged and Ungauged Hillslopes. Water Resources Research 43:1–13.

Y. Fang, P. Broxton, D. Gochis, G.-Y. Niu, J. D. Pelletier, P. A. Troch, and X. Zeng, P.H., 2015. A Hybrid-3D Hillslope Hydrologicalmodel for Use in Earth System Models. Water Resources Research 51:8218–8239.

Chapter 5. General Conclusions

This dissertation was motivated by the "snow drought" of 2015 in the Oregon Cascades when, despite the nearly normal total precipitation over the winter, the winter snowpack never reached 20% of the average snowfall across the Cascades Mountain Range. In the Oregon Cascades, many of the watersheds has streams that are snowmelt driven, especially for late-summer streamflow (Nolin and Daly, 2006). With the historically low snowpack, the summer streamflow was expected to reach historical lows. The reduced snowpack is equivalent to a 4ºC climate warming scenario, presenting a unique opportunity to test fundamental hypotheses of headwater stream response to changes in the amount and timing of recharge during drought conditions. We seek to describe the hydrological responses of such anomalous - but near future normal - recharge conditions.

With the reduced snowpack, climate models predicted that the summer flows would be greatly reduced, and thus new historic streamflow would be observed from the following summer hydrograph. In contrast to most model predictions, the 2015 hydrographs from watersheds did not result in any record low streamflow during the summer months despite reaching new minimums during spring flows. The late summer streamflow did not reach new record lows despite the lack of precipitation inputs through early fall, with the shape of the hydrograph remaining rather horizontal. The hydrographs falling limb that remains horizontal instead of continuing to decline throughout the summer would indicate a recession plot that is not a constant slope, but instead with an increased slope during very late flows making the stream less sensitive to drought due to the presence of a sustaining baseflow.

While understanding the summer streamflow after the 2015 snow drought in the Oregon Cascades is outside the scope of this dissertation, we do seek to develop a better conceptual and mythological understanding of recession analysis that ultimately could be applied to larger regional questions. This work will seek to provide to answers such as characterizing what drought looks like, how watersheds and stream systems respond to drought, and how severely climate change will affect the hydrology of the

watershed streamflow. In this dissertation, recession analysis is used as a tool to aids in the development of a conceptual framework for understanding and improving predictions for drought flow. This work is possible because of recent improvements in recession analysis that removes computation artifacts associated with the computational aspects of taking the derivative of flow (Kirchner, 2009; Roques *et al.*, 2017; Rupp and Selker, 2006a). By removing the obscuring computation artifacts, it is possible for this work to focus on low flow behavior has not been possible in the past in order to advance our thinking about advancing our thinking about how we can use recession analysis, conceptually and methodologically.

If a watershed does exhibit a sustaining baseflow it indicates that a watershed is more resilient to drought that originally thought. This dissertation has attempted to identify issues surrounding the current understanding of watershed responses to drought and provide improvements by: 1) introduced a methodology that can greatly expand the number of watershed analyzed using recession analysis with water height instead of discharge, 2) analyze the impacts of different recession analysis methods on the parameter estimations, supporting the use of individual recession to describe average watershed response, and 3) the rotation of flow vectors in 3D that results in an increased path length and residence time that isn't captured when modeling hillslope drainage in 2D. While this dissertation has developed a framework for better understanding and predicting drought flows there are still opportunities to improve the characterization.

Expanding the number of watersheds analyzed using recession analysis opens door for characterizing watersheds and regions that were previously inaccessible, uncovering data that were there but we just didn't have access to. Because small and headwater basins are disproportionally ungauged, the first explorative step to characterizing the watersheds could be recession analysis using water height measurements (Mcmanamay *et al.*, 2014; McManamay and Derolph, 2019). With the introduction of satellite products measuring water height at precise vertical scales, the accessibility of data for this analysis and thus the watersheds that could be characterized will skyrocket. Increasing the accessibility to recession analysis would also smaller

watersheds to be monitored that are within a larger monitored basin. Using this nested approach allows us to examine how the individual responses at smaller watersheds combine into the larger response. This would be interesting when considering the heterogeneity between watersheds and the variability in the ensemble response, comparing it to the validity of the Boussinesq aquifer "meta hillslope" representation. The analysis of the Swiss watersheds revealed a slope ratio less than 1, contradictory to the classical analytical solutions of early and late-time drainage for recession analysis. This methodology provides an opportunity to look at many more watersheds and characterize them based on high and low flow regimes, challenging the early to late-time drainage regimes so fundamental to recession analysis.

Currently, literature describes two drainage regimes as early-time and late-time. However, the variability between individual recessions including higher slopes at lower flows suggests that these two flow regimes don't capture controlling factors of recessions sufficiently. In order to systematically look at controlling factors of recession analysis beyond early and late-time drainage, we constructed synthetic hydrographs to assess the effects of event inter-arrival time, magnitude, and antecedent conditions on the distribution of individual recession events that comprise the pattern of collective recessions. Analyzing the events collectively was found to be an artifacts of the distribution of the individual recessions and not representative of watershed responses, while the median individual events were representative of a typical watershed response pattern. Looking at individual recessions as a representative form of watershed response, we found that the event magnitude controlled the starting discharge for the individual recession, the event length controlled the length of the individual recession, and the antecedent conditions controlled the variability in recession constants for individual recessions. Using log-normally distributed event magnitudes and inter-arrival times along with linear superposition of events, we were able to reproduce the variability of individual recessions using the synthetic hydrograph compared to a USGS gaged site. The superposition of events does produce the variability in individual events, but we acknowledge that there are other ways to create watershed memory that would also generate variability, and the effects of parameter

estimation from different reservoir models for combing events into a hydrograph would be worthwhile research to peruse. It could be interesting to use baseflow separation to separate baseflow from quick flow for recession analysis to characterize each flow contribution using two different types reservoir models instead of a single model reservoir representation type. This could introduce recession variability that differs between high flow events and low flow events.

Throughout this dissertation, individual recessions are referred to with their main attribute being the slope. Analytical solutions suggest that recessions in log-log space should be linear, and thus solely describing individual recessions using slope ignore variability regarding the linearity or apparent non-linearity of an individual recession. While the degree of linearity or non-linearity of individual recessions is not explicitly addressed in this research, we do think it is important to consider the curvature of individual recessions and the effects on the variability between events. When doing recession analysis on various streams throughout the duration of the research for chapters in this dissertation, we have noticed that some individual recessions are not linear. This has been supported by recent papers noting the concavity or convexity of individual recession, particularly concavity at low flows (Shaw and Riha, 2012; Tashie *et al.*, 2020). It should be noted that advancements in computation aspects of recessions have made analysis on these low flows possible. However, a recent paper on new computational methodology and procedures for taking the derivatives for the recession analysis has shed light on low flow behaviors by removing artifacts and errors associated with taking the derivative at low flows (Roques *et al.*, 2017). The improvements in recession analysis allow for this work to focus on low flow ranges, where previous works wouldn't have been possible because of computational artifacts obscuring interpretation of results. Now that we can see the concavity of some individual recessions at low flow ranges, what does this tell us about the flow regime and how is it different than late-time drainage?

The analytical solution for late-time drainage assumes that a 3/2 slope will continue to be constant for the decreasing flows during the recession event, without exception. However, we and other have observed individual recession curves where the

slope of the recession is greater than the characteristic slope of 3/2. More interestingly these low flow recessions with large slopes also tend to have concavity, where the slope of the individual recession changes with flow; at the begging of the individual recession, the slope is smaller but as the recession continues and the flow decreases the slope increases. This phenomena is hereafter referred to as tailing, identified as the slope increase of an individual recession with decreasing flow. Recession slope is an indicator of how stable discharge is, thus for low flows a small slope indicates an unstable stream flow whereas a large slope indicates a stable streamflow. For an individual recession with tailing, initially the slope is small which means that streamflow continues to decrease (the rate of streamflow decline is constant for a given discharge). The increased slope at low flow means that the streamflow is becoming more stable (ie the rate of streamflow decline is decreasing for a given discharge). Tailing behavior implies that the streamflow will reach a stable flow sooner than traditional modeling approaches imply, and that these watersheds may be resilient to drought conditions from climate change because they have a sustainable baseflow. Figure 21 shows the comparison between the traditional Boussinesq aquifer recession plot, in which you can clearly identify early and late time behavior having constant slopes, and the shape of a theoretical recession curve for a stream with a stabilizing baseflow. The traditional 3/2 late time slope shows that the streamflow magnitude will continue to decrease with time making it sensitive to drought conditions, while the black line shows that the streamflow will stabilize after some time to a magnitude that is equivalent to the x-intercept discharge. A stream that is not sensitive to drought will still exhibit early and late time flows behaviors but at very low flows the flow rate will stabilize and the slope of $-dQ/dt$ will increase. This study suggests that beyond late-time behavior, there is a drought behavior at which the slope of the recession curve is no longer linear. Not all watersheds exhibit the tailing at low flows, which may be a result of underlying geology, geometry, or simply the recession wasn't long enough to express the stable baseflow condition.

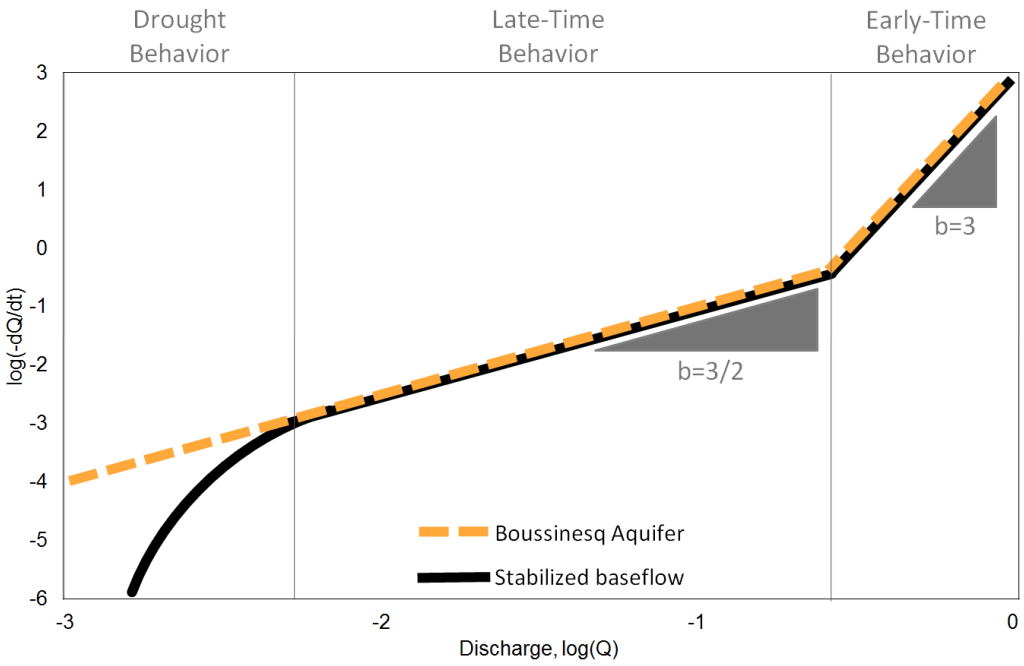

Figure 21. Theoretical comparison between recession plot of drought sensitive and drought resilient streamflow

In the 2015 hydrographs in the Oregon Cascades, the summer streamflow was more stable than models predicted. This could be because recession tailing occurs during drought flows but the models assume late-time behavior. However, we do not fully understand the physical mechanism of tailing. We hypothesize that the representations of drainage in 2D at low flows fundamentally ignores the effects of changing path lengths that are represented in 3D models may results in this tailing behavior. The initial assumptions proposed by Brutsaert of a horizontal and homogenous unconfined aquifer were instrumental for how early and late time behavior is defined. Because the aquifer is horizontal, the driving force is diffusion and is dominated by the water table gradient that is perpendicular to the stream length. These assumptions are an inaccurate representation of watersheds in the Oregon Cascades which are three-dimensional, not flat, a connection of smaller catchment systems within a watershed, not homogenous. We shouldn't expect for the classical Boussinesq aquifer to represent these extreme landscape cases. But what we don't know is whether this sustaining baseflow is extraordinary or ordinary.

Are the Oregon Cascades and other new volcanic systems more resilient to drought compared to other landscapes, or are we modeling these systems incorrectly further exacerbated by field data is that incorrectly processed with respect to taking the derivatives, so we have just missed it thus far? Are these drought resistant streams geologically reasonable and what geometry and geology would signify that other streams are also drought resistant? While these questions are currently outside of the scope of this research, they are worthy of future research that could be made possible by analysis of recession plot low flow tailing behavior.

Development and testing of a numerical model would add insight about hillslope drainage in 3D watershed, and possibly the physicality of tailing at low flows. Modeling hillslope drainage in a 3D aquifer with both stream slope and hillslope angles could provide a visual representation of the spatial and temporal patterns of hillslope drainage paths and velocities using a parabolic water table. Additionally, the model would allow us to look at drainage patterns at very low flows or when at aquifer fully drains, something difficult to quantify with field experiments. A numeric model could provide improved understanding of the rotation of hillslope drainage vectors as the aquifer drains, with better estimates of path length and residence time changes over the mathematical model that uses a linearized water table. The rotation of flow vectors increases the path length, making residence times greater when the water table is low. The activation of longer path lengths could mean water flow over a longer time period and more complete drainage that could be reproducing tailing behavior. The drainage patterns can be expressed using recession analysis as a possible hydrologic explanation for tailing behavior of the concave individual recessions that result in stabilized late summer flows.

A numerical model could also provide sensitivity analysis for aquifer properties and geometry to characterize the rotation of flow vectors. Further development of a conceptual framework to classify watersheds would be useful in order to create a predictive measure of drainage and outflow patterns for 3D drainage. The models can be used to describe wave propagation in hillslope and streamwise directions as a method to constrain possible scenarios when the rotation of drainage paths using

physics. Because there is no analytical solution for 3D aquifer drainage, this would be a worthwhile quantification to move towards. In the hunt for a 3D aquifer drainage solution, existing aquifer classifications schemes could be considered (Leibowitz *et al.*, 2014; Lyon and Troch, 2007; Wigington *et al.*, 2012). The 3D models could also introduce heterogeneity in in order to characterize drainage patterns at low flows. Both spatial heterogeneity across the landscape and the soil column should be considered.

One interesting implication of the changing flow vectors is the effect on the characteristic timescale of drainage. The characteristic timescale of drainage is assumed to be constant, 45 d ± 15 d (Brutsaert 2008). Previous studies that have looked at timescales of different basins have found significant variability (Berne *et al.*, 2005; Brantley *et al.*, 2017; Cooper *et al.*, 2018; Krakauer and Temimi, 2011; Manga, 1999; Sánchez-Murillo *et al.*, 2015). However, the drainage timescale is not well physically understood and a 3D model with many different watershed configuration could be used to estimate drainage timescales, using geometry and drainage paths to explain timescale variation. Ultimately, watersheds would be highly sensitive to drought is the 45 d timescale holds, which makes it a valuable research avenue to pursue. Because we anticipate an increased path length and residence time with aquifer drainage in 3D, a constant drainage timescale may not be representative. The characteristic timescale is calculated using an exponential relationship between flowrate at the basin outlet and groundwater storage. In practice, finding the timescale of a basin uses recession analysis with $b = 1$ for the lower envelope and estimating the timescale as the inverse of a from the point cloud (Brutsaert, 2008; Lyon et al., 2015). However, given the questionable of the validity of the point-cloud estimation methods described in Chapter 3, the timescale values found in this way may not be physically meaningful. If we calculate the timescale using individual recessions, instead of the point cloud, and individual recessions are concave, is there even a timescale? Moreover, for recessions with very large slopes, appearing nearly vertical on the recession analysis plot, there is no timescale for characteristic drainage. What does calculating the timescale represent? It is useful?

In the face of climate change droughts are predicted to become more persistent, further intensifying the need for accurately predicting the timing and magnitude of summer streamflow. In order to determine the sensitivity of a watershed, there is a need to describe what these drought conditions will look like and to quantify how severe the effects on the rivers and aquifers will be. While this dissertation attempted to develop a framework for better understanding and predicting drought flows there are still opportunities to improve the characterization. Knowing how streams and aquifers will respond to drought, both in magnitude and timing, in future climate change scenarios has great implications for water management, identifying watersheds that are more sensitive or resilient to future drought. Addressing these pertinent concerns will be a large but important task. Further research is required to determine the hydrologic and other physical mechanisms and controls that determine the watershed's sensitivities to drought that may allow some watersheds to reach a sustaining baseflow and continue to exhibit drought resilience even during prolonged droughts. This work will need to be large in scale, requiring a regional analysis in order to create predictive capacity for drought flow. An organized effort to perform recession analysis could be the first step in drought characterization regionally. A strength of the critical zone community is the ability to create a global analysis by comparing across studies (Brooks et al., 2015; Fan et al., 2019). However, a lack of consensus for a standard method for recession analysis procedures exists and thus inhibits recession analysis studies from being widely compared. If streamflow analysis is to be included in a global analysis, results need to be comparable across scales and observatories, including using the most up to date commutation method for taking the derivative and methods for parameter estimation. We suggest that the use the exponential time step method be used in favor of the constant time step method to reduce artifacts when considering low flow range. Additionally, we suggest the use of collective recession analysis be avoided in favor of individual recession analysis as the standard to describe the average and variability in watershed response. After individual studies have been published, a combined effort that uses the ensemble of all studies can be combined to look at trends and predictive capacity of recession analysis parameters using hydrology, geology, and climate.

Understanding the underlying controls of recession and drought flow are crucial to the interpretation of a watershed's vulnerability to climate change.

Bibliography

Alexander, R.B., E.W. Boyer, R.A. Smith, G.E. Schwarz, and R.B. Moore, 2007. The Role of Headwater Streams in Downstream Water Quality. Journal of the American Water Resources Association 43:41–59.

Ameli, A.A., N. Amvrosiadi, T. Grabs, H. Laudon, I.F. Creed, J.J. McDonnell, and K. Bishop, 2016. Hillslope Permeability Architecture Controls on Subsurface Transit Time Distribution and Flow Paths. Journal of Hydrology 543:17–30.

Ameli, A.A., J.J. McDonnell, and K. Bishop, 2016. The Exponential Decline in Saturated Hydraulic Conductivity with Depth: A Novel Method for Exploring Its Effect on Water Flow Paths and Transit Time Distribution. Hydrological Processes 30:2438–2450.

Bart, R. and A. Hope, 2014. Inter-Seasonal Variability in Baseflow Recession Rates: The Role of Aquifer Antecedent Storage in Central California Watersheds. Journal of Hydrology 519:205–213.

Berne, A., R. Uijlenhoet, and P.A. Troch, 2005. Similarity Analysis of Subsurface Flow Response of Hillslopes with Complex Geometry. Water Resources Research 41:1–10.

Biswal, B. and M. Marani, 2010. Geomorphological Origin of Recession Curves. Geophysical Research Letters 37:1–5.

Biswal, B. and M. Marani, 2014. "Universal" Recession Curves and Their Geomorphological Interpretation. Advances in Water Resources 65:34–42.

Boussinesq, J., 1877. Essai Sur La Theorie Des Eaux Courantes. Mem. Acad. Sci. Inst. Fr. 31:252–260.

Brantley, S.L., W.H. McDowell, W.E. Dietrich, T.S. White, P. Kumar, S.P. Anderson, J. Chorover, K. Ann Lohse, R.C. Bales, D.D. Richter, G. Grant, and J. Gaillardet, 2017. Designing a Network of Critical Zone Observatories to Explore the Living Skin of the Terrestrial Earth. Earth Surface Dynamics. doi:10.5194/esurf-5-841-2017.

Brutsaert, W., 1994. The Unit Response of Groundwater Outflow from a Hillslope. Water Resour. Res. 30:2759–2763.

Brutsaert, W. and J.L. Nieber, 1977. Regionalized Drought Flow Hydrographs from a Mature Glaciated Plateau. Water Resources Research 13:637–643.

Camporese, M., C. Paniconi, M. Putti, and J.J. Mcdonnell, 2019. Supporting Information for " Fill and Spill Hillslope Runoff Representation with a Richards Equation- Based Model ." Water Resources Research:2–4.

Carlier, C., S.B. Wirth, F. Cochand, D. Hunkeler, and P. Brunner, 2019. Exploring Geological and Topographical Controls on Low Flows with Hydrogeological Models. Groundwater 57:48–62.

Clark, M.P., D.E. Rupp, R.A. Woods, H.J. Tromp-van Meerveld, N.E. Peters, and J.E. Freer, 2009. Consistency between Hydrological Models and Field Observations: Linking Processes at the Hillslope Scale to Hydrological Responses at the Watershed Scale. Hydrological Processes 23:311–319.

Clarke, R.T., 1999. Technical Note: Uncertainty in the Estimation of Mean Annual Flood Due to Rating-Curve Indefinition. 222:185–190.

Cooper, M.G., J.R. Schaperow, S.W. Cooley, S. Alam, L.C. Smith, and D.P. Lettenmaier, 2018. Climate Elasticity of Low Flows in the Maritime Western US Mountains. doi:10.1029/2018WR022816.

Degagnea, M.P.J., G.G. Douglas, H.R. Hudson, and S.P. Simonovic, 1996. A Decision Support System for the Analysis and Use of Stage-Discharge Rating Curves. Journal of Hydrology 184:225–241.

Dralle, D., N. Karst, and S.E. Thompson, 2015. A, b Careful: The Challenge of Scale Invariance for Comparative Analyses in Power Law Models of the Streamflow Recession. Geophysical Research Letters 42:9285–9293.

Fan, Y., M. Clark, D. Lawrence, S. Swenson, L.E. Band, S. Brantley, P. Brooks, W. Dietrich, A. Flores, G. Grant, J. Kirchner, D. Mackay, J. McDonnell, P. Milly, P. Sullivan, C. Tague, H. Ajami, N. Chaney, A. Hartmann, P. Hazenberg, J. McNamara, J. Pellet, J. Volk, and D. Yamazaki, 2019. Hillslope Hydrology in Global Change Research and Earth System Modeling. Water Resources Research, AGU Centennial Volume on GRAND CHALLENGES IN THE EARTH AND SPACE SCIENCES:1737–1772.

Fenton, J.D. and R.J. Keller, 2001. The Calculation of Streamflow from Measurements of Stage. Cooperative Research Centre for Catchment Hydrology. :84.

FOEN, 2019. https://www.hydrodaten.admin.ch/en/current-situation-table-discharge-and-water-levels.htmlww.bafu.admin.ch/bafu/en/home.html.

Gilmore, T.E., D.P. Genereux, D.K. Soloman, and J.E. Solder, 2016. Groundwater Transit Time Distribution and Mean from Streambed Sampling in an Agricultural Coastal Plain Watershed, North Carolina, USA. Water Resources Research 52:2025–2044.

Godsey, S.E., J.W. Kirchner, and C.L. Tague, 2014. Effects of Changes in Winter Snowpacks on Summer Low Flows: Case Studies in the Sierra Nevada, California, USA. Hydrological Processes. doi:10.1002/hyp.9943.

Goode, D.J. and L.F. Konikow, 1990. Apparent Dispersion in Transient Groundwater Flow. Water Resources Research 26:2339–2351.

Hale, V.C., J.J. Mcdonnell, M.K. Stewart, D.K. Solomon, J. Doolitte, G.G. Ice, and R.T. Pack, 2016. Effect of Bedrock Permeability on Stream Baseflow Mean Transit Time Scaling Relationship. :1375–1397.

Harman, C.J. and C.L. Cosans, 2019. A Low-Dimensional Model of Bedrock Weathering and Lateral Flow Coevolution in Hillslopes: 2. Controls on Weathering and Permeability Profiles, Drainage Hydraulics, and Solute Export Pathways. Hydrological Processes 33:1168–1190.

Herschy, R., 1993. The Stage-Discharge Relation. Flow Measurement and Instrumentation 4:10–15.

Jachens, E.R., D.E. Rupp, C. Roques, and J.S. Selker, 2019. Recession Analysis 42 Years Later - Work yet to Be Done (in Review). Hydrology and Earth System Sciences Discussions:1–16.

Jefferson, A., A. Nolin, S. Lewis, and C. Tague, 2008. Hydrogeologic Controls on Streamflow Sensitivity to Climate Variation. Hydrological Processes. doi:10.1002/hyp.7041.

Kennedy, E.J., 1984. Discharge Ratings at Gaging Stations: Techniques of Water-

Resource Investigations of the United States Geological Survey. doi:10.1016/0022-1694(70)90079-X.

Kiang, J.E., C. Gazoorian, H. McMillan, G. Coxon, J. Le Coz, I.K. Westerberg, A. Belleville, D. Sevrez, A.E. Sikorska, A. Petersen-Øverleir, T. Reitan, J. Freer, B. Renard, V. Mansanarez, and R. Mason, 2018. A Comparison of Methods for Streamflow Uncertainty Estimation. Water Resources Research 54:7149–7176.

Kirchner, J.W., 2009. Catchments as Simple Dynamical Systems: Catchment Characterization, Rainfall-Runoff Modeling, and Doing Hydrology Backward. Water Resources Research 45:1–34.

Kong, J., C. Shen, Z. Luo, G. Hua, and H. Zhao, 2016. Improvement of the Hillslope-Storage Boussinesq Model by Considering Lateral Flow in the Unsaturated Zone. Water Resources Research 52:2965–2984.

Kormos, P.R., C.H. Luce, S.J. Wenger, and W.R. Berghuijs, 2016. Trends and Sensitivities of Low Streamflow Extremes to Discharge Timing and Magnitude in Pacific Northwest Mountain Streams. Water Resources Research 52:4990–5007.

Krakauer, N.Y. and M. Temimi, 2011. Stream Recession Curves and Storage Variability in Small Watersheds. Hydrology and Earth System Sciences 15:2377–2389.

Lang, M., K. Pobanz, B. Renard, E. Renouf, and E. Sauquet, 2010. Hydrological Sciences Journal Extrapolation of Rating Curves by Hydraulic Modelling, with Application to Flood Frequency Analysis Extrapolation of Rating Curves by Hydraulic Modelling, with Application to Flood Frequency Analysis. doi:10.1080/02626667.2010.504186.

Leapold, L.B. and T. Dunne, 1979. Water in Environmental Planning. W.H. Freeman, New York, NY.

Leapold, L.B., M.G. Wolman, and J.P. Miller, 1964. Fluvial Processes in Geomorphology. Dover Publications, Inc., New York, NY.

Leibowitz, S.G., R.L. Comeleo, P.J. Wigington, C.P. Weaver, P.E. Morefield, E.A. Sproles, and J.L. Ebersole, 2014. Hydrologic Landscape Classification Evaluates Streamflow Vulnerability to Climate Change in Oregon, USA. Hydrology and Earth System Sciences 18:3367–3392.

Lovellford, R., 2013. Variation in the Timing of Coho Salmon (Oncorhynchus Kisutch) Migration and Spawning Relative to River Discharge and Temperature. Master of Science Thesis in Water Resources Science at Oregon State University.

Lu, N., B.S. Kaya, and J.W. Godt, 2011. Direction of Unsaturated Flow in a Homogeneous and Isotropic Hillslope. Water Resources Research 47:1–15.

Lyon, S.W. and P.A. Troch, 2007. Hillslope Subsurface Flow Similarity: Real-World Tests of the Hillslope Péclet Number. Water Resources Research 43:1–9.

Maloszewski, P. and A. Zuber, 1982. Journal of Hydrology, 57 (1982) 207--231. 57:207–231.

Manga, M., 1996. Hydrology of Spring Dominated Streams in the Oregon Cascades. Water Resources Research 32:2432–2439.

Manga, M., 1997. A Model for Discharge in Spring-Dominated Streams and Implications for the Transmissivity and Recharge of Quaternary Volcanics in the Oregon Cascades. 33:1813–1822.

Manga, M., 1999. On the Timescales Characterizing Groundwater Discharge at Springs. Journal of Hydrology 219:56–69.

Markovich, K.H., R.M. Maxwell, and G.E. Fogg, 2016. Hydrogeological Response to Climate Change in Alpine Hillslopes. Hydrological Processes. doi:10.1002/hyp.10851.

McDonnell, J.J., J. Freer, R. Hooper, C. Kendall, D. Burns, K. Beven, and J. Peters, 1996. New Method Developed for Studying Flow on Hillslopes. EOS Transactions American Geophysical Union 77:465–472.

McDonnell, J.J., M. Sivapalan, K. Vaché, S. Dunn, G. Grant, R. Haggerty, C. Hinz, R. Hooper, J. Kirchner, M.L. Roderick, J. Selker, and M. Weiler, 2007. Moving beyond Heterogeneity and Process Complexity: A New Vision for Watershed Hydrology. Water Resources Research 43:1–6.

McGuire, K.J. and J.J. McDonnell, 2006. A Review and Evaluation of Catchment Transit Time Modeling. Journal of Hydrology 330:543–563.

McGuire, K.J., J.J. McDonnell, M. Weiler, C. Kendall, B.L. McGlynn, J.M. Welker, and J. Seibert, 2005. The Role of Topography on Catchment-Scale Water Residence Time. Water Resources Research 41:1–14.

Mcmanamay, R.A., M.S. Bevelhimer, and S.C. Kao, 2014. Updating the US Hydrologic Classification: An Approach to Clustering and Stratifying Ecohydrologic Data. Ecohydrology 7:903–926.

McManamay, R.A. and C.R. Derolph, 2019. Data Descriptor: A Stream Classification System for the Conterminous United States. Scientific Data 6:1–18.

McMillan, H.K., M.P. Clark, W.B. Bowden, M. Duncan, and R.A. Woods, 2011. Hydrological Field Data from a Modeller's Perspective: Part 1. Diagnostic Tests for Model Structure. Hydrological Processes 25:511–522.

van Meerveld, H.J., J. Seibert, and N.E. Peters, 2015. Hillslope-Riparian-Stream Connectivity and Flow Directions at the Panola Mountain Research Watershed. Hydrological Processes. doi:10.1002/hyp.10508.

Meyer, J.L., D.L. Strayer, J.B. Wallace, S.L. Eggert, G.S. Helfman, and N.E. Leonard, 2007. The Contribution of Headwater Streams to Biodiversity in River Networks. Journal of the American Water Resources Association 43:86–103.

Mirus, B., J. Smith, J. Godt, and R. Baum, 2016. Simulated Effect of Topography and Soil Properties on Hydrologic Response and Landslide Potential under Variable Rainfall Conditions in the Oregon Coast Range,. Landslides and Engineered Slopes:1431–1439.

Mote, P.W., S. Li, D.P. Lettenmaier, M. Xiao, and R. Engel, 2018. Dramatic Declines in Snowpack in the Western US. Npj Climate and Atmospheric Science 1:2.

Mutzner, R., E. Bertuzzo, P. Tarolli, S. V. Weijs, L. Nicotina, S. Ceola, N. Tomasic, I. Rodriguez-Iturbe, M.B. Parlange, and A. Rinaldo, 2013. Geomorphic Signatures on Brutsaert Base Flow Recession Analysis. Water Resources Research 49:5462–5472.

Nadeau, T.L. and M.C. Rains, 2007. Hydrological Connectivity between Headwater Streams and Downstream Waters: How Science Can Inform Policy. Journal of the American Water Resources Association 43:118–133.

Nolin, A.W. and C. Daly, 2006. Mapping "at Risk" Snow in the Pacific Northwest.

Journal of Hydrometeorology 7:1164–1171.
Ploum, S.W., S.W. Lyon, A.J. Teuling, H. Laudon, and Y. van der Velde, 2019. Soil Frost Effects on Streamflow Recessions in a Sub-Arctic Catchment. Hydrological Processes 33:1304–1316.
Polubarinova-Kochina, P.Y., 1962. Theory of Ground Water Movement. Princeton Univ. Press, Princeton, N.J.
Reitan, T. and A. Petersen-Øverleir, 2004. Estimating the Discharge Rating Curve by Nonlinear Regression - The Frequentist Approach. http://www.nve.no/Global/Publikasjoner/Publikasjoner%5Cn2004/Report%5Cn2004/Trykkefil%5Cnreport%5Cn6-04.pdf.
Reitan, T. and A. Petersen-Øverleir, 2008. Bayesian Power-Law Regression with a Location Parameter, with Applications for Construction of Discharge Rating Curves. Stochastic Environmental Research and Risk Assessment 22:351–365.
Rodhe, A. and J. Seibert, 2011. Groundwater Dynamics in a till Hillslope: Flow Directions, Gradients and Delay. Hydrological Processes. doi:10.1002/hyp.7946.
Roques, C., D.E. Rupp, and J.S. Selker, 2017. Improved Streamflow Recession Parameter Estimation with Attention to Calculation of − DQ/Dt. Advances in Water Resources 108:29–43.
Rupp, D.E. and J.S. Selker, 2006a. Information, Artifacts, and Noise in DQ/Dt - Q Recession Analysis. Advances in Water Resources 29:154–160.
Rupp, D.E. and J.S. Selker, 2006b. On the Use of the Boussinesq Equation for Interpreting Recession Hydrographs from Sloping Aquifers. Water Resources Research 42:1–15.
Rupp, D.E. and G.M. Smart, 2007. Comment on "Flow Resistance Equations without Explicit Estimation of the Resistance Coefficient for Coarse-Grained Rivers" by Raul Lopez, Javier Barragan, and M. Angels Colomer. Journal of Hydrology 346:174–178.
Safeeq, M., G.E. Grant, S.L. Lewis, and C.L. Tague, 2013. Coupling Snowpack and Groundwater Dynamics to Interpret Historical Streamflow Trends in the Western United States. Hydrological Processes 27:655–668.
Sánchez-Murillo, R., E.S. Brooks, W.J. Elliot, E. Gazel, and J. Boll, 2015. Baseflow Recession Analysis in the Inland Pacific Northwest of the United States. Hydrogeology Journal 23:287–303.
Shaw, S.B. and S.J. Riha, 2012. Examining Individual Recession Events Instead of a Data Cloud: Using a Modified Interpretation of DQ/Dt-Q Streamflow Recession in Glaciated Watersheds to Better Inform Models of Low Flow. Journal of Hydrology 434–435:46–54.
Smart, G.M., M.J. Duncan, and J.M. Walsh, 2002. Relatively Rough Flow Resistance Equations. Journal of Hydraulic Engineering 128:568–578.
Stoelzle, M., K. Stahl, and M. Weiler, 2013. Are Streamflow Recession Characteristics Really Characteristic? Hydrology and Earth System Sciences 17. doi:10.5194/hess-17-817-2013.
Tague, C. and G.E. Grant, 2004. A Geological Framework for Interpreting the Low-Flow Regimes of Cascade Streams, Willamette River Basin, Oregon. Water Resources Research 40:1–9.

Tague, C. and G.E. Grant, 2009. Groundwater Dynamics Mediate Low-Flow Response to Global Warming in Snow-Dominated Alpine Regions. Water Resources Research 45:1–12.

Tague, C., G. Grant, M. Farrell, J. Choate, and A. Jefferson, 2008. Deep Groundwater Mediates Streamflow Response to Climate Warming in the Oregon Cascades. Climatic Change 86:189–210.

Tashie, A., T. Pavelsky, and L.E. Band, 2020. An Empirical Reevaluation of Streamflow Recession Analysis at the Continental Scale Department of Geological Sciences , University of North Carolina at Chapel Hill , Chapel. Water Resources Research. doi:10.1029/2019WR025448.

Tashie, A., C.I. Scaife, and L.E. Band, 2019. Transpiration and Subsurface Controls of Streamflow Recession Characteristics. Hydrological Processes 33:2561–2575.

Thomas, B.F., R.M. Vogel, and J.S. Famiglietti, 2015. Objective Hydrograph Baseflow Recession Analysis. Journal of Hydrology 525:102–112.

Troch, P.A., A. Berne, P. Bogaart, C. Harman, A.G.J. Hilberts, S.W. Lyon, C. Paniconi, V.R.N. Pauwels, D.E. Rupp, J.S. Selker, A.J. Teuling, R. Uijlenhoet, and N.E.C. Verhoest, 2013. The Importance of Hydraulic Groundwater Theory in Catchment Hydrology: The Legacy of Wilfried Brutsaert and Jean-Yves Parlange. Water Resources Research 49:5099–5116.

Troch, P.A., C. Paniconi, and E. Emiel van Loon, 2003. Hillslope-Storage Boussinesq Model for Subsurface Flow and Variable Source Areas along Complex Hillslopes: 1. Formulation and Characteristic Response. Water Resour. Res. 39:1316.

USGS, 2018. WaterWatch: Customized Rating Curve Builder. https://waterwatch.usgs.gov/?id=mkrc. Accessed 10 Sep 2019.

Wang, D., 2011. On the Base Flow Recession at the Panola Mountain Research Watershed, Georgia, United States. Water Resources Research 47:1–10.

Weiler, M. and J.J. McDonnell, 2007. Conceptualizing Lateral Preferential Flow and Flow Networks and Simulating the Effects on Gauged and Ungauged Hillslopes. Water Resources Research 43:1–13.

Wigington, P.J., S.G. Leibowitz, R.L. Comeleo, and J.L. Ebersole, 2012. Oregon Hydrologic Landscapes: A Classification Framework. JAWRA Journal of the American Water Resources Association:1–20.

Y. Fang, P. Broxton, D. Gochis, G.-Y. Niu, J. D. Pelletier, P. A. Troch, and X. Zeng, P.H., 2015. A Hybrid-3D Hillslope Hydrologicalmodel for Use in Earth System Models. Water Resources Research 51:8218–8239.

Appendix. Comment on: "Base flow recession from unsaturated-saturated porous media considering lateral unsaturated discharge and aquifer compressibility", by Liang, X., H. Zhan, Y.-K. Zhang, and K. Schilling (2017)

Clément Roques[1], David E. Rupp[2], Elizabeth R. Jachens[3], and John S. Selker[3]

[1]Department of Earth Sciences, ETH Zürich, Zürich, Switzerland

[2]Oregon Climate Change Research Institute, College of Earth, Ocean, and Atmospheric Sciences, Oregon State University, Corvallis, Oregon, USA

[3]Biological and Ecological Engineering Department, Oregon State University, Corvallis, Oregon, USA

For Submission to:

Water Resources Research (WRR)

Status: Accepted

Abstract

Liang et al. (2017) presented an analysis of the impacts of unsaturated zone processes on streamflow recession using methodology from Brutsaert and Nieber (1977) with a constant time step in computation of the time derivative of flow. Over the past 10 years many authors have demonstrated that this method may produce artifacts that lead to incorrect interpretations. To demonstrate the impact of the choice of analysis methods, this comment presents an estimation of recession parameters using the Liang et al. (2017) discharge data that eliminates artifacts introduced through the constant time-step. Here we use the exponential time step method, which revealed recession coefficient *b* greater than 1 which are inconsistent with the fitting framework used in Liang et al. (2017).

Main Text

Liang et al. (2017; here after LZZS) presented an illuminating treatment of the impacts of unsaturated zone processes on streamflow recession. While the focus of LZZS was to derive semi-analytical solutions for hydraulic head and discharge accounting for lateral unsaturated flow and aquifer compressibility, this comment only addresses the field data analysis, interpretation, and related conclusions used in LZZS. In their validation of their concepts they carried out recession analysis of field data that followed the guidance of Brutsaert and Nieber (1977). As has been shown in recent literature, the Brutsaert and Nieber (1977) approach employed by LZZS turns out to be effectively fitting a model to data confounded both by artifacts (Roques et al., 2017; Rupp and Selker, 2006) and non-idealized properties of the environment (e.g. Troch et al., 2013). Since Brutsaert and Nieber (1977), multiple methods have been proposed that improve upon their methodology including smoothing techniques (e.g. Thomas et al., 2015), binning (e.g. Kirchner 2009), and improved computational techniques (Roques et al., 2017; Rupp and Selker, 2006), none of which were implemented in LZZS. We would like to alert readers to this consideration, and explore the likely impact of the choice of analysis methods on the results of LZZS.

Oftentimes discharge is discretized by virtue of the resolution of the devices used to measure stream stage. This can lead to periods of time where no change in flow

is reported, or the flow "jumps" by an increment of measurement, which can lead to artifacts when computing time-derivatives of flow. To avoid errors when computing the rate of change in discharge $-dQ/dt$, we have shown that the methodological framework (Exponential Time Step, ETS) described by Roques et al. (2017) is robust and effectively removes the artifacts incurred by using, as LZZS did, a constant time step dt (which we refer to here as the Constant Time Step, or CTS, method). While the ETS method described by Roques et al. (2017) is the latest methodology to address the errors associated with the CTS and propose a solution, other variable time step methods exist that reduce error and bias and could have been implemented (Rupp and Selker, 2006; Clark et al., 2009; Rupp et al., 2009). The ETS method is a numerical method that increments the time step exponentially along the recession and quantifies the local $-dQ/dt$ value from a linear regression fit. Single recessions have been isolated by detecting peak flows in the discharge time series, i.e. data samples that are larger than their two neighbors, and the nearest minimum. For the current analysis, we set the minimum recession duration to be considered to be 7 days, and we omit the first day of recession to reduce potential influence of overland flow after rainfall events. The maximum time interval allowed to compute the derivative $n \times dt$, with n samples and sampling interval dt, was set to 20% of the total duration of each recession. The a and b recession coefficients in $-dQ/dt=aQ^b$ were estimated by fitting a log-log linear regression based on a least-squares error optimization. The method weights the fitting procedure according to the local residual R^2 computed from the local $-dQ/dt$ estimation. The a and b values are estimated on late times of recessions only, i.e. for flows between Q_{10} and Q_{75} of the entire time series. Q_{10} is chosen as minimum flow value to be considered in the fitting procedure to avoid highly uncertain $-dQ/dt$ values at base flow. The distribution in b values obtained for each time series is then analyzed.

Figure 22 shows the comparison between the artifact-sensitive approach using CTS versus the robust analysis based on ETS. It is clear that our recession analysis shows no significant break in slope from b=3 to b=1; its presence would indicate a transition from early to late-time behavior that LZZS sought as corroborating their model.

Moreover, our computation revealed recession coefficients *b* greater than 1 which are inconsistent with the solution of LZZS. Our computation revealed recession coefficient *b* greater than 1 which do not agree with LZZS fitting framework. We thus would caution that Figure 13 of LZZS should be taken as a non-definitive representation of the data and temporal dynamics of the system. Sadly, LZZS are not alone in continuing this artifact-effected approach (e.g. Arciniega-Esparza et al. 2017). The impact on interpretation of recession is dramatic; for instance in the case of the data analyzed by LZZS, a pattern appears of recession parameter *b* systematically greater than 1.5 (

Figure 23), quite at odds with LZZS's statement in their abstract that "For late times, the power *b* … is 1." We see no evidence that *b* approaches 1 at late time and in many instances it appears as if *b* actual increases at extremes of low flow. As the literature suggests recession analysis is a powerful technique but methodology must be implemented to account for potential artifacts when computing the derivative for –dQ/dt to avoid spurious conclusions.

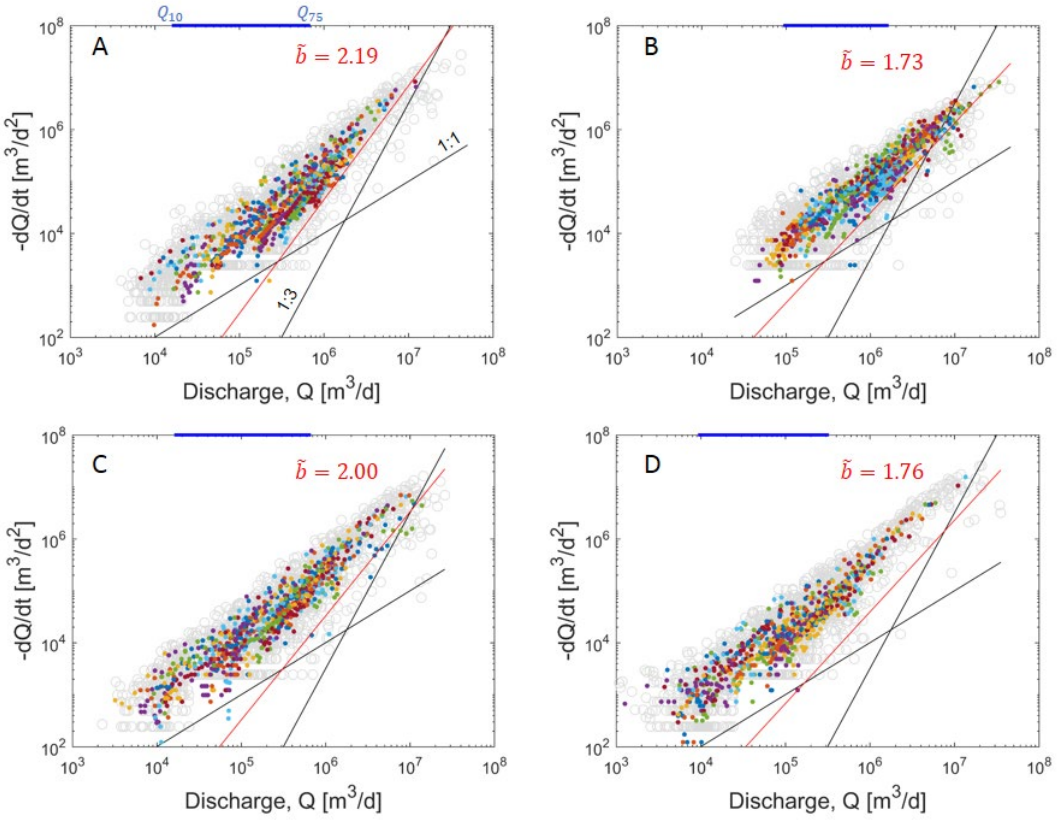

Figure 22. Recession plots log(-*dQ/dt*) vs log(Q) for the observed data investigated in Liang et al. (2017) using the ETS (colored points) and CTS (light gray circles) methods. Different colors represent different recession events. A: Floyd River near Sioux City, B: Raccoon River upstream of Des Moines, C: Turkey River near Garbe and D: West Fork Cedar River at Finchford. Black lines correspond to b=3 and b=1 for references. Red lines are drawn with corresponding median values of *b* obtained from single recession analysis (using an arbitrary a value). The blue horizontal lines at top of each panel represent the range of discharge values considered for the fitting of *a* and *b* parameters at late times, i.e. [Q10, Q75].

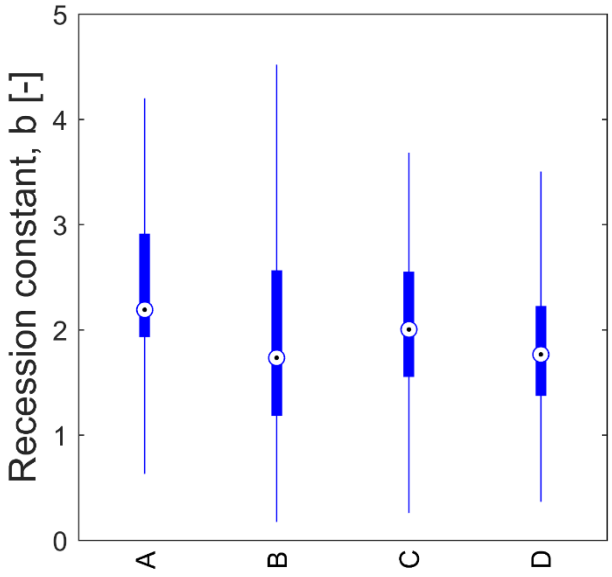

Figure 23. Distribution of *b* values obtained from ETS single recession analysis at late times [Q_{10} Q_{75}] for four locations (see Figure 22). The median (points), 25th and 75th percentiles (blue box) are identified. The vertical blue lines represent the variability outside the interquartile range (whiskers).

Acknowledgements

The data used in available in the supporting materials section for Liang et al. (2017) and the methodology is provided in Roques et al. (2017).

References

Arciniega-Esparza, S., Breña-Naranjo, J. A., Pedrozo-Acuña, A., & Appendini, C. M. (2017). HYDRORECESSION: A Matlab toolbox for streamflow recession analysis. Computers & Geosciences, 98, 87–92. https://doi.org/10.1016/j.cageo.2016.10.005

Brutsaert, W., & Nieber, J. L. (1977). Regionalized drought flow hydrographs from a mature glaciated plateau. Water Resources Research. 13, 637–643. http://dx.doi.org/10.1029/WR013i003p00637

Clark, M. P., D. E. Rupp, R. A. Woods, H. J. Tromp-van Meerveld, N. E. Peters, & J. E. Freer (2009). Consistency between hydrological models and field observations: Linking processes at the hillslope scale to hydro- logical responses at the watershed scale. Hydrological Processes, 23, 311–319. http://dx.doi.org/10.1022/hyp.7154

Kirchner, J.W. (2009). Catchments as simple dynamical systems: Catchment characterization, rainfall-runoff modeling, and doing hydrology backward. Water Resources Research, 45, 1–34. https://doi.org/10.1029/2008WR006912

Liang, X., Zhan, H., Zhang, Y.-K., & Schilling, K. (2017). Base flow recession from unsaturated-saturated porous media considering lateral unsaturated discharge and aquifer compressibility. Water Resources Research, 53. http://dx.doi.org/10.1002/2017WR020938

Roques, C., Rupp, D. E., & Selker, J. S. (2017). Improved streamflow recession parameter estimation with attention to calculation of − dQ/dt. Advances in Water Resources, 108, 29–43. https://doi.org/10.1016/j.advwatres.2017.07.013

Rupp, D.E., Schmidt, J., Woods, R.A., & Bidwell, V.J. (2009). Analytical assessment and parameter estimation of a low-dimensional groundwater model. Journal of Hydrology, 377, 143–154. https://doi.org/10.1016/j.jhydrol.2009.08.018

Rupp, D. E., & Selker, J. S. (2006). Information, artifacts, and noise in dQ/dt-Q recession analysis. Advances in Water Resources, 29, 154-160. https://dx.doi.org/10.1016/j.advwatres.2005.03.019

Thomas, B.F., Vogel, R.M., & Famiglietti, J.S. (2015). Objective hydrograph baseflow recession analysis. Journal of Hydrology, 525, 102–112. https://doi.org/10.1016/j.jhydrol.2015. 03.028

Troch, P., Berne, A., Bogaart, P., Harman, C., Hilberts, A., Lyon, S., Paniconi, C., Pauwels, V., Rupp, D. E., Selker, J, Tueling, A., Uijlenhoet, R., & Verhoest, N. (2013). The importance of hydraulic groundwater theory in catchment hydrology: The legacy of Wilfried Brutsaert and Jean-Yves Parlange. Water Resources Research, 49, 5099-5116. doi: 10.1002/wrcr.20407